TREATMENT OF PHARMACEUTICAL EFFLUENTS BY HYBRID ADVANCED OXIDATION PROCESS

A thesis submitted
in partial fulfillment of the requirements
for the degree of

Doctor of Philosophy

by

SURABHI PATEL

(Roll No.: 166107013)

Department of Chemical Engineering

Indian Institute of Technology Guwahati

Guwahati–781039

Assam, India

February 2022

TREATMENT OF PHARMACEUTICAL EFFLUENTS BY HYBRID ADVANCED OXIDATION PROCESS

A thesis submitted

in partial fulfillment of the requirements

for the degree of

Doctor of Philosophy

by

SURABHI PATEL

(Roll No.: 166107013)

Department of Chemical Engineering

Indian Institute of Technology Guwahati

Guwahati–781039

Assam, India

February 2022

Dedicated

To

My Parents

STATEMENT

I do hereby declare that the content embodied in this thesis entitled "**TREATMENT OF PHARMACEUTICAL EFFLUENTS BY HYBRID ADVANCED OXIDATION PROCESS"** is the result of investigations carried out by me at Department of Chemical Engineering, Indian Institute of Technology Guwahati, Guwahati, India, under the guidance of Prof. Subrata Kumar Majumder and Prof. Pallab Ghosh. In keeping with the general practice of reporting scientific observations, due acknowledgments have been made wherever the work described is based on the findings of other investigators.

CERTIFICATE

This is to certify that the thesis entitled **"TREATMENT OF PHARMACEUTICAL EFFLUENTS BY HYBRID ADVANCED OXIDATION PROCESS"** submitted by **Mrs. Surabhi Patel (Roll No.: 166107013)**, a research scholar in the Department of Chemical Engineering, Indian Institute of Technology Guwahati, for the award of the degree of Doctor of Philosophy, is a record of the original research work carried out by him under my supervision and guidance. The thesis has fulfilled all requirements as per the regulations of the institute and, in my opinion, has reached the standard needed for submission. The work documented in this thesis has not been submitted to any other University or Institute for the award of any degree.

Prof. Subrata K Majumder
Professor
Department of Chemical Engineering
Indian Institute of Technology Guwahati
Guwahati–781039, Assam, India.

Prof. Pallab Ghosh
Professor
Department of Chemical Engineering
Indian Institute of Technology Guwahati
Guwahati–781039, Assam, India.

Acknowledgements

The entire duration of this doctoral program has been full of memorable and enriching experiences for me. Not only have I been fortunate enough to understand my limitations and improve upon them on a professional front, but I have also learned valuable lessons that have made me a better person. As I near the tenure of my Ph.D. study, I would like to express my earnest and heartfelt gratitude to the people who have supported me throughout the journey. First and foremost, I would like to thank my thesis supervisors Prof. Subrata Kumar Majumder and Prof. Pallab Ghosh, for their patience, wisdom, and guidance, which aided me in enduring and resolving challenges that I encountered during my Ph.D. tenure. I sincerely thank him for allowing me the latitude to explore scientific pursuits and provide a guiding light throughout this study. I am grateful to the members of my doctoral committee, Prof. Vaibhav V. Goud, Prof. Chandan Das, and Dr. Lalit Mohan Pandey, for accepting to evaluate my thesis and provide insightful comments.

During my Ph.D. study, I had the wonderful experience of learning from my lab seniors Dr. Somen Mondal, Dr. Ritesh Prakash, Dr. Bharat Kumar Goshika, Dr. Fahad K M, and Mrs. Ruby Kumary who not only assisted me in developing technical knowledge but also provided constant encouragement. I would also like to thank Mr. Jinesh Machale for the stimulating discussions.

I am thankful to the members of our research group Mr. Bongliba T. Santham, Ms. Stuti Dubey, Mr. Kartikey Kumar, Mr. Awadh Kishore, Mr. Rohit Agarwaal, Mr. Gaurav Yadaw, Mohd. Tauheed Khan, Mr. Pathari Yash Subhash, Mr. Ashutosh Singh, and Mrs. Bhavana V. for providing a collaborative research environment. I earnestly appreciate the help, support, and guidance from each of them. I would be grateful to all the faculty members and staff of the Department of Chemical Engineering and Central Instruments Facility, IIT Guwahati.

Most importantly, I would like to thank my support system, which includes Ms. Anushree Ghosh, Ms. Shreya Mukherjee, Mrs. Sutapa Das, Ms. Kajal Ingtipi, Dr. Sushma Chakraborty, Ms. Shivani Gupta, Ms. Jenasree Hazarika, Mrs. Nilanjana Chakraborty, Dr. Siddhartha Thakur, Mr. Jinesh Machale, Mr. Atanu K. Paul, Mr. Sukumar Purohit, Saptarishi Gupta, and Dr. Piyal Mondal for their constant faith and patience.

Last but not least, this thesis would not have been complete without the endless trust and support of my parents Mrs. Sushma Patel and Lt. Girish Chandra Patel, my brother Vaibhav Patel, my husband, Mr. Prateek Shukla, my grandparents Mrs. Saroj Katiyar and Lt. Ram Sevak Katiyar and parents-in-law Lt. Yatra Shukla and Mr. Surendra N. Shukla.

Last but not least, I want to express my gratitude to everyone who has been directly or indirectly involved in my work over the years.

Abstract

Detection of pharmaceuticals in surface and ground water has become very frequent worldwide. The elevated concentration of pharmaceuticals is also raising concerns among researchers. These active organic compounds have become a major concern owing to their toxicity towards aquatic and human life. Excretion and improper disposal by the manufacturers are the main contributors. Most pharmaceuticals are found in the aquatic environment in their original or slightly modified form due to ineffective treatment in the urban wastewater treatment plants. Various processes have been applied for the degradation of pharmaceuticals. The formation of toxic metabolites and low mineralization were the main issues to be tackled.

The development of an efficient and economical technique to mineralize pharmaceutical compounds is the need of the hour. Over the last three decades, advanced oxidation processes (AOPs) have proven to be an excellent technique for removing refractory organic compounds from synthetic and real effluents. The hydroxyl radical is generated as the primary oxidant in most AOPs. The non-selective nature of the AOPs and the prospect of a high degree of mineralization have made them appealing. Ozone alone has been recognized as a strong oxidant, and it is capable of degrading recalcitrant organic compounds. Ozone selectively attacks organic compounds having a high electron density, whereas hydroxyl radical is a non-selective oxidant, and the latter reacts with a variety of organic compounds.

This work focuses on the degradation of pharmaceuticals synthetic and real industrial effluents by ozonation system. Three best-selling pharmaceuticals, naproxen, diclofenac, and ranitidine have been degraded by ozone in the presence of H_2O_2. To analyze the mass transfer of ozone from gas to a liquid, volumetric mass transfer coefficients were calculated in pure water for a pH range of 4–9. Concentration of pharmaceuticals was measured during and after ozonation by HPLC. Pseudo-first-order rate constants were calculated for all three

pharmaceuticals. Effect of pH (i.e, 4 – 9), ozone dosage (i.e., 0.44 – 0.50 mg s^{-1}), initial drug concentration (i.e., 50 – 125 mg dm^{-3}), and hydroxyl radical generation were assessed for ozonation process. The contribution of hydroxyl radicals in the degradation process was analyzed in a scavenging agent. Metabolites formed after ozonation were identified with the help of HR–LCMS. Probable mechanisms of their formation were predicted for all drugs. At pH 9 and 48 – 50 mg s^{-1} ozone supply, all three drugs were completely removed in less than 10 min. Degradation follows the pseudo-first-order reaction rate for NPX, DCF, and RNT, with rate constants ranging from 0.043 to 0.0979 min^{-1}. A model had been developed to analyze the effect of operation parameters on the rate of degradation. Decarboxylation, dichlorination, and hydroxylation are the major mechanisms involved in the degradation process.

After achieving efficient degradation of NPX, DCF, and RNT in ultra-pure water, a separate set of experiments was conducted in wastewater to ensure the degradation of drugs in real systems. The present study focused on degrading real pharmaceutical industrial effluent efficiently and economically. Real pharmaceutical industrial effluents were procured from two leading drug manufacturers in India. Characterization of effluents revealed that it contains mainly anti-cancer, anti-psychotics, anti-depressants, painkillers, and antibiotics. Water quality parameters were estimated for raw effluents, i.e., COD, TSS, TDS, color, alkalinity, ammonia, phenolic contents, etc. In the case of the first effluent, ozonation was used as a pre-treatment followed by adsorption by activated char. COD removal efficiencies were in the range of 75 – 88.5% in 3 h by ozonation. The minimum value of COD for the hybrid process achieved was 190 mg dm^{-3}. Recalcitrant metabolites were formed, which were removed by adsorption on activated char.

Ozonation was used as a post-treatment technique for the second effluent, and coagulation was used to remove TSS as pre-treatment. Coagulation with $FeCl_3.6H_2O$ removed

10% COD and 63% TSS at optimum circumstances. At pH 11, $O_3 + H_2O_2$ removes 91.6% of COD. After the treatments, no toxicity was discovered in any effluent.

In the present work, synthetic and real effluents pharmaceuticals were successfully degraded by ozonation techniques.

Table of Contents

List of tables

List of figures

CHAPTER I

INTRODUCTION AND LITERATURE REVIEW

Chapter I

Introduction and Literature Review

This chapter represents a general outline of the wastewater released from the pharmaceutical industries and its treatment techniques. The characteristics of the wastewater, its fate in the aquatic environment, and the health hazards created by its presence are discussed in detail. Advanced oxidation processes and their use in wastewater treatment are also reviewed. A literature review of the AOPs for each target compound and pharmaceutical wastewater is summarized. The objectives of the present research work are also defined.

1.1. Background

Advances in lifestyle and disease profiling have resulted in a shift in medication use patterns. In 2020, the worldwide pharmaceutical industry was valued at USD 1265.2 billion, with a projected growth rate of 3–6% by 2024 [1–3]. Figure 1.1 presents the global market of pharmaceuticals for the last 20 years [1–3]. An increased sale of antibiotics was also recorded due to the ongoing breakout of COVID-19. 216 million excess doses of antibiotics were sold between June and September 2020 in India [4].

Figure 1.1. Revenue of the pharmaceutical industries in last 20 years around the world [1–3].

Pharmaceutical plants are considered low-volume, high-value, and multi-product, which generally use the batch process for production. Various types of catalysts, solvents, reactants, and water are involved in the production processes. The impurity present in the drug is the major cost-deciding factor, which makes the separation and purification steps vital.

Ultrapure water is used as the extractant and solvent for purification. It cannot be reused due to the strict regulations for the purity of the drug. The discharged water from the pharmaceutical industries contains non-biodegradable recalcitrant organic substances, which have high toxicity towards aquatic and human life. The ratio of treated and untreated wastewater discharged worldwide is shown in Figure 1.2.

This picture is ommited due to copyright issue

Figure 1.2. The ratio of treated and untreated wastewater discharge [Source: UNEP-GPA, 2004].

60 – 80% of the prescribed pharmaceuticals are excreted as parent drugs, and they make their way to the sewage treatment plants and environment [5]. Most of the pharmaceuticals are found in the aquatic environment in their original or slightly modified form due to the ineffective treatment in the wastewater treatment plants (WWTPs) [6,7]. The primary concern is that the effluent from the pharmaceutical industry contains many antibiotics, which can develop resistance in pathogens and mammals. According to a survey conducted by World Health Organization (WHO), 7 lac people die every year due to anti-microbial resistance, and the fatality can increase up to 10 million by 2050 [8]. The main contributors to pharmaceutical contamination in the surface and groundwater are lenient regulations for the treatment, improper disposal, and inefficient removal technologies. Pharmaceuticals were first detected as a pollutant in the aquatic system in 1970 [9]. Nowadays, pharmaceuticals are frequently detected in freshwater bodies such as lakes, ponds, and rivers around the world [10–13]. Several researchers [14–17] have detected pharmaceuticals in the ground and surface water in the range of 15 – 1200 ng dm^{-3}. Although the amounts of pharmaceuticals were in the range of 90 – 31000 µg dm^{-3}, the chronic effects of these compounds were caused by their long-term

exposure [18,19]. The current situation predicts that the number of deaths due to anti-microbial resistance will surpass the combined number of deaths due to cancer and diabetes. Villages adjacent to the pharmaceutical industries are in alarming condition due to the highly contaminated groundwater, which leads to serious health problems such as cancer, miscarriage, and skin disorders [20]. There are many confirmed cases of fish death in the water bodies and resistance developed in humans towards antibiotics [20].

For the past two decades, active organic compounds in aquatic bodies have drawn many researchers' attention. A robust, efficient, and cost-effective technology is needed to overcome the inefficiency of conventional wastewater treatment methods for removing pharmaceuticals.

1.2. Pharmaceuticals in wastewater: sources, occurrence, and fate

Due to the extensive use of pharmaceuticals, their demands have been increasing for the past two decades. Industries have been adopting unethical ways of wastewater disposal and treatment to meet the demands. The effluent generated after one process needs to be discarded to retain the qualitative parameters of drugs produced. Continuous discharge of effluent creates problems in the treatment of wastewater. It is also essential to characterize the wastewater and recognize its components before applying the degradation techniques. The nature of wastewater generated is not uniform due to the vast variety of pharmaceuticals produced, various solvents, and different processes [21]. On the other hand, pharmaceutical residues present in urban wastewater show recalcitrant behaviour towards the wastewater treatment facilities [22]. Hence, they make their way out either untreated or in slightly modified form. Apart from industrial pharmaceutical wastewater, contamination of surface water, groundwater, and soil occur by various pathways from several sources. Figure 1.3 shows the possible ways of pharmaceutical contamination in surface and potable water.

Figure 1.3. Possible pathways of pharmaceutical contamination in surface and groundwater.

The reliability of global healthcare on the pharmaceutical system is increasing day by day. The major factors behind the higher pharmaceutical usage are increasing population, higher disease profiling, and a constantly-growing market. Increased healthcare activities have led to the generation of large quantities of hospital wastewater. Hospital wastewater contains a higher amount of antibiotics, analgesics, steroids, and gene modifiers than household wastewater. These effluent streams can act as a threat due to improper handling and partial treatment. Reports from WHO suggest that the requirement of water is 40 – 60 dm^3 d^{-1} for each in-patient in well-functioned healthcare units. For operating theatres, the water usage can increase up to 100 – 400 dm^3 d^{-1} [23,24].

Cattle manure is often used as solid and liquid fertilizers, and it may contain veterinary pharmaceutical residues. Residues present in soil can further leach into the groundwater. Pesticide sprays and agricultural runoff water from contaminated soil can contaminate surrounding water bodies. Recycling treated wastewater for irrigation purposes also contributes to the contamination of pharmaceuticals into groundwater. It is reported that 200 million hectares of land are irrigated with treated or raw wastewater worldwide [25]. Treated effluent from the wastewater treatment plant is disposed of into sewer or surface water bodies. These treated streams can have pharmaceuticals and their metabolites and can act as the source of contamination. Expired and unused therapeutic doses of drugs and personal care products are sometimes thrown out in the garbage, sewer, and household drains [26], which can make their way to potable and surface water in their original or slightly modified form.

Currently, there is no law or regulatory guidelines enforcing the upper limit of the concentration of these contaminants in effluents, surface, and groundwater. However, studies

reporting frequent detection of pharmaceuticals in the surface and groundwater are drawing the attention of the government. In the United States, a preparatory regulation was brought into action to eliminate the invasion of endocrine disruptors in wildlife and people [27]. The Water Framework Directive and its amended versions have outlined 45 priority substances and ten variable harmful substances to assess the risk imposed by them [28]. Further, European Union (EU) also restricts the upper limit of pharmaceuticals in surface water (10 ng dm^{-3}) and soil (< 1 μg kg^{-1}). Metabolites formed after the treatment of pharmaceuticals can also impose a higher risk than the parent compound itself. Thus, the presence of metabolites is also regulated by WHO and EU [29]. Various pharmaceuticals such as diclofenac (DCF), ibuprofen (IBF), carbamazepine (CBZ), atenolol, naproxen (NPX), and erythromycin were categorized as the prime contaminants in the water cycle by the Global Water Research Coalition [30].

1.3. Characteristics of pharmaceutical wastewater

Characterization of a pharmaceutical effluent is crucial for understanding its composition before applying the treatment techniques [61]. Pharmaceutical industries produce various products. Thus, the effluents discharged are usually different in nature. They may contain a variety of antibiotics, lipid regulators, hormones, solvents, phenol, and micro plastic used for packaging. Generally, the organic content of the effluent is more than its inorganic content. These effluents may also contain micro plastics, PVC, and nano-particles, which have endocrine-disrupting and gene-altering effects on aquatic organisms [62].

Various studies have found that the pharmaceutical industry effluents not only contain active pharmaceutical ingredients but are also laced with various solvents, metabolites, impurities, catalysts, and raw materials used [61,63]. Figure 1.4 exhibits the types of pollutants present in pharmaceutical wastewater. Table 1.2 summarizes the characteristics of industrial, pharmaceutical wastewater [21].

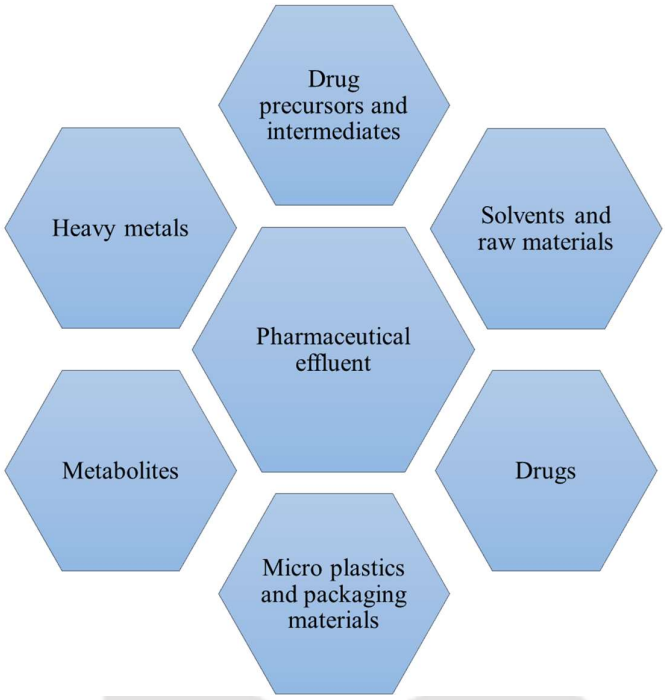

Figure 1.4. Pollutants present in pharmaceutical effluents [21].

1.4. Health hazards due to pharmaceutical contamination

Traces of pharmaceuticals in potable water and the active food chain pose a great risk to humans. One of the major concerns is the increasing anti-microbial resistance (AMR) cases. AMR can be defined as the resistance developed by the bacteria, fungi, viruses, and parasites against medication, making infections difficult to treat. As a result of AMR, antibiotics and other medications become ineffective towards infections, and they can cause severe illness, spread disease, and fatalities.

In 2014, WHO had raised a concern over growing AMR. Other health experts also warned that we are entering a "post-antibiotic era," resulting in millions of deaths per year. In India, particularly, the most vulnerable elements of society are suffering because of the rising AMR. The Washington-based Center for Disease Dynamics, Economics, and Policy published its first 'State of the World's Antibiotics' report in 2015, noting that 58,000 infants had died in

India in 2013 as a result of drug-resistant bacterial infections [64]. Pharmaceuticals' probable source and fate must be considered in the regulation and environmental risk assessment strategy. The formation of non-extractable residues (NERs) causes the pharmaceuticals to dissipate to other natural sources [65]. NERs are the main reasons for increased bio-availability, bio-magnification, and bio-accumulation of pharmaceuticals in plants, mammals, animals, and soil. The pharmaceuticals' ability to amplify and bio-accumulate has been studied in top food chain members such as top predators, large mammals, predatory fish, and birds of prey. According to a report, the most vulnerable species to the pharmaceuticals were found in the Arctic region, such as polar bears, polar foxes, and whales [66].

IBF is proven to pose a risk of chronic toxic effects on aquatic organisms and hinder postembryonic development in the amphibians [6,67]. NPX and ketoprofen are harmful in the aquatic environment [6,67]. Reduction in hemacrotic values in fishes and Asian vultures are reported due to contamination of DCF [67–69]. Unwanted doses of ciprofloxacin affect the lungs and kidneys of humans [6,67]. Resistant bacterial strains can harm both terrestrial and aquatic creatures due to the presence of azithromycin [67,70]. Traces of atenolol can hamper embryonic stem cell growth in humans [71,72]. Propranolol can slow down the process of cell regeneration [67,72].

1.5. Treatment technologies for pharmaceutical removal

It is a well-established fact that pharmaceuticals are increasing their presence in the surface and groundwater. An efficient removal technique should be prioritized inasmuch as the conventional techniques are failing. The composition of wastewater is the key factor for the selection of the removal technique. Various conventional and modern techniques are described in the sub-sections that follow.

1.5.1. Activated sludge process

This is one of the most common methods used in municipal wastewater treatment facilities. In this process, sludge laced with microorganisms is mixed with wastewater to degrade the carbon-containing organic matter. This method is designed to target organic contaminants, flocculants, and suspended solids. The removal efficiency achieved for the pharmaceuticals is in the range of 30 – 70% for long retention time [73,74]. The removal of pharmaceuticals depends on the pharmaceuticals present in the stream, microorganism used, COD, BOD, DO, pH, and temperature [75,76]. Some studies have reported the aerobic and anaerobic degradation of IBF, NPX, and bezafibrate at low concentrations in the effluent streams [77]. At high concentrations of antibiotics, the microorganism becomes inactive and restricts the process. Some pharmaceuticals, i.e., DCF, CBZ, and CA, show recalcitrant behaviour towards the microorganism and leave the treatment facility unaltered [78]. Thus, it can be concluded that the activated sludge processes are rather inefficient for pharmaceutical removal, especially the antibiotics. Pre-treatment of pharmaceuticals is required in order to improve their biodegradability.

1.5.2. Sequencing batch reactor (SBR) treatment

SBR is a modern activated sludge method with a completely mixed system such as the CSTR. It offers various advantages over conventional activated sludge methods. In SBR, all the unit operations such as reaction, settlement, and aeration take place in one tank independently. The major advantage of SBR over the activated sludge method is that no sludge reduction takes place during the process, and a lesser amount of space is required for equipment installation.

Wastewater streams with a low concentration of pharmaceuticals can be treated in SBR with 63 – 69% COD removal [73]. Total 94% BOD_5 and 83% COD removal were achieved when a highly contaminated non-penicillin pharmaceutical wastewater was treated in SBR with a retention time of 24 h [79]. Some researchers have used SBR in a hybrid process to improve

biodegradability. Wastewater with a low COD load (100 mg dm^{-3}) was treated in an SBR coupled with the solar-photo-Fenton process. The COD removal was found to be 98%, and BOD_3/COD was increased to 0.54 [79]. The SBR technique is practised in various countries for wastewater treatment as an alternative to conventional activated sludge. Although SBR provides a better removal efficiency than the conventional process, the removal of pharmaceuticals and their metabolites was not satisfactory.

1.5.3. Membrane biological reactor (MBR) treatment

MBR treatment technology is a hybrid process consisting of membrane separation and an activated sludge process. Membrane filtration traps the microorganism into the reactor in the effluent to provide an unhindered medium for the activated sludge process. Nowadays, these processes are gaining more attention due to cost-effectiveness, high removal rate, and lesser sludge generation. MBR treatment process can be classified into three categories on the basis of the mechanism, i.e., rejection, extraction, and diffusive MBR. Until now, MBR has been effectively used by many countries for industrial and urban wastewater treatment. MBR provides 15 – 42% higher removal efficiency (for the micro-pollutants) than the activated sludge method [80]. However, in the case of wastewater containing antibiotics, the removal efficiencies for both methods were found to be poor. To improve the removal efficiency, MBR is used as a pre-treatment step before ozonation, Fenton, and reverse osmosis [81]. The efficiency of the membrane reactor depends on hydraulic and sludge retention time. The main drawbacks of the MBR reactor are membrane blockage and a high maintenance cost.

1.5.4. Electro-coagulation (EC) treatment

Electro-coagulation (EC) is a wastewater treatment technique in which electricity is applied to alter the surface charge of the pollutants and allow agglomeration without adding any

chemicals. This technology has been widely practiced in the United States and European countries for the last two decades for the removal of metal from industrial wastewater [82]. Electrodes are made of aluminium, stainless steel, and iron in the EC process due to their low cost and easy availability [83]. The EC process has various advantages over the conventional treatment processes, i.e., low operation cost, no requirement of pH adjustment, lesser sludge production, no chemical requirement, and higher efficiency of pollutant removal [84]. It has also been reported that the EC has been employed for wastewater treatment in the mining, pulp and paper, textile, and petroleum industries [85–88]. COD removal for the textile and petroleum industries was found to be in the range of 74 – 99% [89] and 77% [90], respectively. In recent times, EC has been used as the treatment technique for recalcitrant organics such as antibiotics, estrogens, and natural organic matter. Doxycycline has been degraded by EC, and 90% removal was achieved in 80 min at pH 7 [91]. TOC removal of 80 – 90% was recorded for atenolol, acetaminophen, and antipyrine after the application of Fe- assisted EC [92].

1.5.5. Adsorption by activated carbon (AC)

Adsorption is emerging as a sustainable and effective technique for the treatment of complex wastewater treatment. In this method, the pollutants present in the wastewater build up on the surface of the adsorbent by physical or chemical binding. This process is often used as a polishing step for the removal of organic contaminants present in low concentrations, without leaving any by-product. Adsorption has various benefits, such as a good removal efficiency, possibility of reuse and regeneration, and requirement of low operation energy [93]. Many types of adsorbents are available, but AC is the most common adsorbent used for wastewater treatment. AC can be produced from a variety of carbonaceous materials such as wood chips [94], and agricultural waste, tea, and paper-mill wastes [95–97]. Operational parameters (i.e.,

adsorbent dose, pH, temperature, loading of pollutant, and ionic strength) play an important role in the adsorption process. Some studies also highlight the good adsorption capacity of AC for pharmaceuticals [98,99]. One of the critical aspects of the adsorption process is its kinetics. However, in the case of pharmaceutical adsorption, the controlling factors are mass transfer and the overall area available for adsorption. Generally, adsorption is coupled with oxidative removal techniques. The latter degrade the recalcitrant compound followed by the former technique to eliminate the toxicity efficiently. Several studies have shown that the recalcitrant micro-pollutant can be removed by adsorption on AC. However, the efficiency for removal declines due to the blockage of pores [100,101].

1.5.6. Ozonation

Ozone has emerged as one of the most popular treatment techniques for complex compounds. Ozone has been replacing chlorine for water treatment in the last two decades due to its environmental advantages. For any treatment application, ozone has to be generated *in situ* due to its unstable nature. Ozone has a high oxidation potential (i.e., 2.07 V) and follows two mechanisms of degradation, i.e., direct attack by molecular ozone and via the generation of hydroxyl radicals (from the decomposition of ozone). Ozonation has several advantages inasmuch as it generates a lesser amount of sludge, removes the recalcitrant pharmaceutical efficiently, and low operating cost. Mass transfer of ozone from the gas to the liquid phase plays an important role in its availability for reacting with the organic compound. Although the selective reaction tendency of ozone restricts the robust degradation of some pharmaceutical compounds, the addition of H_2O_2, UV, and catalyst enhances the generation of hydroxyl radicals resulting in higher removal efficiency.

1.5.7. Advanced oxidation processes (AOPs)

It has been highlighted earlier (Sec. 1.1) that the conventional methods often fail to treat the wastewater containing pharmaceuticals. AOPs have the capability to degrade a variety of organic and inorganic compounds. These treatments are based on the generation of free radicals (i.e., •OH, $O_2^{\bullet-}$, and $HO_2^{\bullet}$). The most common and effective method is the generation of hydroxyl radicals. They have a high oxidation potential, and they are non-selective in nature. Various studies indicate that the hydroxyl radicals successfully degrade various pharmaceuticals, including antibiotics [102–104]. A detailed discussion on the different AOPs is given in Section 1.6.

1.6. AOPs and their mechanisms

These processes remove pollutants using hydroxyl radicals. In 1980, the AOPs came into the limelight when they were used in water treatment [105]. Afterward, processes that involved the generation of SO_4^{-2} were also considered as AOPs. Nowadays, AOPs are replacing the conventional oxidation and chlorination methods. Both chlorine and ozone have good oxidation and disinfection properties, but in the case of chlorination, the intermediates produced exhibit more toxicity than the parent compound. Ozone is a relatively selective oxidant, whereas the hydroxyl radical is non-selective in nature, and it has a higher oxidation potential than ozone. Hydroxyl radicals have a very short lifetime, which leads to a low concentration of these radicals for the degradation of the pollutant [106,107]. To overcome the low concentration of the oxidant, the generation of radicals should be continuous and *in situ*. The hydroxyl radicals are considered to be very powerful because they convert the recalcitrant pollutant into almost non-toxic products [108]. Previous studies [108] have described the various AOPs with plausible mechanisms. Various AOPs for water treatment are given in Figure 1.5.

This picture is ommited due to copyright issue

Figure 1.5. Various AOPs for wastewater treatment.

1.6.1. Hydroxyl-radical-based AOPs

Hydroxyl radical is considered an ultimate oxidizing agent because of its non-selective and vigorous reactivity, which can break the aromatic ring. The rate constant for this oxidation process is in the range of 10^8 to 10^{10} mol^{-1} dm^3 s^{-1}. Hydroxyl radicals generally react via four basic paths, i.e., radical addition, hydrogen abstraction, electron transfer, and radical combination. The reaction of hydroxyl radicals with an organic compound leads to the formation of carbon-centred radicals. Upon reacting with oxygen, these radicals can be transformed into peroxide radicals. These highly-reactive radicals lead to high degradation rates and efficient mineralization despite their short half-life [108].

1.6.2. Ozone-based AOPs

Ozone is a very selective oxidant, and the rate constant of the reactions involving ozone usually lie in the range of 1.0 – 10^3 mol^{-1} dm^3 s^{-1}. Ozone reacts with the organic compounds in either ionized or dissociated form. A mechanism has been proposed for the generation of hydroxyl radicals, as shown below [109].

$$3O_3 + 2H_2O \rightarrow 2HO\bullet + 4O_2 \quad (1.1)$$

In the presence of another oxidizing agent, H_2O_2 can also be used to yield the HO•. The production of HO• in the presence of H_2O_2 occurs as follows:

$$H_2O_2 \rightarrow HO_2^- + H^+ \quad (1.2)$$

$$HO_2^- + O_3 \rightarrow HO\bullet + O_2^- + O_2 \quad (1.3)$$

Sometimes, radiation is also used for producing the HO•.

$$O_3 + H_2O + h\nu \rightarrow H_2O_2 + O_2 \quad (1.4)$$

The generation of hydroxyl radical was found to be enhanced at basic conditions since the presence of hydroxyl ions initiates the decomposition of ozone [108]. The generation of hydroxyl radicals favoured the degradation process due to their higher oxidative power than ozone. The presence of hydroxyl radicals reduced the lifetime of ozone in the aqueous phase. Hence, higher dissociation of ozone was achieved. The initiation of ozone decomposition in the alkaline medium involves multiple steps, as follows:

$$O_3 + OH^- \rightarrow OH_2^- + O_2 \quad (1.5)$$

$$O_3 + HO_2^- \rightarrow O_3^{\bullet -} + HO_2^{\bullet} \quad (1.6)$$

$$HO_2^{\bullet} + OH^- \Leftrightarrow O_2^- + H_2O \quad (1.7)$$

$$O_3 + O_2^{\bullet -} \rightarrow O_3^{\bullet -} + O_2 \quad (1.8)$$

$$O_3^{\bullet -} + HO\bullet \rightarrow O_2^{\bullet -} + HO_2^{\bullet} \quad (1.9)$$

$$O_3^{\bullet -} + HO\bullet \rightarrow O_3 + HO^{\bullet -} \quad (1.10)$$

1.6.4. Fenton-based AOPs

Some metals are capable of activating the H_2O_2 to produce HO•. Iron is the most extensively used metal as an activator. The Fenton reagent is a combination of H_2O_2 with ferrous ion as catalyst. This highly reactive process produces the HO• via the following reactions:

$$Fe^{2+} + H_2O_2 \rightarrow Fe^{3+} + HO\bullet + OH^+ \quad (1.11)$$

$$Fe^{3+} + H_2O_2 \rightarrow Fe^{2+} + HO_2^{\bullet} + H^+ \quad (1.12)$$

$$HO\bullet + Fe^{2+} \rightarrow Fe^{3+} + OH^- \quad (1.13)$$

$$Fe^{3+} + HO_2^{\bullet} \rightarrow Fe^{2+} + O_2H^+ \quad (1.14)$$

$$Fe^{2+} + HO_2^{\bullet} + H^+ \rightarrow Fe^{3+} + H_2O_2 \quad (1.15)$$

$$2HO_2^{\bullet} \rightarrow H_2O_2 + O_2 \quad (1.16)$$

The generation of hydroxyl radicals is shown in Equation (1.11), and the quenching of these radicals is described by Equations (1.12) and (1.13). Excess of hydroxyl radicals may lead to poor efficiency. That is why scavenging of hydroxyl radicals is required because an optimum ratio of iron ions and hydroxyl radicals has to be maintained. Production of Fe^{3+} and its reduction in Fe^{2+} is described in Equations (1.12) and (1.11). The effectiveness of hydroxyl radicals is high in acidic conditions. Iron cannot be used as a catalyst in wastewater treatment due to sludge formation. Due to these restrictions, three modified Fenton processes were proposed, i.e., Fenton-like reaction, electro-Fenton system, and photo-Fenton system. Fe^{2+} was replaced by Fe^{3+} in the Fenton-like reactions. The UV-based photo-Fenton radiation is used for the enhancement of reduction of Fe^{3+} to Fe^{2+}. In the electro-Fenton process, both ions are generated electrochemically.

1.6.5. Ultrasound (US)-based AOPs

Other unconventional methods like US beam irradiation can also perform advanced oxidation. Three stages like, nucleation, growth, and implosive, were generated due to the compression

and amplification of sound waves. Cavities are generated by these stages, which are made of vapour and gas microbubbles. High temperature and high-pressure conditions are achieved by the collapsing microbubbles. Under this condition, water molecules can be fragmented into hydroxyl radicals.

$$H_2O \rightarrow HO\bullet + H\bullet \quad (1.17)$$

1.6.6. AOPs based on sulfate radicals

Sulfate ion is one of the strongest oxidants with an oxidation potential of 2.01 V. Activation by heat, ultra-sonication, UV radiation, high pH, and transition metals can form powerful sulfate radicals having an oxidation potential of 2.6 V [110].

$$S_2O_8^{2-} \xrightarrow{\Delta/UV} 2SO_4^{-} \quad (1.18)$$

$$S_2O_8^{2-} + M^{n+} \rightarrow SO_2^{\bullet -} + M^{n+1} \quad (1.20)$$

A poorly-defined mechanism for the generation of activated sulfate radicals was presented in the literature [111]. According to this mechanism, the generation of activated persulfate is possible in the temperature range of 308.15 to 403.15 K. Metal activation method is less effective than heat and UV radiation methods. Sulfate radicals have a very short lifetime like the hydroxyl radicals, but they follow a different mechanism. The hydroxyl radical absorbs the H atom from the C–H bond or attaches to the C=C during the reaction. On the other hand, the sulfate radical removes the electron from the carbon and tends to produce organic radicals.

$$SO_4^{\bullet -} + H_2O \rightarrow HO\bullet + SO_4^{2-} + H^+ \quad (1.21)$$

$$SO_4^{\bullet -} + OH^- \rightarrow HO\bullet + SO_4^{2-} \quad (1.22)$$

From Equation (1.22), it is clear that in the alkaline solution, the yield of hydroxyl radical is higher than that in the acidic medium.

1.7. Literature survey

1.7.1. AOPs for pharmaceutical removal

In recent years, the use of AOPs for pharmaceutical degradation has increased. AOPs are found to be effective for the removal of various pharmaceuticals from real as well as synthetic wastewater. Various studies have been conducted for the removal of pharmaceuticals by using AOPs. Generally, AOPs have the capacity of completely removing the pharmaceuticals, but complete mineralization may not be achieved. In several cases, the intermediates generated are more biodegradable and less toxic than the parent compounds, thus implying that biodegradation may be feasible as a post-treatment technique for achieving complete mineralization. Although the removal of pharmaceuticals by the AOPs is generally studied on synthetic wastewater, the real effluents from the industries have received less attention. In the case of natural wastewater, various factors, i.e., water matrix and a cocktail of drugs, compromise the removal efficiency. While, in the case of synthetic wastewater, the AOPs perform extremely well.

The most common and best-selling pharmaceuticals are IBF, NPX, DCF, CBZ, and 17β-estradiol. IBF is a non-steroidal anti-inflammatory drug generally used for headaches, fever, and inflammation. Various studies have suggested that it is frequently detected in the aquatic medium [112–114]. The low rate constant of IBF degradation (i.e., 9.6 mol^{-1} dm^3 s^{-1}) for ozonation suggests its recalcitrant nature towards ozonation [104]. Ozonation was used to degrade a mixture of IBF and CA. Three sets of tests were conducted. The first test used atmospheric air as the feed for ozone production. The second test used H_2O_2 as the catalyst,

and the third test used concentrated O_2 for O_3 production. When compared to the first and second methods, the third method showed a 99% increase in degradation within 150 s, i.e., a 60% increase in mineralization for the same initial concentration and 75% reduction in hydraulic retention time. The degradation rate for the third case was found to be higher than the first and second. The mineralization rate was the same for the second and third methods, i.e., 60% in 10 min. According to the results of toxicity tests with *S. capricornium*, the compounds formed by ozone treatment led to an increase in toxicity in the first case. It was also reported that ozonation alone was not sufficient for countable degradation. It was reported that the 1 mg dm^{-3} ozone dose resulted in only 12% removal of IBF when its initial concentration in water was 2 μg dm^{-3}. The addition of H_2O_2 and a high dose of O_3 might improve the removal efficiency.

AOPs with optimized operating conditions were applied for removing sixteen common pharmaceuticals [115], i.e., CA, clarithromycin (CAM), CBZ, DCF, fenoprofen (FEP), gemfibrozil (GFZ), IBF, indomethacin (IDM), isopropyl antipyrine (IPA), ketoprofen (KEP), NPX, phenobarbital (PB), phenacetine (PNC), and phenytoin (PNT). Two personal care products were present in the medium, i.e., triclocarban (TCC) and triclosan (TCS). This study has suggested the best method of degradation for individual drugs. DCF, NPX, IDM, IPA, and TCS were easier to remove, whereas the removal of IBF and PB was found to be very challenging. CA, FEP, KEP, PNT, and TCC had high mineralization with the UV-based techniques, but the O_3-based techniques were not efficient. On the other hand, the O_3 based techniques were found to be effective for the degradation of CAM, CBZ, GFZ, and PNC.

Ozonation of lincomycin was found to be dependent on the pH ($k_{O_3} > 10^5$ at pH > 7). However, the contribution of hydroxyl radical was negligible [116]. There was a primary attacking site for ozone, i.e., pyrolidine nitrogen. The possibility of additional ozone attacking

sites was suggested, such as sulfur of the methylthio group. Based on the kinetic model, the second-order rate constants for lincomycin were reported to be 3.26×10^{5} and 2.43×10^{6} mol^{-1} dm^3 s^{-1}, for the neutral and acidic media, respectively. Lincomycin was also degraded by the catalytic photo process using a TiO_2 catalyst [117]. It was reported that TiO_2 strongly enhanced the degradation since complete removal was achieved within 120 min at pH 6 and 293.15 K. A mechanism for degradation was also proposed, involving S-oxidation of the methylthio group and oxidation of the pyrrolidine ring, followed by breaking of the amide bond. Advanced oxidation of other antibiotics such as penicillin, amoxicillin, and sultamicillin was studied to enhance their biodegradability [118]. Degradation of penicillin G-procaine was conducted by a photo-Fenton-like reaction by using a 125 W black-light-emitting UV-A in the range of 300 to 370 nm. By optimization of the reaction conditions, 56% of the COD and 42% of the TOC were removed within 30 min of the process. It was also reported that the process became less effective in the absence of UV-A. Biodegradability was also improved from 0.25 to 0.45. Ozonation of amoxicillin was performed to analyze its kinetics [119]. It was observed that the reaction rate constant was strongly dependent on the pH of the system (4×10^3 mol^{-1} dm^3 s^{-1} at pH 2.5 to 6×10^6 mol^{-1} dm^3 s^{-1} at pH 7). The addition of H_2O_2 and UV led to the generation of hydroxyl radicals and a higher rate constant (3.93×10^9 mol^{-1} dm^3 s^{-1} at pH 5.5). No clear evidence for S-oxidation of the amoxicillin was observed, but hydroxylation of the phenol ring was confirmed. It was suggested that there was no further degradation, maybe due to the short reaction time and absence of hydroxyl radicals.

Ceftriaxone, a *β*-lactam antibiotic, was degraded by ozonation, and the extent of mineralization was studied [120]. TOC and COD were reduced by 50 and 74%, respectively, when an ozone dose of 2.96 g dm^{-3} was applied at pH 7. The highest COD removal (i.e., 82%) was recorded at pH 11. A higher COD removal at the alkaline medium suggested the role of

hydroxyl radicals in the degradation process. Biodegradability was also improved from 0 to 0.1 after the ozonation treatment. A comparative study was conducted for the removal of five other pharmaceuticals containing ofloxacin, i.e., CBZ, propranolol, CA, DCF, and SMX, by O_3, H_2O_2/UV, and TiO_2-aided photo-catalysis [121]. It was observed from their study that the ozonation and H_2O_2/UV processes were capable of removing ofloxacin completely at pH 7.4 at 298.15 K, whereas TiO_2 photo-catalysis was found to be inefficient.

Complete removal of sulfadiazine was achieved by electrochemical oxidation in 60 min [122]. Titanium suboxide mesh and stainless-steel plate were used as anode and cathode, respectively. Electrochemical oxidation of SMX was performed by using a boron-doped diamond anode and stainless steel cathode. Complete removal of SMX was obtained in 180 min [123]. Toxicity studies on electrolyte solutions were conducted to get insight into the intermediates produced during the process, and the results demonstrated that the solution was well within the safety limits. Ultrasonication-assisted electrochemical oxidation was used for the degradation of ofloxacin on Ti/RuO_2 catalyst [124]. 91.2% removal was recorded at the optimum condition, whereas the COD removal was 70%. It was also concluded that the synergistic effect enhanced the removal.

In recent times, hybridization of several processes has been applied to improve removal efficiency and mineralization. A combination of processes, such as ozonation followed by adsorption, application of AOP followed by biodegradation, and simultaneous AOP and adsorption, were found to perform better than the individual approaches. The sono-photo-Fenton process was used to degrade ampicillin and nafcillin in a real wastewater matrix [125]. The anti-microbial activities of nafcillin and ampicillin were reduced to 96.3 and 90.5%, respectively. The initial concentration of both antibiotics was 30 µg, and the ultrasonic power was kept at 24.4 W for the removal. A quinolone-based antibiotic, enrofloxacin, was subjected

to ozonation followed by adsorption on zeolite [126]. It was observed that the 2.96 g dm^{-3} of ozone dose at pH 7 decreased 90% of the COD and 50% of the TOC in 60 min. The removal of COD at pH 3 and 11 was found to be low, i.e., 65 and 79%, respectively. The presence of hydroxyl radicals did not affect the degradation process. Biodegradability was increased from 0.07 to 0.38. Decontamination of enrofloxacin was done successfully from the drug-loaded zeolite in 30 min. It was concluded that the zeolite–ozone method was useful for the degradation of antibiotics.

1.7.2. Removal of DCF by AOPs

DCF is an NSAID, which is used to treat mild to moderate pain. It is also prescribed for the symptoms of rheumatoid arthritis and osteoarthritis. It limits prostaglandin biosynthesis *in vitro* and *in vivo*, and this inhibitory activity accounts for the mechanism of action. The chemical structure of DCF is given in Figure 1.6.

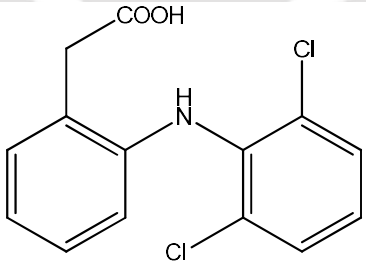

Figure 1.6. Structure of DCF.

In animal studies, the sodium salt of DCF was found to have a wide therapeutic range. Although it is a proven fact that DCF can be removed by natural photolysis [136,137], yet it is one of the most frequently detected pharmaceuticals in the water bodies such as groundwater [137,138] and surface water [139,140], at concentrations up to 1.2 μg dm^{-3} [5,141]. Although its concentration detected in the water bodies has been found to be much lower than the effective concentration limit, DCF can exhibit acute toxicity to the organisms due to the cocktail effect

in the presence of other pharmaceuticals [142]. In addition, there is evidence that the persistent exposure of DCF can affect the health of fish, including the development of tumours and distortion of gills even at the lowest detected concentration (i.e., 5 μg dm^{-3}) [143]. The removal efficiencies of DCF in the conventional biodegradation processes were found to be very low (i.e., 20 – 40%) in WWTPs due to poor biodegradability and low sorption efficiency [144]. Frequent detection of DCF in the aquatic environment and its acute toxicity towards the organisms necessitates an economical and efficient removal technique. Various removal processes based on physical or chemical methods, including membrane filtration [145], adsorption [146–149], coagulation [150], ion exchange [151], activated sludge [152,153], and photocatalytic oxidation [154,155], have been extensively studied for the degradation of DCF present in wastewater. DCF was highlighted by the Water Frame Work Directive in a list of 33 active chemicals, which can be a possible threat to the aquatic environment in the next ten years [156]. Many researchers have suggested that DCF has a high reactivity towards ozone and other AOPs [104,128,130].

A bench-scale experiment to degrade various pharmaceuticals using O_3/H_2O_2 was performed [157]. It was reported that only DCF was degraded by O_3 but with very low efficiency (i.e., 3%). The combination of O_3/H_2O_2 was effective and led to a higher degradation (i.e., 80 – 90%) than ozone alone. It was concluded that the degradation of pharmaceuticals could be improved by using O_3/H_2O_2, but the degradation efficiency of AOPs was found limited to the radical scavenging capacity. It was suggested that the concentration of O_3 should be at least the same as the dissolved organic carbon (DOC) for a better degradation of the pharmaceuticals (i.e., > 90%). A comparative study was conducted to assess the DCF degradation by UV/H_2O_2 and O_3 [121]. It was reported that both the processes led to significant degradation of DCF. The degree of mineralization was 32 and 39% for ozonation and

UV/H_2O_2, respectively, after 9 min of ozone treatment. Both reactions followed a similar pathway (but not identical) and led to the formation of the hydroxylated intermediates and C−N cleavage products. The reported values of the kinetic constants for this reaction were in the range of $1.76 \times 10^4 – 1.84 \times 10^4$ s^{-1} for DCF ozonation, in the pH range of 5 − 6. Similarly, the second-order rate constant for the ozonation of DCF was 1×10^6 mol^{-1} dm^3 s^{-1} at pH range of 5 – 10 [104] at 298 K. However, some investigators have reported lower values of the rate constant under identical operating conditions (i.e., 1.76×10^4 to 1.84×10^4 mol^{-1} dm^3 s^{-1} at pH 5 − 6 at 298.15 K) [121]. Information on the intermediates and their path of formation is scarce in the literature. One study has identified the steps during the ozonation of DCF. These steps include the hydroxylation of the aromatic rings and cleavage of diphenyl amine followed by ring-opening resulting in 95% chlorine removal and 30% removal of TOC in 90 min [121]. Various investigators have also implemented additional techniques in order to achieve high mineralization. The impact of H_2O_2 on the ozonation process was also investigated, with the conclusion that H_2O_2 increased the formation of hydroxyl radicals, resulting in a higher elimination of DCF [121,130]. Degradation of DCF was performed by H_2O_2/UV and direct photosynthesis. It was found that the addition of H_2O_2 led to higher mineralization (i.e., 40% TOC and 50% chlorine removal). However, the conversion of DCF achieved in this process was found to be lower than ozonation. Since the acidic degradation environments affected Fe, the Fenton-type methods yield unsatisfactory results [133]. It was found that the acidic and neutral media had a negligible effect on the conversion of DCF because of the precipitation of iron hydroxide instead of the drug [135]. When the pH of the system was not lowered by the buffer, the system performed better than the acidic media for the degradation, and the optimum pH was found to be 4.5 – 5 for higher degradation.

Various processes such as photocatalytic ozonation, photocatalytic oxidation, and non-thermal dielectric barrier discharge (DBD) have achieved the degradation of DCF and IBF

[158]. It was reported that the degradation of both drugs by direct ozonation resulted in a higher removal efficiency than photocatalytic oxidation. A combination of ozonation and photo-catalysis gave an enhanced rate of mineralization and degradation. It was also emphasized that the degradation achieved by the DBD reactor was dependent on the gaseous environment and energy input. The presence of Fe^{+2} accelerated the degradation in the case of the DBD reactor. It was also discovered that ozonation in the absence of light was the best strategy for degrading DCF, but some carboxylic acids generated as intermediates impeded the process yield, resulting in less mineralization.

Four pharmaceuticals, i.e., CBZ, DCF, SMX, and trimethoprim, were eliminated by advanced oxidation using O_3 at different experimental conditions [159]. Various intermediates were formed during ozonation that had not been reported previously in the literature. The initial concentration of the pharmaceutical was 5 mg dm^{-3} for the O_3 doses of 1.6, 2.3, 2.8, and 4.5 mg dm^{-3}, respectively, while the final concentration of each pharmaceutical was less than 1 mg dm^{-3}. The majority of the intermediates exhibited strong resistance to O_3. It was also suggested that the combination of oxidation processes with other techniques might increase the degradation.

Three different techniques, i.e., O_3, UVA, and TiO_2, were employed for the decomposition of DCF under various operational conditions [160]. It was observed that 100% removal of DCF and 60 – 75% elimination of TOC were achieved within 60 min. The optimum concentration of TiO_2 was in the range of 0.5 − 2.5 g dm^{-3}, and the O_3 consumption was approximately 6 mg for the removal of 1 mg of TOC. It was also suggested that DCF has some nucleophilic sites, and 100% removal was achieved in 10 min by the UVA, whereas 90% of the TOC was eliminated within the first 15 min.

Ozonation, sonolysis, and a combination of both were applied to degrade DCF [161]. Under the specified condition, the extent of mineralization was found to be 22 and 36% by ozonation and sonolysis, respectively, after 40 min of the treatment. From the combination of both the processes, the total mineralization achieved was 40% at the same time, which was more efficient than the individual techniques. The rate constants were calculated in terms of TOC removal, which were 0.169, 0.106, and 0.211 mg dm^{-3} min^{-1} for US, O_3, and US + O_3, respectively. A combination of US and O_3 yielded a higher removal due to the synergistic effect, which led to collapsing bubbles for the generation of free radicals. It was found that some metabolites produced during the degradation were highly recalcitrant to almost all degradation techniques. To achieve higher mineralization, removal of these metabolites was necessary. Adsorption, as a post-treatment technique, was found to be efficient in removing the metabolites generated during the AOP.

An integrated process of ozonation and adsorption was applied to degrade DCF [162]. Three types of AC were used in these experiments, and it was reported that AC named P110 Hydraffin had the highest BET surface area. Non-catalytic ozonation led to 100% removal of DCF in 15 min, whereas a combination of O_3 and AC gave better TOC and DCF removal rates. The influence of pH was also discussed, with the conclusion that there was only a minor effect of pH in ozonation alone. It was also stated that it was difficult to find the rate constant in the catalytic ozonation due to the mass transfer resistance. The combination of ozonation and adsorption gave better results than adsorption or ozonation carried out individually. By adsorption, 100% removal of DCF was achieved in 20 min, whereas by ozonation, it took 15 min. 90−95% TOC was removed in 120 min. Intermediates such as maleic, malonic, pyruvic, and carboxylic acids were detected. Most of the acids were degraded with time except oxalic and pyruvic acids.

A comparative investigation of DCF ozonation in the presence and absence of the HO• scavenger, *t*-BuOH, was carried out to assess the involvement of hydroxyl radicals in the degradation of DCF [163]. In this study, most of the intermediates formed in the degradation process were identified. The second-order rate constant was estimated to be 6.8×10^5 mol^{-1} dm^3 s^{-1} at 293.15 K. 100% mineralization of DCF was achieved when the ratio, O_3/DCF, was 5:1 in the presence of *t*-BuOH, and it was found to be 8:1 in its absence. The intermediates and their quantity were estimated, which were DCF-2, 5-iminoquinone, 5-hydroxy DCF, and 2,6-dichloroaniline, and their quantities were 32, 7, and 19%, respectively, in the presence of *t*-BuOH. In the presence of HO•, the detected intermediates were 5-hydroxy DCF, DCF-2, 5-iminoquinone, and 2,6-dichloroaniline, and their quantities were estimated to be 4.5, 2.7, and 6%, respectively. In the presence of HO•, 95% of chlorine was released whereas, in its absence, 45% of the same was released.

1.7.3. Removal of NPX by AOPs

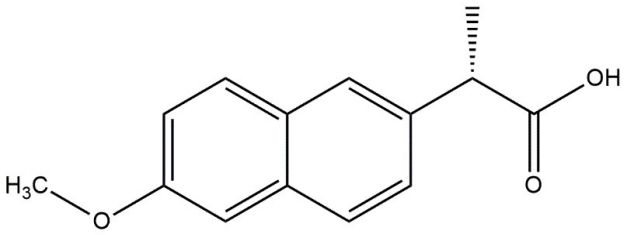

Figure 1.7. Structure of NPX.

NPX, a derivative of propionic acid (Figure 1.7), is one of the bestselling non-steroidal anti-inflammatory drugs. It is present in the range of 0.1 ng dm^{-3} to 7.69 µg dm^{-3} in wastewater [112,168,169] and 0.1 – 0.25 µg dm^{-3} in surface water [112,170]. It was listed among the top four pharmaceuticals found in the wastewater streams in the range of 7.0 – 1301.8 g d^{-1} [171]. Although the conventional wastewater treatment methods can remove more than 90% of NPX, it requires primary treatments and longer retention times (e.g., 5 – 10 d) [172–174]. The biodegradation methods require a very high retention time. Sedimentation and coagulation have been found to be ineffective for NPX removal. However, ozonation, chlorination, and adsorption can remove it effectively [170]. Some recent works have shown the low removal efficiencies of various treatment methods, e.g., anoxic–aerobic photo-bioreaction (28 – 35%) [39], chlorination and UV/chlorine (43.1 – 56.9%) [175], and membrane bioreaction (32 – 40%) [171].

A comparative study was conducted for the NPX removal by hydrodynamic cavitation (HC) and ozonation [176]. Only 28.9% removal of NPX was achieved in 120 min on the application of HC alone, whereas the complete removal of NPX was achieved within 40 min of reaction when a combination of HC and O_3 was used. The integrated HC–aerobic oxidation method was also found to be more efficient for the full mineralization of NPX from the aqueous solution. Because of the pre-treatment with HC + O_3, the biodegradability index increased from

0.35 to 0.70. These findings demonstrate that the HC-based pre-treatment could transform the non-biodegradable contaminants into biodegradable intermediates. Overall, it can be stated that the use of HC in combination with ozone, followed by conventional aerobic oxidation, is one of the most effective methods for removing NPX and reducing COD.

$CuFe_2O_4$ was used as a catalyst to activate peroxymonosulfate and oxidize NPX [177]. In the presence of 0.3 g dm^{-3} $CuFe_2O_4$ and 2 mmol dm^{-3} peroxymonosulfate, 92.3% of NPX was degraded, and 50.3% of organic carbon was eliminated in 60 min. This degradation system performed well throughout a wide pH range of 4 to 10. According to the free radical scavenger studies and electron spin resonance analyses, the primary active species were hydroxyl and sulfate radicals. The degradation path was also suggested, which involved hydroxylation, chain cracking, and ring-opening.

UV-based AOPs were used to degrade NPX [178]. As an alternative to the H2O2-based AOPs, a combination of UV and chlorine was used to degrade NPX. The pathways of degradation and metabolites formed were predicted and compared for both processes. Both AOPs degraded NPX via pseudo-first-order kinetics. The first-order rate constant (k') for the UV/chlorine method was 4.9 times higher than that for the UV/H_2O_2 method at pH 7. In the UV/chlorine process, the hydroxyl radical and reactive chlorine species contributed 15.9 and 76.3% of the NPX degradation, respectively. At the pH range of 6 – 9, UV/chlorine had better efficiency than UV/H_2O_2, but when the pH increased from 6 to 9, k' in the UV/chlorine method declined from 6.10×10^3 s^{-1} to 2.98×10^3 s^{-1}. However, in the UV/H2O2 method, pH had only a minor effect on k'. The k' increased linearly with increasing oxidant dosages (i.e., chlorine or H_2O_2) from 20 to 200 mol dm^{-3} in both the AOPs. The water matrix had less impact on the UV/H_2O_2 process than the UV/chlorine process. The value of k' was reduced by 23.2 and 9% in the UV/chlorine and UV/H_2O_2 processes, respectively, in tap water.

Different AOPs were used to explore the degradation of NPX as a target compound, i.e., UV (254 nm), VUV (172 nm), and UV/VUV (254/185 nm) photolysis [179]. For the highest concentration studied (i.e., 1.0×10^{-4} mol dm^{-3}), total photodecomposition of NPX was achieved after 20 min of UV, 10 min of VUV, and 8 min of UV/VUV photolysis. Four aromatic by-products and some aliphatic carboxylic acids were detected during these processes. The rate of degradation of NPX was determined by its initial concentration. Only the maximum concentration of dissolved O_2 had an effect on UV photolysis. It significantly reduced the transformation rate during VUV photolysis and had minor effects while applying the combined technique. The UV/VUV degradation rates of NPX were similar to those reported during VUV photolysis in deoxygenated conditions, but a synergistic impact of UV and VUV lamps was found in the presence of dissolved O_2. The radical pathway appears to dominate during the UV/VUV photolysis of NPX in the absence of O_2. In contrast, direct photolysis appears to contribute more to the overall transformation of NPX in solutions saturated with O_2. The initial rate of mineralization was highest under UV/VUV photolysis. However, only the VUV light could remove the TOC completely.

NPX was successfully mineralized by thermally activated persulfate (TAP) [180]. The TAP system can be a great oxidant regardless of the aqueous matrix in which pollutants are dissolved. In a highly charged non-treated hospital wastewater, the results demonstrated complete degradation of NPX. According to the TOC data, complete mineralization of pharmaceutical wastes and hospital wastewaters was achieved in optimum conditions. Inorganic additives such as $MgNO_3$ increased the NPX degradation rate constant by 154%, while $CaCl_2$ lowered the rate constant by 18.5%. All of the reactions followed pseudo-first-order kinetics. At 343 K, the highest achievable k_{obs} was 0.0214 mmol^{-1} dm^3 s^{-1}. Both hydroxyl and sulfate radicals played a key role in the degradation process. However, the dominance of

sulfate radical was observed. This finding was reinforced by the fact that no hydroxylated NPX species were found in the transformation products. Mainly decarboxylated NPX molecules were discovered as metabolites.

The use of TiO_2 as a photocatalyst in the heterogeneous photocatalytic degradation of NPX was also studied [181]. As the operating parameters, the effects of TiO_2 loading, volumetric flow rate, temperature, and dissolved oxygen content were investigated in a 0.078 dm^3 Duran reactor. 90% removal of NPX with only 5% mineralization after 3 h of photolysis was achieved. On the other hand, photo-catalysis using TiO_2 resulted in a lower removal (i.e., 40%) but improved mineralization (i.e., 20%). According to the by-product analysis, demethylation and decarboxylation were the primary steps in the degradation of NPX. The Microtox test (based on the bioluminescent bacterium *Vibro fisheri*) was used to assess the toxicity of the treated solution to examine the acute toxicity of NPX and its photo products. Under the operational parameters examined, photo-catalysis did not improve biodegradability. Mineralization data, on the other hand, looks interesting for future research.

Various studies on NPX degradation have suggested that the NPX could be removed by most of the AOPs. Nevertheless, the rate of mineralization was found to be low, and the information on the intermediates has been scarce.

1.7.4. Removal of ranitidine (RNT) by AOPs

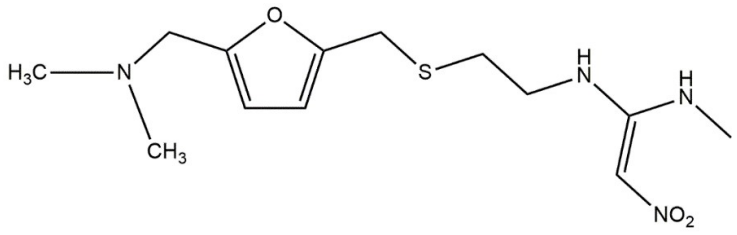

Figure 1.8. Structure of RNT.

RNT (Figure 1.8), with the pKa values of 8.13 and 1.95 [182], is often used in the treatment of ulcers, gastrointestinal hyper-secretory disorders, and gastroesophageal refluxes (popular trade names are Zantac, Taladine, Nu-Ranit, and Raniplex) [183,184]. RNT works as a histamine H_2-receptor antagonist due to the presence of a furan ring [185]. RNT has been discovered in surface waters and wastewaters, according to many investigations [75,186]. STP effluents in Greece had a median concentration of 1059 ng dm^{-3} [187], and river waters in Spain had a median concentration of 396.5 ng dm^{-3} [188] . In urine and excreta, it is excreted partly as an unaltered (i.e., 30 – 70%) compound and partly as its primary metabolites, RNT N-oxide, N-desmethyl RNT, and RNT S-oxide [189,190].

Electrochemical methods [191], photochemical oxidation [192], photolysis [193], ozonation [184], and solar photo-catalysis have already been used to remove RNT from ultrapure water and wastewater effluent. The AOPs showed good removal rates of RNT.

Ozonation of RNT was conducted under various operating conditions, i.e., system pH and ozone supply rate [194]. The elimination rate of RNT during ozonation was strongly impacted by the ozone concentration and pH. High pH and ozone concentration resulted in a higher removal rate. Mineralization reached 22% at neutral and acidic pH. When water matrices reacted with ozone, the total elimination of RNT was reduced, especially at the higher RNT concentrations. Inorganic ions in the aqueous matrix appeared to have little effect on the ozonation of RNT. Eleven transformed products (TPs) have been discovered, and their structures were deduced. The oxidation of the alkyl-part of the RNT molecule, more specifically at the double bond or the neighbouring secondary amine, with the abstraction of the NO_2 moiety, produced TPs with an aldehyde moiety and an imine C=N bond in most of the cases. The synthesis of oxidized derivatives of RNT with a carboxylic group in their structure resulted from further oxidation. The structure of RNT S-oxide had been validated through the

study of a reference standard. It had also been recognized as an ozonation product.

Some more parameters were studied for the ozonation of RNT, i.e., initial concentration of RNT and presence of free radical inhibitors [184]. The evolution of RNT over time indicates that it has high reactivity with molecular ozone. Mineralization levels of 20 – 25% indicate that the $(CH_3)_2$–N–CH_2– moiety linked to the furan ring might be isolated from the remainder of the RNT structure and mineralized further. Only alkaline conditions (e.g., pH 11) are capable of increasing the TOC conversion to levels around 70%. The competitive kinetic method for determining the direct ozonation rate constant for RNT demonstrated an undesirable reliance of the aforementioned constant on the reactivity of the reference molecule.

Radiation-based techniques also exhibited a high removal rate for RNT. UV light was used to irradiate aqueous solutions of RNT and other pharmaceuticals (i.e., tetracycline and lincomycin) in homogeneous and heterogeneous environments [117]. Two commercial polycrystalline TiO2 powders (supplied by Degussa P25 and Merck) were employed as photocatalysts. After 300 min, tetracycline and RNT showed a significant photolytic degradation, while the degradation of lincomycin was substantially lower. In terms of mineralization, tetracycline showed a slight drop in the TOC values, whereas lincomycin and RNT showed no differences. Tetracycline was almost totally mineralized in the presence of the Degussa P25 TiO_2, but lincomycin and RNT had a 60% drop in their initial TOC. When the Merck TiO_2 was used, there was less substantial mineralization.

In a pilot plant scale Compound Parabolic Collector (CPC) reactor, the mechanisms of solar photo-degradation of RNT were investigated. Catalyzed by a titanium dioxide semiconductor and Fenton reagent (Fe^{2+}/H_2O_2), two types of heterogeneous photocatalytic tests were carried out both with the distilled water and synthetic wastewater effluent matrix [195]. RNT was degraded at a comparable pace in both procedures. However, it was slower in the

synthetic effluent than in distilled water, owing to the negative effects of other organic molecules commonly found in municipal wastewater effluents. This suggests the importance of analyzing kinetics while considering the influence of the matrix before applying the AOPs for wastewater treatment. In both TiO_2 and photo-Fenton processes, the early steps of photocatalytic degradation of RNT were hydroxylation (i.e., attack by HO•), deamination, dealkylation, and oxidation by HO• and O_3. Additional unidentified products generated by the reduction of RNT by conductive band electrons were identified in the case of TiO_2-assisted photo-catalysis. Carboxylic acids were found at the end of the TiO_2 and photo-Fenton studies, implying that the high molecular weight intermediates were either mineralized or converted to the products (of reduced molecular weight) that are less damaging to the environment.

In the case of RNT degradation, it was observed that the few metabolites produced during the process imposed more threat than RNT itself. NDMA (i.e., N-nitrosodimethylamine) is a carcinogenic disinfection by-product that poses a major hazard to human health and the environment. RNT is a key precursor of NDMA. Photo-catalysis was found to be a useful and effective technology for degrading RNT and eliminating its potential to form NDMA [196]. A simple hydrothermal process was used to make MoS_2/RGO composites with various mass ratios. The MoS_2-RGO-3 heterojunction has the best photocatalytic performance for RNT degradation among the composites. Under visible light, the MoS_2-RGO-3 composite (with 23.2 wt% RGO) achieved the best photocatalytic degradation of RNT, with 74% degradation in 60 min. In addition, this composite had the highest RNT mineralization efficiency (i.e., 50%) and the least NDMA formation probability (i.e., 6.76%). Furthermore, the generated hydroxyl and superoxide radicals were involved in the RNT photocatalytic degradation reaction, where the hydroxyl radical was the most active component.

1.7.5. Industrial wastewater treatment by the AOPs

Organic wastewater generated by the industries has caused numerous environmental issues as civilization has progressed. The great majority of organic contaminants found in the water bodies persist in the environment, providing a health risk to humans and animals. As a result, effective treatment solutions for highly concentrated organic wastes are critical. AOPs are becoming increasingly used in the treatment of organic wastes. They have a high oxidation efficiency and produce no secondary pollutants when compared with other chemical techniques. Various studies have been conducted on the treatment of real industrial pharmaceutical wastewater by the AOPs. In most cases, AOPs are used for pre-treatment to improve the biodegradability of the recalcitrant effluent followed by biological treatments or a simultaneous application.

A biological activated-sludge system was used to treat wastewater released from a pharmaceutical manufacturing factory (i.e., TevaKS, Israel). It was followed by ozonation [197]. Before discharging the effluent to the municipal wastewater treatment plant, the purpose was to minimize the quantities of the medicines, i.e., CBZ and VLX. Both pharmaceuticals were found in the raw wastewater at unusually high amounts (i.e., [CBZ] = 0.84 ± 0.19 mg dm^{-3}; [VLX] = 11.72 ± 2.2 mg dm^{-3}), and they defied the biological treatment. CBZ was efficiently decomposed by ozone: the concentration of CBZ was reduced by more than 99% at an O_3 dose-to-dissolved organic carbon ratio (i.e., O_3/DOC) of 0.55. VLX had a lower removal rate, which was reduced by 98% at the higher O_3/DOC ratio of 0.87. The ozone degradation rate of CBZ was significantly increased when the pH of the biologically-treated effluent was reduced from 7 to 5, while the ozone degradation rate of VLX was decreased considerably for the same decrease in the pH. The concentrations of DOC and filtered chemical oxygen demand in the effluent did not change after the ozone treatment (COD). However, after ozonation, the

effluent's biological oxygen demand (BOD_5) and BOD_5/COD ratio both increased significantly. Several organic by-products were generated following the reaction of ozone with the target medicines and the organic matter present in the effluent. However, these by-products were predicted to be eliminated through the biological treatment in the municipal WWTP.

Real pharmaceutical wastewater containing the antibiotic amoxicillin was treated in a multistage treatment system by ozonation and ozonation coupled with aerobic biodegradation [198]. The wastewater had a high concentration of organic matter (i.e., TOC = 803 mg dm^{-3} and COD = 2775 mg dm^{-3}), a high amoxicillin content (i.e., 50 mg dm^{-3}), and acute ecotoxicity (*Aliivibrio fischeri aTU*: 48.22). Ozonation was found to be successful for amoxicillin destruction (up to 99%), as well as complete removal of the original colour of the wastewater, with an average ozone consumption of 1 g for dm^3 of the effluent. On the other hand, the ozonation system was unable to accomplish complete mineralization on its own. As a result, a multistage method combining ozonation and biodegradation was developed to reduce the cost and improve treatment efficiency. With roughly 500 mg of ozone consumption, the multistage treatment system achieved degradation of more than 99% of the amoxicillin, more than 98% of the original COD, and 90% of the initial toxicity.

Pharmaceutical wastewater based on antibiotic fermentation was treated using continuously-operated laboratory size anaerobic and aerobic moving bed biofilm reactors (MBBRs) using an O_3/H_2O_2 process [199]. Under the optimum conditions of the anaerobic MBBR at an influent pH of 6.5, hydraulic retention time (HRT) of 12 h, and organic loading rate of 13 kg COD /(m^3 d) for the hydrolysis/acidification process, 26.6% of COD was removed, and 931.75 mg dm^{-3} of volatile fatty acids (VFAs) was produced. Furthermore, the aerobic MBBR eliminated 91% of COD at a rate of 1.5 m^3 h^{-1} of aeration. Ultimately, the non-

biodegraded pollutants were mineralized using an O_3/H_2O_2 oxidation reaction with an H_2O_2/O_3 molar ratio of 0.5 and a 15 min reaction period. The total COD and color removal efficiencies were 99.2 and 98.7%, respectively. The findings of this study suggest that the total mineralization could be achieved by a hybrid AOP technique.

A study of the treatability of pharmaceutical effluent was conducted [200]. Both industrial (6000 m^3) and municipal wastewater (128 m^3) were discharged untreated into an adjacent evaporation pond per day. COD, TSS, and oil grease content were found to be in the range of 4100–13,023 mg dm^{-3}, 20–330 mg dm^{-3}, and 17.4–600 mg dm^{-3}, respectively in the raw wastewater. The presence of refractory chemicals lowered the BOD/COD ratio (0.25–0.30). The findings revealed that the refractory chemicals and their by-products were resistant to biological treatment and always remained in the treated effluent. It was also observed that the Fenton process, as a pre-treatment, enhanced biodegradability.

Ozone coupled with Fe^{2+} and nano zero-valent iron (nZVI) were used to enhance the biodegradability of pharmaceutical industrial wastewater [201]. BI was improved from 0.18 to 0.63 on the application of O_3 + nZVI. COD and toxicity were reduced by 62.3 and 82%, respectively. Spinach seeds were used for toxicity assessment, and a better germination rate in the treated effluent paved the removal of toxicity.

Photocatalytic oxidation of a pharmaceutical synthetic effluent was performed using silver decorated g-C_3N_4/ZnO nanorods [202]. The heterostructure of the silver nano-particles and nanorods was synthesized using environment-friendly methods. Efficient degradation of amoxicillin (i.e., 85.3%), cefalexin (i.e., 71.74%), and paracetamol (i.e., 41.36%) was achieved using a very small dosage (i.e., 0.08 mg dm^{-3}) of Ag/g-C_3N_4/ZnO nanorods. The initial concentration of the drugs in the effluent was high (i.e., 40 mg dm^{-3}). The recyclability of the nanorods was found to be significantly good as they removed 78% of the paracetamol after 5

cycles. Although the experiments were not performed on the real wastewater, it was emphasized on the scale-up for treatment of real effluent.

It can be concluded that although many research works have been performed on synthetic wastewater employing various treatment methods, including the AOPs, studies on real pharmaceutical effluents are still scarce in the literature.

1.8. Scope of the work

The degradation of pharmaceuticals in synthetic wastewater by various technologies was studied previously. The ozone-based technologies were also used to treat synthetic wastewater, and they exhibited good efficiency. Information on the metabolites produced during ozonation and their formation pathways are also very limited in the literature. Very few studies have been conducted on the treatment of real industrial effluents from the pharmaceutical industries. A qualitative analysis of the effluents plays a key role in the degradation process and its efficiency. It is essential to analyze the pharmaceuticals present in the wastewater stream and other water matrix to achieve a high degree of removal. In some cases, it has been observed that the metabolites generated during the AOPs have recalcitrant behaviour. These types of effluents have toxicity despite higher removal efficiencies. To overcome the recalcitrant metabolites, hybridization of technologies is a useful way to degrade stubborn effluents. This type of approach is not yet explored by the researchers.

The research on the degradation of three pharmaceuticals (i.e., NPX, DCF, and RNT) in the real wastewater and the effect of operating parameters such as the pH of the system, ozone dose, concentration of hydrogen peroxide, and initial concentration of the pollutant is not yet reported in detail. Degradation pathways and identification of intermediates of the above-mentioned pharmaceuticals are also missing from the literature. It is essential to study

the feasibility of degradation of pharmaceuticals present in the real effluents released from the pharmaceutical industries using hybrid technologies such as O_3/H_2O_2.

1.9. Objectives of the study

The main objectives of the present work are as follows:

[1] Intensification of degradation of naproxen aided by the ozone in a plant prototype: its kinetic and mass transfer studies

[2] Ozonation of diclofenac in a laboratory-scale bubble column: intermediates, mechanism, and mass transfer studies

[3] Ozonation of ranitidine and development of a kinetic model for degradation

[4] Treatment of a real effluent released from the pharmaceutical industry by a hybrid process of advanced oxidation and adsorption by activated charcoal

[5] Treatment of a mixture of effluents released from the pharmaceutical industries by a combination of coagulation and O_3/H_2O_2

1.10. Organization of the thesis

The present work deals with the removal of pharmaceuticals from synthetic and real industrial wastewater by AOP (i.e., O_3 + H_2O_2) coupled with other pre-and post-treatment (i.e., adsorption and coagulation). Literature relevant to the target compounds and applied techniques have been reviewed. The chapter-wise outline of the thesis is given below.

Chapter I (Introduction): This chapter presents an overview of pharmaceutical effluents and the techniques for the treatment of wastewater. The application of different types of AOPs for wastewater treatment is also discussed. A brief review of the literature is presented for each

target pharmaceutical and real industrial effluent. This chapter also presents the objectives of the present research work.

Chapter II (Materials and Methods): This chapter describes the experimental setup used for the ozonation. The list of the chemicals used, as well as their source and purity, is provided. A detailed description of the preparation of samples and experimental procedures is presented. The steps for carrying out the experiments and analyzing the samples are also given in this chapter.

Chapter III (Ozone Microbubble-aided Intensification of Degradation of NPX in a Plant Prototype: Kinetic and Mass Transfer Studies): In this chapter, degradation of NPX in synthetic wastewater is conducted by the ozone microbubble system in the presence of H_2O_2. The effect of various operating parameters such as the pH of the medium, ozone supply rate, and the effect of H_2O_2 are analyzed. The pseudo-first-order reaction rate constants are estimated at different pH and ozone doses. The axial variation of ozone concentration in the reactor is analyzed by the dispersion model. Mass transfer study of ozone from the gas to the liquid phase is also discussed in detail. The volumetric mass transfer coefficients for the ozonation of pharmaceuticals by the ozone microbubbles are also determined. Identification of intermediates and the mechanism of their formation are predicted and reported in detail.

Chapter IV (Ozonation of DCF in a Laboratory-scale Bubble Column: Intermediates, Mechanism, and Mass transfer study): The effects of various parameters on the degradation of DCF in the aqueous medium are reported in this chapter. The effect of the pH of the medium, initial concentration of DCF, presence of radical scavenger, and water matrices are studied in detail. The present study aims to predict the degradation pathways of DCF during ozonation and detect the metabolites formed. The kinetic parameters for the ozonation of DCF are

determined, and a kinetic model is developed for the ozonation process. The involvement of the hydroxyl radicals in the degradation process is also investigated. Mass transfer of ozone in the aqueous phase is analyzed, and the parameters for mass transfer are calculated. Removal of TOC and release of chloride ions during the reaction are also studied.

Chapter V (Degradation of RNT by O_3 + H_2O_2: Kinetics, Modelling, and Mechanism): A synthetic wastewater containing RNT is treated with O_3/H_2O_2. The effect of several parameters such as ozone dose, initial RNT concentration, system pH, and water matrices are studied. A few intermediates are also predicted during and after ozonation. Pseudo-first order rate constants are also calculated for the pH range of 4 – 9 and ozone supply (0.44 – 0.50 mg s^{-1}). Elimination of TOC and toxicity are also analyzed. A model is developed for RNT ozonation to account for the effect of hydroxyl radicals on the reaction rate.

Chapter VI (Treatment of a Real Pharmaceutical Industrial Effluent by a Hybrid Process of Advanced Oxidation and Adsorption by Granular Activated Char (GAC)): A real industrial effluent is treated with a hybrid process of O_3/H_2O_2 and adsorption on GAC. This chapter includes the complexities encountered for real wastewater treatment, i.e., the presence of matrices and interference of other organic compounds. The pharmaceuticals present in the effluent are identified and classified. The presence of anti-cancer, anti-psychotic, anti-depressant, and antibiotic drugs is confirmed in the effluent. The effluent was treated with ozone in the presence of H_2O_2. The pretreated wastewater is passed through a bed of GAC for further reduction of the COD. The effects of pH, the concentration of H_2O_2, and ozone feed rate are studied. The water quality parameters of the raw and treated wastewater are analyzed and discussed.

Chapter VII (Treatment of Mixture of Pharmaceutical Industrial Effluents with a Combination of Coagulation and O_3/H_2O_2): A mixture of two pharmaceutical effluents is treated with a hybrid technology consisting of coagulation by $FeCl_3$ and O_3/H_2O_2. This study aims for the higher removal of TOC, COD, and toxicity of the effluent. In the pre-treatment process, coagulation is done by $FeCl_3$. Next, oxidation is performed by using O_3/H_2O_2. The effect of the pH of the medium and the dose of $FeCl_3$ on COD removal are studied during the coagulation treatment. The concentrations of various metals in the effluent are detected before and after the treatment. Toxicity analysis with the help of *E. coli* is also performed to assess the removal of the same.

Notations

Abbreviations

AC	Activated char
AMR	Anti-microbial resistance
AOP	Advanced oxidation process
BI	Biodegradability index
BDL	Below detection limit
BET	Brunaur-Emmett-Teller
BOD	Biological oxygen demand
CA	Clofibric acid
CAM	Clarithromycin
CBZ	Carbamazepine
COD	Chemical oxygen demand

COVID-19	Coronavirus disease
CPC	Compound parabolic collector
CSTR	Continuous stirring tank reactor
DBD	Dielectric barrier discharge
DCF	Diclofenac
DO	Dissolved oxygen
DOC	Dissolved organic carbon
EC	Electro-coagulation
EU	European Union
FEP	Fenoprofen
GAC	Granular activated carbon
GFZ	Gemfibrozil
HC	Hydro cavitation
HRT	Hydraulic retention time
IBF	Ibuprofen
IDM	Indomethacin
IPA	Isopropyl antipyrine
KEP	Ketoprofen
MBR	Membrane batch reactor
MBBR	Moving bed biofilm reactor
nNZVI	Nano zero valent iron
NSAID	Non-steroidal anti-inflammatory drug
NDMA	N-nitrosodimethylamine
NPX	Naproxen

NRE	Non-extractable residue
PB	Phenobarbital
PNC	Phenacetine
PNT	Phenytoin
PVC	Polyvinyl chloride
RGO	Reduced graphene oxide
RNT	Ranitidine
SBR	Sequencing batch reactor
SXM	Sulfamethoxazole
STP	Sewage treatment plant
TAP	Thermally-activated persulfate
TCC	Triclocarban
TCS	Triclosan
TOC	Total organic carbon
TP	Transformation product
TSS	Total suspended solids
US	Ultra-sonication
USD	United States dollar
UV	Ultraviolet
VFA	Volatile fatty acid
VLX	Venlafaxine
VUV	Visible ultraviolet
WHO	World health organization
WWTP	Wastewater treatment plant

CHAPTER II

MATERIALS AND METHODS

CHAPTER II

Materials and Methods

This chapter contains the details of the experimental setup used to degrade synthetic and real wastewater. The reagents and chemicals used in the present work have been listed with their sources. The experimental methods used to degrade various drugs have been described in detail. The details of the analytical instruments used for the various analysis are also described along with the analysis procedure.

2.1. Experimental setup

2.1.1. Ozonation setup

Ozonation system used to degrade pharmaceutical wastewater consists of an oxygen concentrator, an ozone generator connected with a sparger, a glass reactor, and an ozone destructor to diminish the excess ozone. Figure 2.1 represents the setup for ozonation process.

An assembly of an oxygen concentrator (make: Oz-Air, model: HG 03, country: India) and an ozone generator (make: Oz-Air, model: ISM 10 Oxy, country: India) was used to supply ozone to the reactor vessel. The oxygen concentrator worked on the pressure swing adsorption method [203,204], which isolated the oxygen from air based on its molecular characteristics and affinity towards the adsorbent. It produced pure oxygen and fed it to the ozone generator. The ozone generator worked on the corona discharge method [205]. In this method, the applied voltage generated nascent oxygen, and it combined with the oxygen molecule to generate ozone. The ozone thus generated was supplied through a sparger to a glass reactor of 1 dm^3 volume. The excess ozone escaping from the reactor was captured and passed into the ozone

destructor (make: Oz-Air, model: Dest 50, country: India), which converted the unreacted ozone to oxygen. A rotameter (make: Instrumentation Engineers Pvt. Ltd., model: 1114C, country: India) was used to measure the flowrate of the mixture of ozone and oxygen coming out from ozone generator. The range of the rotameter was 8–80 $cm^3\ s^{-1}$. The pore size of the sparger (make: Oz-Air, model: S4, country: India) used in this study was 40 μm. It was resistant to ozone. It was observed that the pores were distributed nonuniformly throughout the sparger surface. The pH of the samples was monitored by an inline pH meter (make; Equiptronics, model: EQ 610, country: India).

The surface morphology and pore structure of the sparger used were analyzed by FESEM (make: Jeol, model: JSM-7610F, country: Japan).

Figure 2.1. Schematic of the experimental setup for ozonation process.

2.2. Chemical and reagents used

All the chemicals and reagents used in the present work have been listed in Table 2.1 and their purity and source. All the chemicals were of analytical grade and solvents used in HPLC analysis were of HPLC grade. Synthetic wastewater and control solutions were prepared in milli-pore water (make: Millipore, model: Elix-3, country: USA) of pH 6.5.

Table 2.1. List of chemicals and reagents (for water quality test) used in present work

Chemical	Purity (%)	Source
Acetonitrile (HPLC grade)	99.8	Merck (India)
Diclofenac (DCF)	98	MP biomedical (France)
Glacial acetic acid (HPLC grade)	99.8	Merck (India)
Glacial ammonium acetate (HPLC grade)	99.6	Merck (India)
Granular activated char	98%	Loba chemicals (India)
Hydrogen peroxide	30	Merck (India)
Hydrochloric acid	35	Merck (India)
Isopropyl alcohol	99.5	Merck (India)
Manganese di oxide	99	Merck (India)
Methanol (HPLC grade)	99.8	Merck (India)
Naproxen (NPX)	98	Sigma-Aldrich (India)
Ranitidine (RNT)	98	MP biomedical (France)
Sodium thiosulfate pentahydrate	99.9	Merck (India)

Sodium hydroxide pallets	99	Rankem (India)

Reagents	Source
Alkalinity	Palintest (UK)
Ammonia	Palintest (UK)
Chloride ion	Palintest (UK)
Colour	Palintest (UK)
COD	Hach (USA)
Nitrate ion	Palintest (UK)
Phenols	Palintest (UK)
DPD-4	Palintest (UK)

2.3. Analytical methods

2.3.1. Measurement of NPX, DCF, and RNT concentration

For quantitative analysis of NPX, DCF, and RNT, 5 cm^3 of the sample was withdrawn from the reactor and quenched with bubbling nitrogen gas to remove the residual ozone. Samples were filtered by a 0.2 μm syringe filter. Then, the sample was analyzed in the high-pressure liquid chromatograph-UV (HPLC-UV) (make: LC-20AD, model: Shimadzu, country: Japan), equipped with a C18 column (make: Agilent, model: XDB C18, country: USA). The dimensions of the column were 5 mm × 4.6 mm × 250 mm. Sample injection volume was kept at 20 mm^3. Analysis was performed in the isocratic elution mode. All experiments were replicated at least three times. Analysis conditions for NPX, DCF, and RNT are given in Table 2.2. The detection limits for NPX, DCF, and RNT were 2.2×10^{-5}, 5.0×10^{-5}, and 5.6×10^{-5},

respectively. Figures 2.2a, 2.2b, and 2.2c show the HPLC peaks for NPX, DCF, and RNT, respectively.

Table 2.2. Operating conditions for HPLC analysis

Compound	HPLC analysis conditions				
	Mobile phase	**Flow rate (cm^3 s^{-1})**	**Ratio**	**Wavelength (nm)**	**Retention time (min)**
NPX	aqueous solution of 1% acetic acid and acetonitrile	1.2	50:50	260	8.574
DCF	aqueous solution of 1% acetic acid and acetonitrile	1.0	30:70	276	5.024
RNT	100 mM ammonium acetate and methanol	1.0	35:65	322	3.16

This Figure is ommited due to copyright issue

Figures 2.2. HPLC peaks for (a). NPX, (b). DCF, and (c). RNT.

2.3.2. Characterization of real pharmaceutical effluents

Both pharmaceutical effluents were qualitatively analyzed by HR-LCMS at the Sophisticated Analytical Instrument Facility (SAIF) of IIT Bombay (India). The separation of the

pharmaceuticals was achieved by the HPLC using an analytical C18 column (100 mm × 2.1 mm × 3 μm) (make: Thermo Fisher Scientific, model: Hypersil, country: USA). The details of the mobile phase composition and the gradient method are given in Table 2.3. In the mass spectrophotometer (make: Agilent Technologies, model: G6550A; country: USA), the capillary voltage applied was 3500 V, the gas flow rate was 13 dm^3 min^{-1} (at 523 K), the sheath gas flow rate was 11 dm^3 min^{-1} (at 573 K), the nebulizer pressure was 2.4 bar, and the nozzle voltage was 1000 V.

Table 2.3. Details of the mobile phase composition, and the gradient method of flow

Time (min)	**1% formic acid in water (Flowrate %)**	**90% acetonitrile + 10% H_2O + 0.1% formic acid (Flowrate %)**	**Flow rate (cm^3 min^{-1})**	**Pressure (MPa)**
1.0	95	5	0.3	120
20.0	0	100	0.3	120
25.0	0	100	0.3	120
26.0	95	5	0.3	120
30.0	95	5	0.3	120

The properties of the raw wastewater were measured by a photometer (make: Palintest, model: 7100, country: UK).

For the chloride test, the samples were acidified to avoid interference from the reducing and complexing agents. Then, a reagent containing silver nitrate was added, and the chloride present in the sample reacted with it forming a turbid dispersion of silver chloride. The turbidity thus developed, was measured in terms of the chloride concentration. The samples were filtered through a glass fiber filter for color intensity measurement to remove the suspended solids. In

the ammonia test, it reacted with salicylate and gave a green–blue color due to the formation of indophenol in the presence of chlorine. Phenol and phenol substitutes gave red color by reacting with 4-amino-antipyrine. Before analysis, the sample was neutralized to prevent hindrance of the metal ions. A photometer measured the intensity of the red color.

2.3.3. Measurement of COD, BOD, TOC, and dissolved ozone

The properties of the raw wastewater were measured by a photometer (make: Palintest, model: 7100, country: UK). The samples were filtered with Whatman filter paper (Grade 1, pore size: 0.45 μm) for the COD analysis and diluted with Milli Q water. The COD reagents were added carefully in the COD vials and digested for 2 h in the COD digester (make: Velp Scientifica, model: ECO 25, country: India) at 423 K. Then, the digested samples were kept at room temperature to cool, and the COD was measured. BOD (biological oxygen demand) of effluent was measured by the respirometric method [206]. A known amount of wastewater and inocula were used in 0.3 dm^3 bottles.

The TOC studies were carried out using a TOC (make: O. I. Analytical, model: Aurora 1030, country: USA) analyzer equipped with a non-dispersive infrared (NDIR) detector according to the procedure described in the literature [207]. To convert the total inorganic carbon (TIC) in the sample to CO_2, it was acidified with phosphoric acid (5 % v/v) and sparged. The TIC-free sample was next oxidized with heated sodium persulfate (10% v/v, 373 K), where the organic compounds were oxidized and the carbon was converted into CO_2. The NDIR detector then evaluated and quantified it. The instrument displays the carbon content present in the sample as TOC content in mg dm^{-3}.

A photometer was used to quantify the concentration of dissolved ozone in the reactor using an ozone-specific reagent DPD (diethyl-p-phenylenediamine). As per standard procedure [208], the measurements were taken shortly after the samples were collected. The colorimeter

measured dissolved ozone levels in the range of 0–10 mg dm^{-3}. Higher dissolved ozone concentrations required adequate dilutions using Milli-Q water, as per the colorimeter supplier's guideline.

2.3.4. Identification of intermeddles for NPX, DCF, and RNT ozonation

The intermediates formed during NPX ozonation were identified by a liquid chromatography-mass spectrophotometer (LC–MS) (make: Waters, model: Q-Tof Premier, country: USA). The electrospray ionization source operated in negative and positive modes. The intermediates formed during NPX ozonation were scanned in the negative mode. For MS, the desolvation gas flow rate, cone gas flow rate, capillary voltage, desolvation temperature, and source temperature were 0.111 $dm^3\ s^{-1}$, 0.0139 $dm^3\ s^{-1}$, 2.45 kV, 623 K, and 358 K, respectively. The sample injector volume was set at 20 mm^3.

Intermediates formed during DCF and RNT were analyzed using a mass spectrophotometer in positive mode (make: Agilent Technologies, model: G6550A; country: USA) established in SAIF IIT Bombay. The parameters for source and scan source are already mentioned in Sec 2.3.2.

2.3.5. Toxicity analysis

The toxicity of effluent before and after treatment was measured by the well test with *E. coli* and *S. Aureus*. Effluent pH was kept neutral with the help of Naand HCl. Nutrient broth was prepared with beef extract (10 g dm^{-3}), peptone (10 g dm^{-3}), and NaCl (5 g dm^{-3}) for *E. coli* growth. The concentration of *E. coli* was 10^8 cfu cm^{-3} and it was placed in Mueller-Hilton agar (MHA) [209]. Sample was collected after the ozonation for the assessment of toxicity. Sterile discs were prepared with inoculated MHA to be impregnated of 20 μdm^{-3} sample. Then, the

plates were kept in incubation for 24 h at 310 K [210]. The zones of inhibition were formed due to toxicity.

2.4. Experimental methods

Ozonation of NPX, DCF, RNT and real effluents were carried out in 1 dm^3 glass reactor equipped with a sparger of pore size of 40 µm that was capable of generating fine bubbles [211]. The reaction time was 10 – 120 min that varied with the target drug, ozonation system, and the pH. The pH of the aqueous solutions varied from 4 to 11. Three different ozone supply rates (0.42–0.78 mg s^{-1}) were applied for ozonation. The samples were withdrawn after a certain time, depending on the ozone supply rate. All the experiments were repeated 3 – 4 times to ensure their repeatability. The experiments were carried out at room temperature (i.e., 298 K).

In case of hybrid process treatment of real effluents, adsorption was performed. The ozonated water was further treated by activated carbon in a glass column (length: 15 cm, diameter: 2 cm) for pH range of 5–11.

Notations

Abbreviations

BOD	Biological oxygen demand
COD	Chemical oxygen demand
DCF	Diclofenac
DPD	Diethyl-p-phenylenediamine
FESEM	Field emission scanning electron microscope
HPLC	High-performance liquid chromatography
HR-LCMS	High-resolution liquid chromatograph-mass spectrometer
IIT	Indian institute of technology
LC-MS	Liquid chromatograph mass spectrometer
NDIR	Non-dispersive infrared
NPX	Naproxen
RNT	Ranitidine
SAIF	Sophisticated analytical instrument facility
TOC	Total organic carbon
UV	Ultra-violet

CHAPTER III

OZONE MICROBUBBLE-AIDED INTENSIFICATION OF DEGRADTION OF NAPROXEN IN A PLANT PROTOTYPE: KINETICS AND MASS TRASNFER

[1] S. Patel, S. K. Majumder, P. Ghosh, P. Das, Ozone microbubble-aided intensification of degradation of naproxen in a plant prototype, J. Environ. Chem. Eng. (2019), 7 (3), 103102. DOI: 10.1016/j.jece.2019.103102.

[2] S. Patel, R. Agarwal, S. K. Majumder, P. Ghosh, P. Das, Kinetics of ozonation and mass transfer of pharmaceuticals degraded by ozone fine bubbles in a plant prototype, Heat and Mass Trans. (2019), 56, 385-397. DOI: 10.1007/s00231-019-02718-7.

CHAPTER III

Ozone Microbubble-aided Intensification of Degradation of NPX in a Plant Prototype: Kinetic and Mass Transfer Studies

This chapter contains the study of naproxen (NPX) removal by a combination of ozone and hydrogen peroxide in a microbubble system. The effects of different parameters such as system pH, ozone supply rate, and H_2O_2 doses have been studied thoroughly. Gas to liquid mass transfer of ozone was also studied and a model was also developed for the same. The Hatta number was calculated for various operational parameters to assess the mass transfer of ozone. The metabolites generated were identified along with their path of formation. The pseudo-first-order reaction constants were also computed for the ozonation of NPX at different pH and ozone supply rates.

3.1. Introduction

NPX is a nonsteroidal anti-inflammatory medicine (NSAID) that works by decreasing hormones in the body that induce inflammation and pain. NPX is a pain reliever used to treat illnesses like arthritis, tendinitis, ankylosing spondylitis, bursitis, and menstrual cramps. Traces of NPX have been found in the water bodies due to extensive use of it as a pain reliever. The inefficiency of conventional treatment methods and toxicity of metabolites generated during oxidation have been reported in previous studies [174,212,213].

The primary objective of this study was to investigate the degradation of NPX using a combination ozone and hydrogen peroxide. This work focuses on the complete removal of NPX under different operation variables, and the intermediates generated during the process. Furthermore, the kinetic parameters, mass transfer for ozonation, and degradation pathway have been investigated. The results have demonstrated that the combination of O_3 and H_2O_2 was an effective treatment technique for NPX removal.

3.2. Results and Discussion

3.2.1. Hydrodynamics characteristics of the microbubble

A photographic technique was used for measuring the size of the microbubbles. The images of the microbubbles were captured by a digital camera (D5300 24 MP, Nikon, India) in an illuminating field created by a halogen lamp (500 W). The camera was positioned at a distance of 0.5 m from the reactor wall. To obtain clear images, the background was set black. The captured images were enhanced and analyzed by an image processing software (Digimizer version: 4.2, MedCalc Software, Belgium). The boundaries of the microbubbles were clearly marked, avoiding their overlap. The size distribution was calculated by analyzing 300 – 500 microbubbles at each flow rate. For each flowrate, 4 – 6 images were captured and the images having the best quality were chosen for the analysis. A typical size analysis of the microbubbles is shown in Figure 3.1. The Sauter mean bubble diameter (d_{32}) can be expressed as

$$d_{32} = \frac{\sum_{i=1}^{n} n_i d_{bi}^3}{\sum_{i=1}^{n} n_i d_{bi}^2} \qquad (3.1)$$

This Figure is ommited due to copyright issue

Figure 3.1. A typical example of image analysis for measuring the size of the microbubbles.

The size range of the microbubbles was 0.44 – 1.06 mm and the Sauter mean diameter was found to be 0.63 mm. The size distribution of the microbubbles is shown in Figure 3.2, which was fitted by the log-normal distribution, given by

$$f_n(d_b) = \alpha + \frac{\beta}{d_b \delta \sqrt{2\pi}} \exp\left[-\frac{\{\ln(d_b / \gamma)\}^2}{2\delta^2} \right] \tag{3.2}$$

where f_n is the distribution density function, and α, β, γ, and δ are the parameters of the log-normal distribution, which are functions of the superficial gas velocity (u_g). As per the

$$\alpha = 0.015 - 1.78u_g \tag{3.3}$$

$$\beta = 2.04 \exp(-155.79u_g) \tag{3.4}$$

$$\gamma = 0.046 \exp(1318.22u_g) \tag{3.5}$$

$$\delta = 0.13 - 31.16u_g \tag{3.6}$$

This Figure is ommited due to copyright issue

Figure 3.2. Size distributions of the microbubbles at different superficial gas velocities at pH 4.

The pressure drop across the reactor was determined by using Equation (3.7), given below.

$$\Delta P = \rho_m g H_m (1 - \varepsilon_g) \tag{3.7}$$

The effect of gas flow rate on the gas holdup in the reactor is shown in Figure 3.3. The gas holdup increased almost linearly with the increasing gas flow rate from 0.02 to 0.08 $dm^3\ s^{-1}$. The maximum average gas holdup (i.e., 0.4) was attained at the maximum gas flow rate of 0.08 $dm^3\ s^{-1}$. The pressure drop, calculated from Equation (3.7) was 588 Pa. Pressure drop and gas hold up have significant effects on the bubble size, and play important roles in mass transfer. A higher pressure drop can lead to the formation of larger bubbles, which would affect the interfacial area and rate of mass transfer of ozone. As the volume of the aqueous phase in the bubble column was increased, the holdup also increased. Superficial gas velocity and gas holdup can be related by Equation (3.8), given below.

$$\varepsilon_g = a u_g^b \tag{3.8}$$

Using the experimental data, the correlations for the coefficients *a* and *b* are as follows:

$$a = 1.13\times10^3 - 1.12\times10^3 V \tag{3.9}$$

$$b = 1.93 - 0.55V \tag{3.10}$$

where *V* is the initial volume of liquid in the reactor.

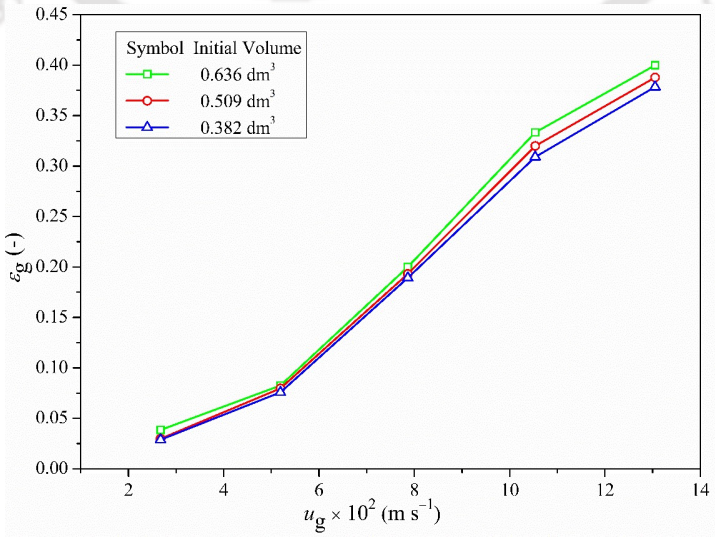

Figure 3.3. Effect of superficial gas velocity on gas holdup at different initial volumes of the liquid.

The FESEM (JSM-7610F, Jeol, Japan) images of the sparger (S4, Oz-Air, India) surface and pore are shown in Figures 3.4a and 3.4b, respectively. The pore size of the sparger was 40 μm (specified by the manufacturer). It was resistant to ozone. It was observed that the pores were distributed non-uniformly throughout the sparger surface.

Figure 3.4. FESEM images of (a) sparger surface, (b) pore, and (c) sparger.

3.2.2. Mass transfer studies

The concentration of ozone dissolved in water increased with time and became constant, corresponding to the steady-state concentration of ozone dissolved in water, c_{ss} at $t \to \infty$. The steady-state concentration was reached when the solute concentrations in the gas and the liquid were constant. For the determination of the volumetric mass transfer coefficient of ozone, two phenomena are important, i.e., the mass transfer of the gaseous ozone into the aqueous phase and the rate of self-decomposition of ozone absorbed into the solution. Many researchers have reported that the decomposition of ozone in water is a function of pH and temperature, which follows a first-order reaction rate [214,215]. When ozone in the gas phase was absorbed in water and it simultaneously underwent decomposition reaction in a completely mixed semi-batch reactor, the mass balance equation can be written as:

$$\frac{dc_{O_3}}{dt} = k_L a\left(c^*_{O_3} - c_{O_3}\right) - k_D c_{O_3} \tag{3.11}$$

The diffusivity of ozone in gas was much larger than that in water, so the resistance to mass transfer in the gas phase is negligible, compared to that in the liquid phase. The equilibrium concentration of ozone in water can be calculated from the following equation.

$$c_{ss} = \left(\frac{k_L a}{k_L a + k_D} \right) c^*_{O_3} \tag{3.12}$$

The solubility of ozone in water was several times higher than that of oxygen (i.e., the mole fraction solubility of oxygen in water is 2.3×10^{-5} and the same for ozone is 9.1×10^{-5} at 298 K and atmospheric pressure). Therefore, when a mixture of ozone and oxygen was passed into water in the form of microbubbles, ozone preferentially dissolves in water. The concentration of ozone in the aqueous phase can be described by Henry's law: $p = Hc$. Henry's law constant, H, depends on pH and temperature. The equilibrium concentration of ozone in the aqueous phase is given by [214]

$$c^*_{O_3} = \left(\frac{\rho RT}{M} \right) \frac{c_G}{H} \tag{3.13}$$

The Henry's law constant, H, depends on pH and temperature, which is given by [214]

$$H = 3.84\times10^7 c_{OH^-}^{0.035} \exp\left(\frac{-2428}{T} \right) \tag{3.14}$$

From Equations. (3.11) and (3.12), the mass balance Equation for ozone can be written as

$$\frac{dc_{O_3}}{dt} = \left(k_L a + k_D \right) \left(c_{ss} - c_{O_3} \right) \tag{3.15}$$

Integration of Equation (3.15) with the boundary condition, at $t = 0$, $C_{O_3} = 0$, yields

$$ln\left(\frac{c_{ss}}{c_{ss} - c_{O_3}} \right) = \left(k_L a + k_D \right) t \tag{3.16}$$

The concentration of ozone in water increases with time and attains equilibrium after a certain time. A plot of $\ln\left(c_{ss}/(c_{ss}-c_{O_3})\right)$ versus t, gives a straight line with a slope of $k_La + k_D$. The value of k_D at different pH can be calculated from the correlation suggested by previous study [216,217]. The volumetric mass transfer coefficients can be calculated by subtracting the k_D from the value of slope for all pH and ozone generation rates.

3.2.3. Determination of rate constant for ozonation of pharmaceutical drug

The rate Equation for the oxidation of pharmaceutical drug with ozone can be expressed by

$$\frac{d[PH]}{dt} = -k[PH]c_{O_3} \tag{3.17}$$

Ozone dissolution in water undergoing a self-decomposition process is first-order in nature. The self-decomposition of ozone depends on pH, temperature and ionic strength [218]. Ozone decomposition is initiated either thermally (in acidic media) or by the hydroxyl ion, OH^- (in alkaline media). The diffusivity of ozone in the gas phase is much higher than that in water. Therefore, the resistance to mass transfer in the gas phase is negligible as compared to the aqueous phase. Incorporating the ozone decomposition and the rate of mass transfer of ozone, the mass balance Equation of ozone can be written as

$$\frac{d[O_3]}{dt} = k_L a\left(c^*_{O_3} - c_{O_3}\right) - k_D c_{O_3} - k[PH]c_{O_3} \tag{3.18}$$

Equations (3.17) and (3.18) are simultaneously solved by the Runge-Kutta fourth-order method to obtain the best-fit values of k_la and k based on the concentration profiles of pharmaceuticals and ozone in the reactor. The direct reaction of ozone with a compound pharmaceutical is expressed as

$$PH + aO_3 \rightarrow \text{Products} \tag{3.19}$$

Here *a* is the stoichiometric coefficient representing the ozone molecule consumed per molecule of pharmaceutical transformed to products. The stoichiometric coefficient allows the establishment of the kinetic regime of ozone absorption when ozone undergoes fast reactions in water. Equation (3.19) represents a general reaction where the by-products have been omitted from the series-parallel reactions of the ozonation. The rate Equation of the reaction can be written as

$$-\frac{d[\mathrm{PH}]}{dt} = k[\mathrm{PH}]c_{\mathrm{O_3}} \tag{3.20}$$

$$-\frac{1}{a}\frac{d[\mathrm{O_3}]}{dt} = k[\mathrm{PH}]c_{\mathrm{O_3}} \tag{3.21}$$

In order to obtain the reaction rate constant (k), the denominated absolute rate constant method under pseudo-first-order conditions was used. According to the method, the concentration profile of a pseudo-first-order reaction performed with excess drug or oxidant in a batch reactor can be expressed as

$$\ln\left(\frac{[\mathrm{PH}]_0}{[\mathrm{PH}]}\right) = k_{\mathrm{app}}t \tag{3.22}$$

A plot of $\ln([\mathrm{PH}]_o / [\mathrm{PH}])$ versus t gives a straight line with a slope of k_{app}. The reaction rate constant of ozonation was then calculated by

$$k_{\mathrm{O_3}} = \frac{k_{\mathrm{app}}}{c_{\mathrm{O_3}0}} \tag{3.23}$$

If neither compound is in excess, the Equation (3.21) can be written as

$$\ln\left(\frac{[\mathrm{PH}]_0}{[\mathrm{PH}]}\right) = k\int C_{\mathrm{O_3}}dt \tag{3.24}$$

A plot of $\ln([\mathrm{PH}]_0/[\mathrm{PH}])$ versus $\int C_{O_3} dt$ represents a straight line with a slope of k.

3.2.4. Axial concentration of ozone in liquid

To observe the concentration profile of ozone in aqueous phase, the axial dispersion model derived by Wang [219] was used. The final form of model equation based on basic mole balance at steady-state operation is given by:

$$\frac{d^2c_G}{dz^2}+\frac{d\left(c_G\mathrm{Pe}_G\right)}{dz}-\mathrm{Pe}_G\xi\phi\varphi_1 c_G+\mathrm{Pe}_G\xi\phi c_L=0 \tag{3.25}$$

$$\frac{d^2c_L}{dz^2}+\mathrm{Pe}_L\frac{dc_L}{dz}+\mathrm{Pe}_L\zeta\phi c_G-\mathrm{Pe}_L\left(\zeta\phi\varphi_2+\mathrm{Da}\right)c_L=0 \tag{3.26}$$

where Pe_G, Pe_L, ξ, ζ, C_G, C_L, Da, and z are dimensionless parameters which are defined by

$$\mathrm{Pe}_G=\frac{Q_GL^2}{V_{Gb}D_{eG}},\ \mathrm{Pe}_L=\frac{Q_LL^2}{V_{Lb}D_{eL}},\ \xi=\frac{RTVa_ik_L}{HQ_G},\ \zeta=\frac{Va_ik_L}{Q_L},\ c_G=\frac{p_b}{p_\alpha},\ c_L=\frac{HC_b}{p_\alpha},\ \mathrm{Da}=\frac{V_{Lb}k}{Q_L},$$

$$z=1-\frac{y}{L}$$

Other parameters are defined by

$$\varphi_1=\cosh(\mathrm{Ha}) \tag{3.27}$$

$$\varphi_2=\lambda Ha\sinh(\mathrm{Ha})+\cosh(\mathrm{Ha}) \tag{3.28}$$

$$\phi=\left(\lambda\cosh\left(\mathrm{Ha}\right)+\sinh\left(\mathrm{Ha}\right)/\mathrm{Ha}\right)^{-1} \tag{3.29}$$

The Hatta number for the first-order reaction is given by

$$\mathrm{Ha}=\frac{\left(k_{\mathrm{app}}D_{O_3}\right)^{1/2}}{k_L} \tag{3.30}$$

Damkohler number Da is related to Hatta number as $\mathrm{Da} = \mathrm{Ha}^2 / \gamma$. The parameters λ and γ are defined by $\lambda = RTk_L /(Hk_G)$ and $\gamma = \delta_L^2 Q_L /(D_L V_{Lb})$.

For the calculation of Hatta number, the value of k_L= 3×10^{-4} m s^{-1} [217,220] and D_{O_3} = 1.3×10^{-9} m^2 s^{-1} [217] were used. As can be seen, *Ha* is always lower than 0.3, which means the ozone reactions are slow. The usual Danckwerts boundary conditions were used to integrate the differential equations (Equations (3.25) and (3.26)). The boundary conditions are:

$$\text{z} = 0;\ \frac{dc_G}{dz} = \frac{dc_L}{dz} = 0$$

$$\text{z} = 1;\ c_G = 1 - \frac{1}{\mathrm{Pe}_G}\frac{dc_G}{dz},\ c_L = -\frac{1}{\mathrm{Pe}_L}\frac{dc_L}{dz} \tag{3.31}$$

The boundary-value problem (Equations (3.25) and (3.26) with Equation (3.31)) was solved analytically by means of the eigenvalues of the differential equations. From Equation (3.25):

$$c_L = \varphi_1 c_G - \frac{1}{\xi\varphi}\frac{dc_G}{dz} - \frac{1}{\xi\varphi\mathrm{Pe}_G}\frac{d^2c_G}{dz^2} \tag{3.32}$$

From Equations. (3.32) and (3.26)

$$\begin{aligned}&\frac{d^4c_G}{dz^4}\left(\frac{1}{\xi\varphi\mathrm{Pe}_G}\right) + \frac{d^3c_G}{dz^3}\left(\frac{1}{\xi\varphi} + \frac{\mathrm{Pe}_L}{\xi\varphi\mathrm{Pe}_G}\right) + \frac{d^2c_G}{dz^2}\left\{\varphi_1 + \frac{\mathrm{Pe}_L}{\xi\varphi} + \frac{\mathrm{Pe}_L}{\xi\varphi\mathrm{Pe}_G}\left(\zeta\varphi\varphi_2 + \mathrm{Da}\right)\right\} + \\ &\frac{dc_G}{dz}\left\{\frac{1}{\xi\varphi} - \mathrm{Pe}_L\varphi_1 + \frac{\mathrm{Pe}_L}{\xi\varphi}\left(\zeta\varphi\varphi_2 + \mathrm{Da}\right)\right\} - c_G\left(\mathrm{Pe}_L\zeta\varphi + \mathrm{Pe}_L\zeta\varphi\varphi_1\varphi_2 + \varphi_1\mathrm{DaPe}_L\right) = 0\end{aligned} \tag{3.33}$$

It is a linear, homogeneous, constant-coefficient ordinary differential equation, which can be solved by characteristics equation:

$$\frac{d^4c_G}{dz^4}+\frac{d^3c_G}{dz^3}\left(\mathrm{Pe}_G+\mathrm{Pe}_L\right)+\frac{d^2c_G}{dz^2}\left\{\xi\varphi\varphi_1+\mathrm{Pe}_G\mathrm{Pe}_L+\mathrm{Pe}_L\left(\zeta\varphi\varphi_2+\mathrm{Da}\right)\right\}+$$
$$\frac{dc_G}{dz}\left\{\mathrm{Pe}_G-\mathrm{Pe}_G\mathrm{Pe}_L\xi\varphi\varphi_1+\mathrm{Pe}_G\mathrm{Pe}_L\left(\zeta\varphi\varphi_2+\mathrm{Da}\right)\right\}- \quad (3.34)$$
$$c_G\left(\mathrm{Pe}_G\mathrm{Pe}_L\xi\zeta\varphi^2+\mathrm{Pe}_G\mathrm{Pe}_L\xi\zeta\varphi^2\varphi_1\varphi_2+\xi\varphi\varphi_1\mathrm{DaPe}_G\mathrm{Pe}_L\right)=0$$

From Equation (3.34)

$$s^4+s^3\left(\mathrm{Pe}_G+\mathrm{Pe}_L\right)+s^2\left\{\xi\varphi\varphi_1+\mathrm{Pe}_G\mathrm{Pe}_L+\mathrm{Pe}_L\left(\zeta\varphi\varphi_2+\mathrm{Da}\right)\right\}+$$
$$s\left\{\mathrm{Pe}_G-\mathrm{Pe}_G\mathrm{Pe}_L\xi\varphi\varphi_1+\mathrm{Pe}_G\mathrm{Pe}_L\left(\zeta\varphi\varphi_2+\mathrm{Da}\right)\right\}- \quad (3.35)$$
$$\left(\mathrm{Pe}_G\mathrm{Pe}_L\xi\zeta\varphi^2+\mathrm{Pe}_G\mathrm{Pe}_L\xi\zeta\varphi^2\varphi_1\varphi_2+\xi\varphi\varphi_1\mathrm{DaPe}_G\mathrm{Pe}_L\right)=0$$

The simplified Eigen Equation for the differential Equations (3.25) and (3.26) can be written as:

$$\left(s^2+\mathrm{Pe}_Gs-\mathrm{Pe}_G\xi\phi\varphi_1\right)\left\{s^2+\mathrm{Pe}_Ls-\mathrm{Pe}_L\left(\zeta\phi\varphi_2+\mathrm{Da}\right)\right\}-\mathrm{Pe}_G\mathrm{Pe}_L\xi\zeta\phi^2=0 \quad (3.36)$$

which has four real roots s_1, s_2, s_3 and s_4. Hence, they obtained general solutions as follows:

$$C_G=A_1e^{s_1z}+A_2e^{s_2z}+A_3e^{s_3z}+A_4e^{s_4z} \quad (3.37)$$

$$C_L=A_1\beta_1e^{s_1z}+A_2\beta_2e^{s_2z}+A_3\beta_3e^{s_3z}+A_4\beta_4e^{s_4z} \quad (3.38)$$

where $\beta_i=\dfrac{s_i^2+\mathrm{Pe}_Gs_i-\mathrm{Pe}_G\xi\phi\varphi_1-\mathrm{Pe}_L\zeta\phi}{s_i^2+\mathrm{Pe}_Ls_i-\mathrm{Pe}_G\xi\phi-\mathrm{Pe}_L(\zeta\phi\varphi_2+\mathrm{Da})}$ (i = 1, 2, 3, 4) (3.39)

A linear Equation system can be represented by using the boundary conditions (Equation (3.31)). The four integration constants A_i are calculated by solving the Equations for the co-current flow as:

$$\begin{bmatrix} s_1 & s_2 & s_3 & s_4 \\ s_1\beta_1 & s_2\beta_2 & s_3\beta_3 & s_4\beta_4 \\ e^{s_1}\left(1+\frac{s_1}{\mathrm{Pe}_G}\right) & e^{s_2}\left(1+\frac{s_2}{\mathrm{Pe}_G}\right) & e^{s_3}\left(1+\frac{s_3}{\mathrm{Pe}_G}\right) & e^{s_4}\left(1+\frac{s_4}{\mathrm{Pe}_G}\right) \\ e^{s_1}\beta_1\left(1+\frac{s_1}{\mathrm{Pe}_L}\right) & e^{s_2}\beta_2\left(1+\frac{s_2}{\mathrm{Pe}_L}\right) & e^{s_3}\beta_3\left(1+\frac{s_3}{\mathrm{Pe}_L}\right) & e^{s_4}\beta_4\left(1+\frac{s_4}{\mathrm{Pe}_L}\right) \end{bmatrix} \begin{bmatrix} A_1 \\ A_2 \\ A_3 \\ A_4 \end{bmatrix} = \begin{bmatrix} 0 \\ 0 \\ 1 \\ 0 \end{bmatrix} \quad (3.40)$$

3.2.5. Ozone concentration profile in bulk liquid and mass transfer coefficient

Typical model parameters and constants those were used to calculate the ozone concentration profile are shown in Table 3.2.

Table 3.2. Typical model parameters and constants

Variable	Value
Ha	0.000116
ξ	2
ζ	6
λ	0.01
γ	0.003
r	1

After solving the equations, the parameters obtained as per the present experimental condition at *H*a = 0.000116 are shown in Table 3.3.

Table 3.3. Calculated values of other parameters which are used in various Equations at *H*a = 0.000116

Variable	Calculated value	Variable	Calculated value
ϕ_1	1	β_1	0.0039
ϕ_2	1	β_2	6.1693
ϕ	1	β_3	0.1353
Da	0.0003	β_4	0.9999
s_1	−104.4081	A_1	0.0009
s_2	−39.4393	A_2	0
s_3	3.8473	A_3	0.024
s_4	0.0002	A_4	0.1665

By using these calculated parameters, one can obtain the ozone concentration profile in the aqueous phase as a function of reactor coordinate (z) according to the Equation (3.41)

$$C_L = 3.52\times10^{-6} e^{-104.4081z} + 3.24\times10^{-3} e^{3.8473z} - 0.17e^{0.0002z} \quad (3.41)$$

The plot of $\ln(C_{ss}/(C_{ss}-C_L))$ versus t, gives a straight line with a slope of $k_La + k_D$ according to the Equation (3.22). The value of the first-order decomposition rate constant of ozone, k_D at pH 5 is 2.33×10^{-4} s^{-1} from [217]. From the values of slope, the mass transfer coefficient was obtained. It was seen that the mass transfer coefficient varied with ozone flowrate at different pH as shown in Figure 3.5 for NPX. The mass transfer coefficients at different ozone flowrates, at different Hatta numbers and different pH for various pharmaceutical drugs are shown in Table 3.4.

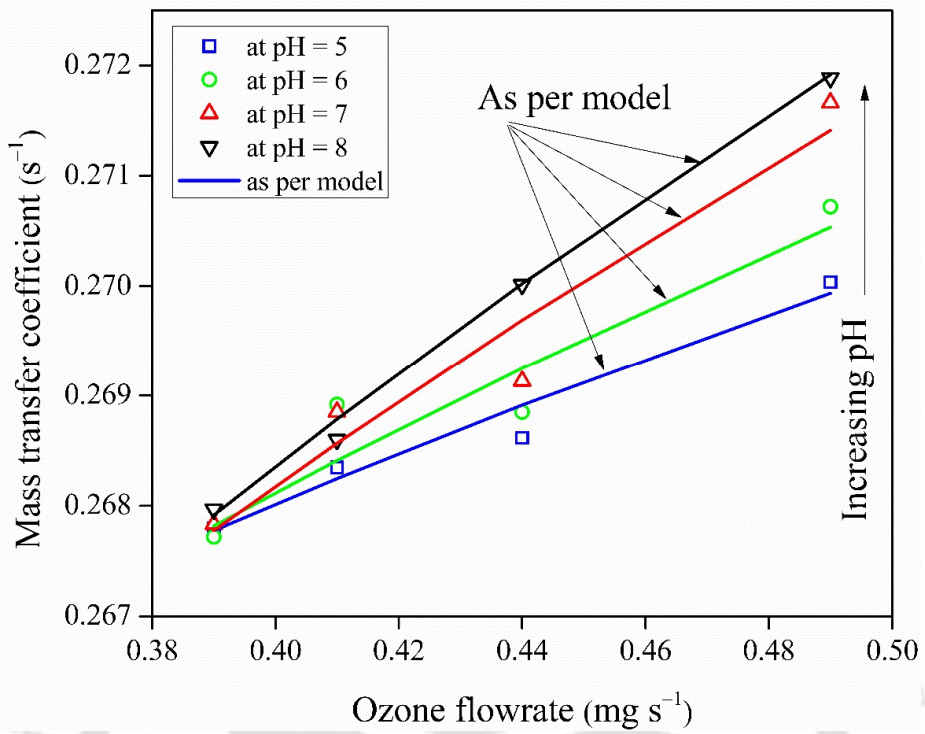

Figure 3.5. Variation of volumetric mass transfer coefficient with ozone flowrate at different pH values in case of NPX.

Table 3.4. The mass transfer coefficient for NPX at different pH and at ozone flowrate 0.39 mg s^{-1} and H_2O_2 = 0.0012 dm^3

Pharmaceutical drugs	**Ozone flowrate (mg s^{-1})**	**pH value**	**$k_{app}\times10^3$ (s^{-1})**	**Ha$\times10^4$ (-)**	**k_La (s^{-1})**
NPX	0.39	5	0.056	1.161	0.26780
		6	0.099	1.544	0.26772
		7	0.165	1.993	0.26783
		8	0.231	2.358	0.26737

	0.42	5	1.100	5.146	0.26835
		6	1.935	6.825	0.26892
		7	3.218	8.802	0.26885
		8	4.502	10.411	0.26849
	0.44	5	1.818	6.616	0.26862
		6	3.198	8.774	0.26885
		7	5.319	11.316	0.26913
		8	7.440	13.383	0.26892
	0.48	5	11.368	16.543	0.27004
		6	19.995	21.940	0.27072
		7	33.257	28.295	0.27166
		8	46.520	33.465	0.27189
CBZ	0.39	5	0.472	26.099	0.03877
IBP	0.39	5	1.070	39.314	0.04147
MIT	0.39	5	69.000	315.700	0.04027
RNT	0.39	5	15.050	147.441	0.04857

A general correlation is developed to predict the volumetric mass transfer coefficient at different pH which can be expressed as

$$k_L a = 0.2497\, pH^{0.0634}\, \dot{M}_{O_3}^{n} \tag{3.42}$$

where

$$n = 3.9\times10^{-3}\, pH^{1.365} \tag{3.43}$$

3.2.6. Effect of pH on NPX degradation

The ozonation of NPX was carried out at various pH (i.e. 5–9). The pH of the system was adjusted before ozonation by using HCl and Nasolutions. The degradation of NPX was highly affected by the pH of the reaction medium. For the same amount of ozone supply and retention time, the degradation was comparatively slower in the acidic medium than the alkaline medium. As shown in Figure 3.6a, for 0.39 mg s^{-1} ozone supply rate, after 100 min, the degradation achieved was 30% at pH 5, which increased to 75% at pH 9. From Figures 3.6b, 3.6c, and 3.6d, it is apparent that the degradation accelerated as the pH of the reaction medium increased.

This Figure is ommited due to copyright issue

Figure 3.6. Effect of pH on NPX degradation for different rates of ozone supply: (a) 0.39, (b) 0.41, (c) 0.44, and (d) 0.48 mg s^{-1}. $[NPX]_0$ = 50 mg dm^{-3}; T = 300 K.

In the acidic reaction system, NPX was degraded by molecular ozone, while at alkaline pH, the hydroxyl radicals played an important role in the degradation. The alkaline medium facilitated hydroxyl radical generation [221], which favored the degradation process due to their higher

oxidative power than ozone. The presence of hydroxyl radicals reduced the lifetime of ozone in the aqueous phase. Hence, higher dissociation of ozone was achieved. The initiation of ozone decomposition in the alkaline medium involves multiple steps, as follows:

$$O_3 + OH^- \rightarrow OH_2^- + O_2 \qquad k_2 = 40\ dm^3\ mol^{-1}\ s^{-1} \qquad (3.44)$$

$$O_3 + HO_2^- \rightarrow \bullet O_3^- + HO_2^\bullet \qquad k_2 = 2.2 \times 10^7\ dm^3\ mol^{-1}\ s^{-1} \qquad (3.45)$$

$$HO_2^\bullet + OH^- \Leftrightarrow O_2^- + H_2O \qquad pK = 4.8 \qquad (3.46)$$

$$O_3 + \bullet O_2^- \rightarrow \bullet O_3^- + O_2 \qquad k_2 = 1.6 \times 10^9\ dm^3\ mol^{-1}\ s^{-1} \qquad (3.47)$$

$$\bullet O^-_3 + H_2O \rightarrow HO\bullet + O_2 + OH^- \qquad k_1 = 20\text{–}30\ s^{-1} \qquad (3.48)$$

$$\bullet O_3^- + HO\bullet \rightarrow \bullet O_2^- + HO_2 \qquad k_2 = 6 \times 10^9\ dm^3\ mol^{-1}\ s^{-1} \qquad (3.49)$$

$$\bullet O_3^- + HO\bullet \rightarrow O_3 + \bullet OH^- \qquad k_2 = 2.5 \times 10^9\ dm^3\ mol^{-1}\ s^{-1} \qquad (3.50)$$

$$O_3 + HO\bullet \rightarrow O_2 + HO_2^\bullet \qquad k_2 = 3 \times 10^9\ dm^3\ mol^{-1}\ s^{-1} \qquad (3.51)$$

At basic pH, the HO• is generated by a single step only, as given by Equation (3.47). A high concentration of hydroxyl ion leads to the generation of O_2, HO_2^-, O_3^-, and HO• [221]. For pH < 7, the generation of HO• is slow, which is reflected by the low-rate constant, as given by Equation (3.48). However, the steps involved in the propagation and termination [i.e., Equations (3.49) – (3.51)] are very fast.

In the acidic medium, a different mechanism of ozone decomposition is involved, i.e. via the thermal decomposition of ozone into oxygen [222]:

$$O_3 \leftrightarrow \bullet O + O_2 \quad (3.52)$$

$$O + H_2O \rightarrow 2HO\bullet \quad (3.53)$$

An oxygen atom is formed during the decomposition, which further reacts with water to form HO•. A perhydroxyl radical is generated by the reaction of HO• with O_3.

$$HO\bullet + O_3 \rightarrow HO_2^{\bullet} + O_2 \qquad k_2 = 1.1 \times 10^8 \text{ dm}^3 \text{ mol}^{-1} \text{ s}^{-1} \quad (3.54)$$

$$HO_2^{\bullet} + O_3 \rightarrow HO\bullet + 2O_2 \qquad k_2 < 10^4 \text{ dm}^3 \text{ mol}^{-1} \text{ s}^{-1} \quad (3.55)$$

$$HO_2^{\bullet} \Leftrightarrow \bullet O_2^- + H^+ \qquad pK = 4.8 \quad (3.56)$$

In the acidic medium, the hydroxyl radicals are mainly generated by the reaction given by Equation (3.53). However, they may be generated by the propagation step [i.e., Equation (3.55)] as well.

3.2.7. Effect of ozone flow rate

High rates of ozone supply led to a drastic increase in the degradation efficiency. The ozone generation rate was varied in the range of 0.39 – 0.48 mg s^{-1} to assess the effect of ozone concentration in the reactor. For 0.39 mg s^{-1} ozone supply rate, 30 – 75% removal of the drug was recorded in 100 min for pH 5 – 9, whereas 99% removal was achieved within 10 min for 0.48 mg s^{-1} ozone supply rate for the same pH range. Therefore, it can be concluded that a small change in the ozone supply rate led to a very high removal rate as a result of the high reactivity of NPX with ozone. The degradation of NPX for different ozone supply rates is shown in Figure 3.7. It is clearly observed that the extent of NPX removal increased up to 99%

at high ozone supply rate. For example, at 0.48 mg s^{-1}, the NPX concentration was reduced to below the detectable range within 4 min. The degradation increased 1.32 – 3.3 times when the ozone supply rate was increased by 1.2 folds.

This Figure is ommited due to copyright issue

Figure 3.7. Effect of ozone supply rate on NPX degradation at different pH: (a) pH 5, (b) pH 6, (c) pH 7, (d) pH 8, and (e) pH 9. $[NPX]_0$ = 50 mg dm^{-3}; T = 300 K.

Some chromatograms obtained by the HPLC analysis at different times during the degradation of NPX are shown in Figure 3.8. The peak for pure NPX appeared at 8.5 min at t = 0 (Figure 3.8a). After 2 min of ozonation (ozone supply rate = 0.48 mg s^{-1}), two peaks appeared (i.e. at 2.25 min and 4.70 min), showing the formation of two significant degradation products. It is also seen that the intensity of the NPX peak decreased, which signifies the degradation of NPX. After 4 min of ozonation, one intermediate converted to another inasmuch as one of the peaks diminished and the other strengthened. The NPX peak disappeared after 6 min of ozonation. The chromatogram suggests the formation of two degradation intermediates, one of which converted to the other. After 10 min, only one degradation product was formed.

This Figure is ommited due to copyright issue

Figure 3.8. (a) atograms for NPX ozonation at (a) t = 0, (b) t = 2, (c) t = 4, and (d) t = 6 min. $[NPX]_0$ = 50 mg dm^{-3}; T = 300 K; ozone supply = 0.48 mg s^{-1}; pH = 7; $[H_2O_2]$ = 1.2 cm^3.

The LC–MS analysis was carried out for identifying these intermediates, discussed further in Section 3.5. For a low ozone supply rate (i.e. 0.39 mg dm^{-3}), the formation and conversion of

the degradation products were very slow comparatively. For the ozone supply rate of 0.39 mg s^{-1}, the chromatograms were analyzed for 50, 100, and 150 min of ozonation. The NPX peak was reduced after 150 min of ozonation. Both the intermediates were present after 150 min, which suggests that some more ozone was required to convert one product into another, as shown in Figure 3.9.

This Figure is ommited due to copyright issue

Figure 3.9. Chromatograms for NPX and the intermediates formed during ozonation at (a) t = 0, (b) t = 50, (c) t = 100, and (d) t = 150 min. $[NPX]_0$ = 50 mg dm^{-3}; T = 300 K; ozone supply rate = 0.39 mg s^{-1}; pH = 7; $[H_2O_2]$ = 1.2 cm^3. (d)

3.2.8. Effect of H_2O_2 on NPX degradation

In alkaline medium, the addition of H_2O_2 increased the generation of hydroxyl radicals, which influenced the degradation process significantly. In addition, it increased ozone consumption because the addition of H_2O_2 decreased the lifetime of O_3. In acidic conditions, the addition of H_2O_2 did not affect the degradation, as shown in Figure 3.10. It may be due to the low ozone dissociation and less amount of hydroxyl radicals. In pure water, ozone decomposition was initiated by the hydroxyl ions, but in the presence of H_2O_2, it was initiated by the anion $\left(OH_2^-\right)$, which has a much higher rate constant than the hydroxyl ion. To illustrate, $k_{O_3,OH_2^-} = (5.5 \pm 1.0) \times 10^6$ dm^3 mol^{-1} s^{-1} and $k_{O_3,OH^-} = 210 \pm 20$ dm^3 mol^{-1} s^{-1} for pH 6 – 11.6 [223]. At higher pH, the H_2O_2 consumption increased by 10 folds for every increase in pH by unity. This increased the generation of HO• rapidly, which accounts for the higher degradation efficiency after the addition of H_2O_2 in the alkaline medium.

This Figure is ommited due to copyright issue

Figure 3.10. Effect of H_2O_2 on NPX degradation at different pH: (a) pH 5, (b) pH 6, (c) pH 7, (d) pH 8, and (e) pH 9. $[NPX]_0$ = 50 mg dm^{-3}; T = 300 K; ozone supply rate = 0.39 mg s^{-1}; $[H_2O_2]$ = 1.2 cm^3.

The mechanism of ozone dissociation by OH_2^- is as follows:

$$H_2O_2 \Leftrightarrow HO_2^- + H^+ \qquad pK = 11.6 \qquad (3.57)$$

$$O_3 + HO_2^- \rightarrow HO\bullet + \bullet O_2^- + O_2 \qquad k_{O_3,OH_2^-} = (5.5 \pm 1.0) \times 10^6 \text{ dm}^3 \text{ mol}^{-1} \text{ s}^{-1} \qquad (3.58)$$

3.2.9. Kinetics of ozonation

The rate constant for ozonation of NPX was determined for the semi-batch operation, in which ozone was continuously supplied to the reactor. The ozone concentration with respect to time was found to be constant due to its continuous supply to the reactor and consumption. The concentration of NPX was much higher than that of ozone. The kinetics of the bimolecular reaction between ozone and NPX can be written as

$$\frac{d[NPX]}{dt} = -k_{o_3}[O_3][NPX] \qquad (3.59)$$

It can be considered as a pseudo-first-order reaction [224], i.e.

$$\ln\left[\frac{[NPX]_0}{[NPX]}\right] = k_{app}t \qquad (3.60)$$

where k_{app} is the apparent rate constant, given by $k_{app} = k_{O_3}[O_3]$. It was calculated from the slope of the plot between $\ln\left[\frac{[NPX]_0}{[NPX]}\right]$ and t as shown in Figure 3.11.

This Figure is ommited due to copyright issue

Figure 3.11. Plot of $\ln\left[\frac{[NPX]_0}{[NPX]}\right]$ versus t for the calculation of k_{app}. $[NPX]_0$ = 50 mg dm^{-3}; T = 300 K; ozone supply rate = 0.39 mg s^{-1}; $[H_2O_2]$ = 1.2 cm^3.

This Figure is ommited due to copyright issue

Figure 3.12. Effect of pH and ozone supply rate on the pseudo-first-order rate constant, k_{app}.

For higher ozone supply rates (i.e., > 0.55 mg s^{-1}), the ozone concentration did not remain constant. So, the reaction cannot be considered as pseudo-first-order for these systems. k_{app} increased with increasing ozone supply rate and pH (see Figure 3.12). The values of the reaction rate constant for different pH and ozone supply rate are summarized in Table 3.5.

Table 3.5. Values of k_{app} for different pH and ozone supply rate with $[NPX]_0$ = 50 mg dm^{-3}

Ozone supply rate	**pH**				
(mg s^{-1})	**5**	**6**	**7**	**8**	**9**
0.39	0.0034	0.0064	0.0098	0.0115	0.0131
0.41	0.0203	0.0224	0.0318	0.0484	0.0536
0.44	0.058	0.069	0.106	0.133	0.199

0.48	0.109	0.243	0.342	0.442	0.677

In alkaline medium, degradation of NPX takes place by the reaction with hydroxyl radicals. It is mentioned in Section 3.2.6, that alkaline medium favors the degradation of NPX. The values of k_{app} confirm this. The values of the rate constant for the O_3/ H_2O_2 system were always higher than those for O_3 alone (see Figure 3.13) due to the involvement of the hydroxyl radicals. In alkaline medium (i.e. pH 8 and 9), this difference was large. It may be due to the insufficient amount of hydroxyl radicals in the alkaline medium for ozone alone.

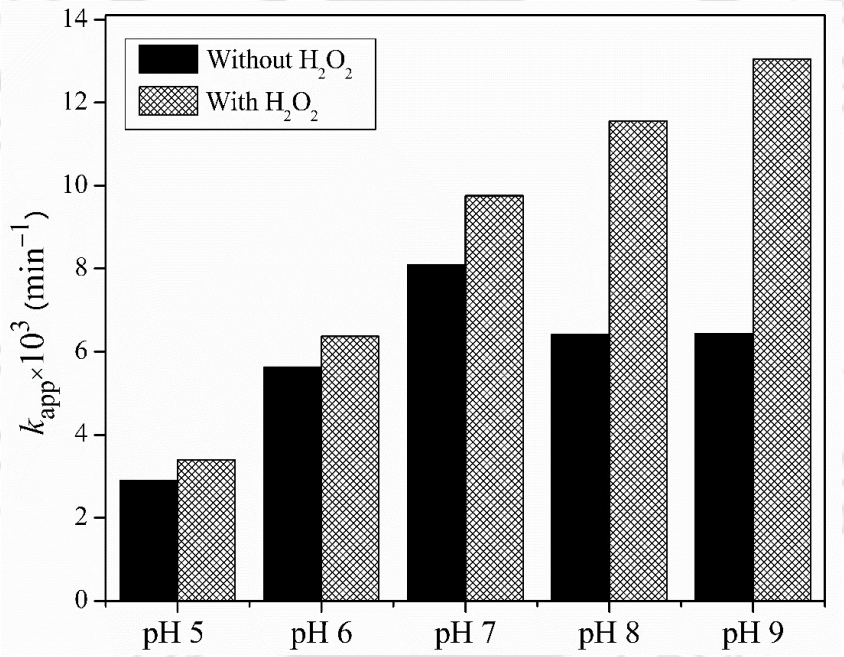

Figure 3.13. Effect of H_2O_2 on the pseudo first-order rate constant, k_{app}.

3.2.10. Identification of intermediates using mass spectrometry

The full-scan ESI mass spectrum of the NPX metabolites (negative ions) was performed on the samples collected from the reactor. These are shown in Figure 3.14. Initially two main peaks of the products were observed due to the loss of CO_2 (m/z = 185.10, 2-methoxy-6-methyl

napthalene), and the losses of one CO_2 molecule and one CH_3 group (m/z = 170.7, 2-methoxy-6-methyl naphthalene) [225,226]. After 8 min of ozonation, only one high-intensity peak was observed, which corresponds to 1-(6-methoxynaphtalen-2-yl) ethyl-hydroperoxide (m/z = 216.6) [179]. The value m/z represents the ratio of mass to charge number of ions.

This Figure is ommited due to copyright issue

Figure 3.14. Full scan electrospray ionization mass spectrum of the NPX intermediates: (a) t = 4 min; (b) t = 8 min. $[NPX]_0$ = 50 mg dm^{-3}; T = 300 K; ozone supply rate = 0.48 mg s^{-1}; $[H_2O_2]$ = 1.2 cm^3.

3.2.11. Mechanism of reaction

Figure 3.15 shows the proposed reaction mechanism for NPX degradation. In the first step, NPX was attacked by the hydroxyl radical and an unstable intermediate was formed. This intermediate was converted to 2-methoxy-6-ethyl naphthalene (m/z = 185.1) and 2-methoxy-6-methyl naphthalene (m/z = 170.7) by the loss of one molecule of CO_2, and one molecule of CO_2 with one methyl group, respectively. Intermediate B further forms 1-(6-methoxynaphthalene-2-yl) ethyl hydroperoxide (m/z = 216.6) due to the combination of the oxygen radicals. These products were also confirmed by other studies [179,225,226].

Figure 3.15. Proposed mechanism of NPX degradation and the intermediates formed.

3.3. Conclusion

Degradation of NPX was studied by using ozone microbubbles in the presence and absence of H_2O_2. The rate of degradation increased with increasing pH (i.e. 5 to 9) of the medium and the ozone supply rate (i.e. 0.39 to 0.48 mg s^{-1}). NPX was degraded to below the detection limit within 4 min of commencement of reaction for 0.48 mg s^{-1} ozone supply rate at pH 9. 50–99% conversion was recorded for ozone supply rates in the range of 0.39 – 0.48 mg s^{-1} and the corresponding reaction times were found to be 100, 750, 30, and 10 min. The hydroxyl radicals present in the reaction system controlled the degradation process significantly, which justifies the higher removal efficiencies in the alkaline medium. From the model, it can be concluded that the concentration of ozone in aqueous phase became constant after 0.27 min; so that we can consider that the ozone concentration is constant as compared to drug concentration throughout the reaction. For the ozone supply rate of 0.39 mg s^{-1}, the k_{app} ranged from 2.89 × 10^{-3} to 6.44 × 10^{-3} min^{-1} for O_3 alone whereas, for the O_3 + H_2O_2 system, it varied from 3.39×10^{-3} to 13.1×10^{-3} min^{-1}. Mainly three intermediates were produced during the ozonation due to decarboxylation of NPX.

Notations

Symbols

a	Coefficient used in Equation (3.8) (-)
a_i	Interfacial area per volume of reactor (m^2 dm^{-3})
b	Coefficient used in Equation (3.8) (-)
C_G	Concentration of ozone in the gas phase (mg dm^{-3})
C_L	Concentration of dissolved ozone in aqueous phase at time t (mg dm^{-3})
$c^*_{O_3}$	Equilibrium ozone concentration in aqueous phase (mg dm^{-3})
c_{ss}	Steady state ozone concentration in aqueous phase at $t\rightarrow\infty$ (mg dm^{-3})
D	Molecular diffusion coefficient in the film (m^{-2} s^{-1})
D_a	Damkohler number (-)
d_b	Bubble diameter (m)
d_{32}	Sauter-mean diameter (m)
f_n	Frequency distribution function (-)
g	Gravity constant (m^2 s^{-1})
H	Henry's law constant (Pa mol fraction^{-1})
H_m	Height of gas-liquid mixture (m)
k	Rate of reaction ($M^{-1}s^{-1}$)
k_{app}	Pseudo-first-order rate constant (s^{-1})
k_D	First-order decomposition rate constant of ozone (s^{-1})
$k_L a$	Volumetric mass transfer coefficient of ozone (s^{-1})
K_{OH}	Rate constants with HO radicals ($M^{-1}s^{-1}$)
K_{O_3}	Rate constants with O_3 ($M^{-1}s^{-1}$)

M Molecular weight of water (kg mol^{-1})

n Number of bubbles (-)

L Length of the reactor (m)

P Pressure (Pa)

p Partial pressure of ozone in the gas phase (Pa)

P Total pressure of the system (N m^{-2})

pK Equilibrium constant (-)

Q Volumetric flow rate (dm^3 s^{-1})

R Gas constant (J mol^{-1} K^{-1})

Re Reynolds number

t Time (s)

T Temperature (K)

u_g Superficial gas velocity (m s^{-1})

V Reactor volume (dm^3)

Greek letters

α Parameter for log normal distribution (-)

β Parameter for log normal distribution (-)

γ Parameter for log normal distribution (-)

δ Parameter for log normal distribution (-)

ε_g Gas holdup (-)

ρ_m Density of mixture (kg dm^{-3})

ρ Density of water (kg dm^{-3})

σ Surface tension of the liquid (N m^{-1})

ε_g Fractional gas holdup

γ Dimensionless number (-)

δ Thickness of diffusion film (m)

ζ Dimensionless number (-)

ξ Dimensionless number (-)

λ Dimensionless number (-)

ϕ Symbol used in Equation (3.35)

Abbreviations

CBZ	Carbamazepine
FESEM	Field emission scanning electron microscope
HPLC	High-performance liquid chromatography
IBP	Ibuprofen
LC-MS	Liquid chromatography–mass spectrometry
MIT	Methylisothiazolone
NPX	Naproxen
NSAID	Nonsteroidal anti-inflammatory medicine
PH	Pharmaceutical
RNT	Ranitidine

CHAPTER IV

OZONATION OF DICLOFENAC IN A LABORATORY-SCALE BUBBLE COLUMN: INTERMEDIATES, MECHANISM, AND MASS TRANSFER STUDIES

[1] S. Patel, S. K. Majumder, P. Ghosh, Ozonation of diclofenac in a laboratory-scale bubble column: Intermediates, mechanism, and mass transfer study. J. Water Process. Eng. (2021), 44, 102325. DOI: 10.1016/j.jwpe.2021.102325.

CHAPTER IV

Ozonation of DCF in a Laboratory-scale Bubble Column: Intermediates, Mechanism, and Mass Transfer Studies

This chapter presents the degradation of diclofenac (DCF) using ozone in the presence of hydrogen peroxide. Effects of various operational parameters, i.e., pH, ozone dose, H_2O_2 concentration, and initial concentration of DCF on the removal rate, were investigated. The removal efficiencies of COD and TOC during ozonation were also reported. The role of hydroxyl radical in the DCF degradation process was confirmed by using a radical scavenger. The release of ammonia and chlorine gas was estimated during the ozonation. The intermediates formed during the degradation were identified, and the path of degradation was also predicted. A kinetic model for DCF ozonation was developed, and the kinetic parameters were determined.

4.1. Introduction

DCF is one of the extensively used analgesic, antiarthritic, and anti-inflammatory non-steroidal drugs (NSAID). Although it is a proven fact that DCF can be removed by natural photolysis [136,137], yet it is one of the most frequently detected pharmaceuticals in water bodies such as groundwater [137,138] and surface water [139,140], at concentrations up to 1.2 μg dm^{-3} [5,141]. Traces of DCF pass through the conventional wastewater treatment facilities without any alteration due to its resistance and high stability.

Photo-Fenton, O_3, O_3/H_2O_2, catalytic ozonation, and UV/H_2O_2 are some of the proven

tools for removing stubborn organic compounds from wastewater with a good mineralization efficiency. Complete mineralization has been found to be expensive due to the extreme reaction conditions [8]. However, in partial degradation, more biodegradable and less toxic intermediates were formed, which was the key to removing toxicity. The potential of the AOPs for the degradation of pharmaceuticals from wastewater has been well-established in previous studies [119,227–231]. Recently, the ozonation of DCF has been reported by many researchers [150,163,232–234]. However, only a limited extent of studies is available for the intermediates and the mechanism of degradation.

The present study aims to predict the degradation pathways of DCF during ozonation and detect the metabolites formed. The effects of system pH, ozone supply rate, and initial concentration of the substrate were studied in detail. A kinetic model was developed for the ozonation of DCF, and the kinetic parameters of the model were determined by using the experimental data. The involvement of the hydroxyl radicals in the degradation process was also investigated. Mass transfer of ozone in the aqueous phase was analyzed, and the parameters for mass transfer were calculated. For the toxicity analysis, the seed germination technique was used. Removal of total organic carbon (TOC) and the release of chloride ion during the reaction were also studied.

4.2. Results and Discussion

4.2.1. Effect of pH of the medium

The oxidation of DCF was conducted in the pH range of 4 – 9. The results are shown in Figures 4.1a – c. The degradation efficiency was usually above 90%. The pH of the solution had a strong effect on the degradation. The impact of the pH on ozone lifetime and its decomposition rate were enunciated by Von Sonntag and Von Gunten [235]. It has been reported that the

lifetime of ozone decreases with the increasing pH of the aqueous phase [236].

Although ozone s short-lived in the alkaline medium, the time required to achieve 99% degradation was less than that in the acidic medium. The increase in the rate of degradation of DCF with the pH of the medium suggests *in situ* generations of the hydroxyl radicals. Non-selectivity and higher oxidizing power of the hydroxyl radicals make them a better oxidizing agent than molecular ozone for the oxidation of DCF. The pseudo-first-order rate constant was increased by 32% when the pH was increased from 4 to 9 (see Figure 4.2). Involvement of the hydroxyl radical in the oxidation of DCF was also confirmed by adding a catalyst and a scavenging agent for the hydroxyl radical (see Section 4.2.2).

This Figure is ommited due to copyright issue

Figure. 4.1. Removal of DCF by ozonation in the pH range of 4 – 9 at the ozone supply rate of (a) 0.44, (b) 0.48, and (c) 0.50 mg s^{-1}. Initial concentration of DCF = 50 mg dm^{-3}.

This Figure is ommited due to copyright issue

Figure 4.2. Variation of the pseudo-first-order rate constant $\left(k_{app}\right)$ with the pH of the medium for the ozone supply rate of 0.44 mg s^{-1} and initial DCF concentration of 50 mg dm^{-3}.

However, system pH was found to be declining during the ozonation process due to the generation of acidic metabolites and NO*x* since the reaction solutions were not buffered during the ozonation. It was also reported in a previous study that during ozone generation, NO*x* production occurred due to electric discharge, which also contributed to the decline in pH [237].

4.2.2. Effect of hydroxyl radical generation *in-situ*

H_2O_2 was added to the aqueous phase for the generation of hydroxyl radicals, and isopropyl alcohol was used for scavenging them. Figure 4.3 shows the effect of hydroxyl radicals present in the reaction system. The addition of isopropyl alcohol (IPA) slowed down the reaction by consuming the hydroxyl radicals. This led to a lower value of the reaction rate constant. k_{app} dropped from 0.4485 to 0.3947 min^{-1} when isopropyl alcohol at a concentration of 13 mol m^{-3} was added to the reaction medium. The addition of 42 mol m^{-3} H_2O_2 led to an increase in k_{app} by 7%. This variation in the rate constant confirmed the involvement of hydroxyl radicals in the degradation of DCF.

Figure 4.3. Effect of addition of H_2O_2 and IPA on the degradation of DCF at pH 7. Initial concertation of DCF = 50 mg dm^{-3}, [H_2O_2] = 42 mmol dm^{-3}, and [IPA] = 13 mmol dm^{-3}.

4.2.3. Effect of initial concentration of DCF

To analyze the effect of loading of the target pollutant, the concentration of DCF was varied in the range of 50 – 125 mg dm^{-3} at pH 9 for the ozone supply rate of 0.44 mg s^{-1}. It was observed that the degradation efficiency of DCF dropped from 99 to 90%, when the initial concentration of DCF was increased from 50 to 125 mg dm^{-3} (see Figure 4.4). These results indicate that the ozone demand increased as the initial concentration of DCF increased. A lesser degradation efficiency at the higher concentration of the target pollutant suggests the unavailability of a sufficient amount of the oxidants (i.e., molecular ozone and hydroxyl radicals) in the aqueous phase for reacting with DCF. To achieve a higher degree of removal of DCF, an optimized ratio of ozone dose and DCF loading is required. Although the degradation efficiency for 125

mg dm^{-3} DCF was decreased by only 10%, a low mineralization efficiency (i.e., 9%) was recorded for this system. It implies that the intermediates formed during ozonation required a higher dose of the oxidant(s) for complete mineralization.

Figure 4.4. Effect of the initial concentration of DCF on its removal at pH 7 and 0.44 mg s^{-1} ozone supply rate.

4.2.4. Effect of ozone supply rate

Ozonation of DCF was conducted at three different ozone supply rates, i.e., 0.44, 0.48, and 0.50 mg s^{-1}. It was found that the removal of DCF was highly sensitive to the ozone supply rate. A slight increase in the ozone supply rate led to a shorter reaction time for the removal of DCF. For all ozone supply rates, complete removal of DCF was achieved. However, the time required for the removal showed significant differences. When the ozone dose was increased by 0.04 mg s^{-1}, the time needed for complete removal of DCF was reduced to 15 min from 70 min. When the ozone dose was increased further by 0.02 mg s^{-1}, the reaction time was 6 – 10 min. An identical behavior was observed for the pH range of 4 – 7. A higher ozone supply rate led to the higher values of the apparent rate constant. The increase in the rate constant with ozone supply rate can be described based on the two-film theory [238]. According to this theory, the higher concentration of ozone at the interface led to an increase in the mass transfer coefficient. However, at a certain value of ozone supply, the water would be saturated with ozone completely. At this point, ozone concentration in water will be constant, and a further increase in the ozone dose will not affect the mass transfer. After achieving the ozone saturation, the degradation process would become dependent on the reaction rate constant. Hence, a further increase in the ozone dose does not affect the degradation efficiency. The other

major factor is the enhanced production of hydroxyl radical, which takes part actively in the degradation process. The effect of ozone supply rate on DCF degradation efficiency at different pH is shown in Figure 4.5.

This Figure is ommited due to copyright issue

Figure 4.5. Effect of ozone supply rate on the degradation efficiency of DCF for (a) pH 4, (b) pH 5, (c) pH 6, (d) pH 7, (e) pH 8, and (f) pH 9 at the initial DCF concentration of 50 mg dm^{-3}.

4.2.5. Production of ammonia and chlorine during DCF d(e) ion

Figure 4.6 shows the ammonia and chloride ion concentration in the reaction medium during the ozonation of DCF. 88% of the total chlorine and 72% of the total nitrogen were released during the mineralization process. In the first 25 min of the reaction, the chloride concentration increased rapidly due to the probable substitution of chloride by the oxygen-containing groups. After 25 min of reaction, the concentration dropped slightly as some chloride ions reacted with the other metabolites (aniline) and formed products such as dichloro aniline, a major intermediate detected. Various chlorine-containing intermediates were detected in the proposed mechanism (see Section 4.2.6). Detection of ammonia reflects the loss of nitrogen atoms in the structure of DCF. The elimination of nitrogen is considered an essential step in the mineralization process because it signifies the rupture of two (f) c rings. Although the final products did not contain nitrogen, a loss of only 72% of the nitrogen illustrates the formation of intermediate nitrogen-containing compounds, which went undetected.

This Figure is ommited due to copyright issue

Figure 4.6. Production of ammonia and chloride ion during the ozonation of DCF at pH 7, 0.44 mg s^{-1} ozone supply rate, and 50 mg dm^{-3} initial DCF concentration.

4.2.6. Mineralization (TOC) and COD removal during ozonation

Figures 4.7a and 4.7b show the TOC and COD removal from the DCF solution for various ozone supply rates. The maximum TOC removal was 60%, achieved at the ozone supply rate of 0.50 mg s^{-1}. For a lower ozone supply rate (i.e., 0.44 mg s^{-1}), the TOC removal was only 20%, which indicates that the recalcitrant intermediates were formed after 30 min of ozonation at the lower ozone supply rate. It can also be observed that at the initial stage of ozonation (i.e., 0.48 and 0.50 mg s^{-1}), the mineralization rate was higher due to the availability of the easily-degradable parent compound. The behavior of COD removal also followed the same pattern as it was found to be maximum, i.e., 80% for the highest ozone supply rate (i.e., 0.50 mg s^{-1}). For a lower ozone supply rate, the COD removal was 40 – 50% only. Direct ozonation of the parent compound led to the production of less degradable intermediates, which can be partially removed by the hydroxyl radicals. This would result in a partial TOC elimination and lower COD removal [239,240].

This Figure is ommited due to copyright issue

This Figure is ommited due to copyright issue

Figure. 4.7. TOC and COD removal during ozonation for various ozone supply rates (i.e., 0.44, 0.48, and 0.50 mg s^{-1}) at pH 9.

4.2.7. Identification of the intermediates and the mechanism proposed

Metabolites formed during the ozonation of DCF were identified in order to propose the probable degradation pathways. To ensure mineralization and determination of the level of toxicity, it is crucial to find the final products and intermediates (formed during ozonation). For the identification study, a separate experiment was conducted without altering the pH. The ozone supply rate was 0.50 mg s^{-1}, and the concentration of H_2O_2 was 42 mol m^{-3}. HR-LCMS (coupled with the National institute of standards and technology (NIST) library) was used to identify and detect the intermediates, and the chromatogram obtained is shown in Figure 4.8.

This Figure is ommited due to copyright issue

Figure 4.8. HR-LCMS chromatogram of the intermediates produced during the ozonation of DCF.

This Figure is ommited due to copyright issue

Figure 4.9. Mechanism of the ozonation of DCF and the proposed structure of the metabolites.

Although the metabolites formed during oxidation depend on the technique applied for degradation, the metabolites detected for sonolysis, Fenton, and ozonation are common [232,241,242].

During the reaction, the solution turned orange after 10 min, which disappeared within 10 min. It was found that the production of diclofenac-2, 5-iminoquinone (M3) was responsible for this color, which also agrees with the recent studies [163,243]. The disappearance of M3 suggests its further degradation. In the HR-LCMS spectrum, eight distinct peaks were visible, out of which five had low intensity. The positive ion spectrum from the LC-MS shows a peak at 9.93 min (m/z = 312) for [M+H]. Further fragmentation shows the loss of a water molecule (m/z = 294) as [M–H_2O]. Both the mass spectroscopic results indicate the presence of 5-hydroxy DCF (M2), which is an unstable compound in the oxidative atmosphere. It tends to be oxidized into DCF-2, 5-iminoquinone, which was also detected as a metabolite in the present study. M2 may also produce the phenyl acetic acid derivatives (M7 and M11, m/z = 152.1). DCF-2, 5-iminoquinone (M3) was detected at RT = 9.8 min (m/z = 310). The probable attack of ozone at the acetate group attached to the benzene ring may release a CO_2 molecule and oxidize the carbon attached to the ring into the aldehyde group (M1). M1 was converted to M4 (i.e., N acetyl 2-amino salicylic acid, m/z = 218, RT = 7.58 min) and 2-chloro benzoate (i.e., M5, m/z = 177, RT = 7.10 min) at the advanced stages of oxidation. Further oxidation breaks the C–N bond and produces various products containing one benzene ring. Cleavage of the C–N bond leads to the generation of a major product, i.e., dichloro aniline (i.e., M6, m/z = 161.9, RT = 7.024 min). Dichloro aniline was commonly found as a metabolite in the previous studies as well [242]. Further degradation of M6 produced 2, 6-dichloro quinone (i.e., M8, m/z = 178), 4-amino, 3, 5-di chlorophenol (m/z = 177), and 2-chloro aniline (m/z = 127). After the C–N cleavage, the ring-opening reactions take place and generate smaller acids (i.e., M13,

M14, and M15). Thus, the ozonation of DCF involves the decarboxylation, dechlorination, and hydroxylation steps. Cleavage of the C–N bond and opening of the benzene rings generated the compounds of lower molecular weight. Smaller carboxylic acids, such as acetic acid, formic acid, and oxalic acid, were produced at the final stage of ozonation, which further mineralized to carbon dioxide and water. Dechlorination was also confirmed by the presence of the chlorine the reaction medium. Figure 4.9 represents the probable mechanism for DCF ozonation.

4.2.8. Kinetic study of ozonation of DCF

The reaction of the target pollutant with ozone is a function of various macroscopic parameters, i.e., ozone supply rate, pollutant loading, and system pH. The ozone in the aqueous phase depends on the extent of mass transfer of ozone from the gas to the liquid phase. The pH of the system also plays a vital role in ozone dissociation and mass transfer. Thus, the kinetics of the DCF degradation reaction was studied under different operating parameters. The dependence of the pseudo-first-order rate constant on the operational parameters was also studied.

Since it is a fact that both molecular ozone and hydroxyl radical act as oxidants, the rate of oxidation of DCF can be written as

$$\frac{d[\mathrm{DCF}]}{dt} = -k_{\mathrm{O_3}}[\mathrm{DCF}][\mathrm{O_3}] - k_{\mathrm{HO}\bullet}[\mathrm{DCF}][\mathrm{HO}\bullet] \qquad (4.1)$$

where [DCF], $[\mathrm{HO}\bullet]$, and $[\mathrm{O_3}]$ denote the concentration of diclofenac, hydroxyl radical, and ozone, respectively at time *t*. $k_{\mathrm{O_3}}$ and $k_{\mathrm{HO}\bullet}$ are the rate constants for the reactions involving ozone and hydroxyl radical, respectively.

Equation (4.1) can be simplified to equation (4.2) by considering the reaction as pseudo-first-order.

$$\frac{d[\mathrm{DCF}]}{dt} = -\left(k_{\mathrm{O_3}}[\mathrm{O_3}] + k_{\mathrm{HO}\bullet}[\mathrm{HO}\bullet]\right)[\mathrm{DCF}] \tag{4.2}$$

$$\frac{d[\mathrm{DCF}]}{dt} = -k_{\mathrm{app}}[\mathrm{DCF}] \tag{4.3}$$

Upon integration, we get

$$\ln\left(\frac{[\mathrm{DCF}]}{[\mathrm{DCF}]_0}\right) = -k_{\mathrm{app}}t \tag{4.4}$$

The value of k_{app} can be determined from the slope of the plot of $\ln\left(\frac{[\mathrm{DCF}]}{[\mathrm{DCF}]_0}\right)$ versus t. The experimental data for the ozonation of DCF fitted equation (4.4) well for different operating conditions. The coefficient of determination was greater than 0.93 in all cases. Therefore, it can be concluded that the degradation of DCF by ozone and hydroxyl radical follows the pseudo-first-order kinetics. The values of k_{app} were in the range of 0.0742 – 0.48 $\mathrm{min^{-1}}$. The highest value of k_{app} was found to be 0.48 $\mathrm{min^{-1}}$ at the ozone supply rate of 0.50 mg $\mathrm{s^{-1}}$ and pH 9.

Degradation of DCF by ozone is a complex process that involves various direct and indirect parameters. Due to the unstable nature of ozone and the constraints encountered during the measurement of the concentration of the hydroxyl radicals in the reaction medium, the ozone supply was considered an independent variable. System pH, ozone dosage, and the initial concentration of DCF were considered as the main parameters that affected k_{app} [244]. The nature of dependency of all three parameters was estimated, and an empirical model was developed for k_{app}. This model is given as

$$k_{\mathrm{app}} = A\exp\left(-\frac{E_a}{RT}\right)\left(\frac{Q_{\mathrm{O_3}}\,t_R}{[\mathrm{DCF}]_0\,V_R}\right)^a(\mathrm{pH})^b = k_{abs}\left(\frac{Q_{\mathrm{O_3}}\,t_R}{[\mathrm{DCF}]_0\,V_R}\right)^a(\mathrm{pH})^b \tag{4.5}$$

where Q_{O_3} is the ozone supply rate (mg s^{-1}) to the system, $[DCF]_0$ is the initial concentration of DCF (mg dm^{-3}), and $\left(-\frac{E_a}{RT}\right)$ was considered as a constant since all experiments were performed at the constant temperature of 298 K.

From the multiple regression, the values of *a* and *b* were estimated as 0.59 and 0.35, with r^2 = 0.922, respectively. Therefore, equation (4.5) can be written as

$$k_{app} = 0.99\left(\frac{Q_{O_3} t_R}{[DCF]_0 V_R}\right)^{0.59} (pH)^{0.35} k_{abs} \quad (4.6)$$

To verify the developed model, the values computed from it were compared with the experimental data. It was found that the relative error for model was < 7%. Therefore, the kinetic model for DCF degradation was considered to be accurate for the range of the operating parameters studied in this work, i.e., ozone supply rate of 0.44 – 0.50 mg s^{-1}, system pH of 4 – 9, and initial concentration of DCF 50 – 125 mg dm^{-3}.

4.2.9. Effect of water matrix on the degradation of DCF

To analyze the effect of the water matrix, a separate experiment was conducted with real wastewater (COD = 50 – 55 mg dm^{-3}) spiked with DCF, and compared with the degradation efficiency achieved in ultra-pure water (COD = 0 mg dm^{-3} and electrical resistivity = 0.0055 µS cm^{-1}). One run was conducted with a lower concentration of DCF, based on the DCF concentrations present in the water bodies [245–247]. The effect of water matrix on the removal efficiency and mineralization is shown in Figure 4.10. It was observed that the organic and inorganic materials present in the real wastewater inhibited the ozonation of DCF to some extent. The removal efficiency was dropped by 17% when the ozonation was conducted in

wastewater instead of ultrapure water. Although the removal efficiency was lower, 83% removal of DCF was achieved in 60 min of the reaction. It can be concluded that the substances present in the wastewater competed with DCF for consuming the oxidant present in the solution. Therefore, the availability of ozone and hydroxyl radicals for oxidizing DCF decreased, and a reduced removal rate was observed. It can be anticipated that the presence of other contaminants inhibited the degradation process, so the removal efficiency achieved in the case of ultra-pure water could not be achieved in real wastewater.

Figure 4.10. Effect of wastewater matrix on the degradation of DCF at pH 7. Ozone supply rate = 0.44 mg s^{-1}; Initial concentration of DCF = 50 mg dm^{-3}.

4.3. Conclusions

Ozonation was found to be a very effective method for removing DCF from water. The removal efficiency was in the range of 95 – 99% in the alkaline as well as acidic media. However, the reaction time required for the complete removal of DCF was less in the alkaline medium. The volumetric mass transfer coefficient was in the range of $1.150 \times 10^3 – 2.717 \times 10^3$ s^{-1} for pH 6 – 9 and ozone supply rate of 0.44 – 0.5 mg s^{-1}. The values of the pseudo-first-order rate constant were in the range of 0.0742 – 0.0979 min^{-1}. The results also confirmed the active participation of the hydroxyl radicals in the degradation process. The rate constant dropped by 11% when 13 mmol dm^{-3} IPA was added as the radical scavenger. The rate of ozone supply to the reactor was proved to be a key factor for the degradation time. An increase of 0.06 mg s^{-1} in the ozone

supply rate led to a rapid fall in the reaction time (i.e., from 60 to 6 min). 88% of the total chlorine and 72% of the total nitrogen were released during the degradation process. With a real effluent having 50 mg dm^{-3} COD, the removal efficiency was dropped by 17%. The mineralization of DCF by ozone mainly consisted of three steps, i.e., attack of the oxidant, cleavage of the C–N bond, and ring-opening. The major intermediates detected in HR-LCMS were dichloro aniline, 5-hydroxy DCF, DCF-2 5-iminoquinone, 2-chloro benzoate, derivatives of phenylacetic acid, and carboxylic acids (e.g., acetic, formic, and oxalic acids). The primary mechanism involved in the degradation process included decarboxylation, dechlorination, and hydroxylation.

Notations

Symbols

A	Pre-exponential factor in the Arrhenius equation (s^{-1})
A'	Coefficient in the correlation given by Equation (4.6) (s^{-1})
a	Coefficient in the correlation given by Equation (4.6) (-)
b	Coefficient in the correlation given by Equation (4.6) (-)
C_{O_3}	Concentration of ozone in the aqueous phase (mg dm^{-3})
E_a	Activation energy (kJ mol^{-1})
k_{app}	Pseudo-first-order rate constant for DCF ozonation (s^{-1})
$k_{\bullet OH}$	Rate constant for oxidation of DCF by ozone (mol^{-1} dm^3 s^{-1})

k_{O_3}	Rate constant for oxidation of DCF by hydroxyl radical (mol^{-1} dm^3 s^{-1})
Q_{O_3}	Ozone supply rate (mg s^{-1})
R	Universal gas constant (kJ mol^{-1} K^{-1})
T	Temperature (K)
t	Time (s)
t_R	Residence time for DCF degradation (s)
V_R	Volume of the reactor (dm^3)

Abbreviations

AOP	Advanced oxidation process
COD	Chemical oxygen demand
DCF	Diclofenac
IPA	Iso-propyl alcohol
NSAID	Non-steroidal anti-inflammatory drugs
NIST	National institute of standards and technology
TOC	Total organic carbon

CHAPTER V

DEGRADATION OF RANITIDINE BY O_3 + H_2O_2: KINETICS, MODELLING, AND MECHANISM

CHAPTER V

Degradation of Ranitidine by O_3 + H_2O_2: Kinetics, Modelling, and Mechanism

In this chapter, synthetic wastewater containing ranitidine (RNT) is treated with O_3/H_2O_2 to degrade the drug. The effects of several parameters on the degradation process such as ozone dose, initial RNT concentration, system pH, and water matrix are studied. The model for the ozonation of RNT is also developed to assess the effect of operation conditions on RNT degradation. Intermediates formed during ozonation are also identified, and the mechanism of their formation is also predicted.

5.1. Introduction

The advanced living style of the developed nations includes daily utilization of synthetic compounds like pharmaceuticals, personal-care products, chemicals, and pesticides [244]. Due to this, the remains of these organic compounds act as contaminants in the wastewater since the conventional wastewater treatment plants fail to degrade them efficiently [245–248]. Although there are many groups of contaminants and organic micro-pollutants of concern, most research works are mainly attracted towards the destiny of the active pharmaceutical compounds in wastewater due to its serious hazards [244,249,250]. These pharmaceuticals and personal-care products (PPCPs) are extensively present in the aquatic environment and perceived as a rising global issue [251–253]. Despite performing separation processes like partial degradation, adsorption, and transformation to remove these organic micro-pollutants, PPCPs are often being traced in the treated water and even in the drinking water [254,255].

Even though the concentration of PPCPs and other pharmaceuticals are found to be in minimal quantities (ng dm^{-3} to µg dm^{-3}) [256], there may be some potential risk in drinking water on the health as the PPCPs are biologically active [257,258]. The conventional methods of treating drinking water, such as flocculation and adsorption, were less effective in eliminating these pharmaceutical compounds due to their recalcitrant nature [259–261].

Many works have been conducted on the treatment of wastewater by biodegradation removing the pharmaceuticals and other contaminants, but it was found that these pharmaceuticals have resistance towards these approaches, which led to the ineffective treatment of wastewaters [262,263]. One of the suitable approaches for the removal of some specific pharmaceuticals like diclofenac, RNT, ketoprofen, gemfibrozil, and ofloxacin is based on membrane separation, but the requirement of a high retention time may lead to concentration polarization during the operation [222,249]. Most commonly, advanced oxidation processes (AOPs) have been found to efficiently treat wastewater that contains bio-refractory pollutants. Ozonation, UV photocatalysis, and Fenton are some of the types of AOPs, which have also been examined for wastewater treatment, removing the pharmaceuticals very efficiently [264]. AOPs are now considered as an alternative to the conventional water treatment methods for removing the pharmaceuticals [265,266].

Among all the AOP methods, results obtained from ozonation have been very encouraging and prove to be an alternative for wastewater treatment. No sludge generation and the decomposition of residual ozone into oxygen make it a more efficient process. The oxidation potential of 2.07 V makes ozone a powerful oxidizing agent. It interacts with the organic micropollutants present in wastewater either directly as an ozone molecule or indirectly by converting into hydroxyl free radicals via a series of chain reactions. These hydroxyl free radicals have an even more oxidizing potential than ozone itself [267]. The decomposition of

ozone via the chain reactions consists of three steps, i.e., initiation, propagation, and chain cleavage [222].

In the present work, the ozonation process has been used to remove RNT, a histamine-2 blocker, by a combination of ozone and hydrogen peroxide. The effect of various operational factors like the pH of the system, initial concentration of RNT, and ozone flow rate on the rate of degradation of RNT had been studied and analyzed. The intermediates formed during the reaction were also identified along with their path of formation. Finally, by studying the dependency of the degradation process on the operational parameters, a mathematical model for the degradation of RNT has been proposed.

5.2. Results and discussion

The effect of degradation of RNT on the various operational factors, i.e., pH of the initial solution, initial concentration of RNT, and ozone flowrate, was studied and analyzed. The results obtained are discussed in the following sub-sections.

5.2.1. Effect of initial pH

One of the significant factors affecting the degradation of RNT is the initial pH of the wastewater. The performance of ozonation depends on the initial pH of the wastewater. The effect of the initial pH of wastewater was studied by fixing the initial concentration of RNT at 50 mg dm^{-3} and varying the pH from 4 to 9. At this initial concentration of RNT, the effect of pH was studied at three different flowrates of ozone, i.e., 0.44, 0.48, and 0.50 mg s^{-1}, as shown in Figure 5.1. The results obtained from the experiment indicate that the degradation rate was more pronounced in the alkaline conditions than the acidic and neutral conditions at all three ozone flow rates. At the ozone flow rate of 0.44 mg s^{-1}, 99.54% of RNT was degraded in 50

min when the pH of the solution was 9. On the other hand, 90, 92, and 98% removal of RNT occurred when the pH was 4, 5, and 8, respectively. At the ozone flow rate of 0.48 mg s^{-1}, 100% degradation of RNT occurred in 17 min at pH 9, while the same reduced to 96% at pH 4 in the same time i.e., the degradation rate was higher when the solution was alkaline. Similar results were obtained for the ozone flow rate of 0.50 mg s^{-1}. This behavior confirms the involvement of hydroxyl radicals. In the alkaline medium, ozone decomposes rapidly and produces hydroxyl radicals *in situ*, which is a better oxidant than ozone itself [234,268,269]. In the acidic medium, molecular ozone was found to be responsible for the degradation. Molecular ozone is a selective oxidant and attacks only a few sites [266]. The presence of hydroxyl ions accelerates the decay of ozone into hydroxyl radical, as shown in Equations (5.1 – 5.5) [231].

$$O_3 + OH^- \rightarrow OH_2^- + O_2 \quad (5.1)$$

$$O_3 + HO_2^- \rightarrow HO\bullet + O_2^{\bullet -} + O_2 \quad (5.2)$$

$$O_3 + O_2^{\bullet -} \rightarrow O_3^{\bullet -} + + O_2 \quad (5.3)$$

$$O_3^{\bullet -} \rightleftarrows O^{\bullet -} + O_2 \quad (5.4)$$

$$O^{\bullet -} + H_2O \rightarrow HO\bullet + OH^- \quad (5.5)$$

This Figure is ommited due to copyright issue

(a)

Figure 5.1. Degradation of RNT by ozone at pH 4 · [RNT]$_0$ = 50 mg dm^{-3} for the ozone supply rate (a) 0.44 mg s^{-1}, (b) 0.48 mg s^{-1}, and (c) 0.50 mg s^{-1}.

5.2.2. Effect of initial concentration of RNT

The results from the experiment indicated that the degradation of RNT was favorable at the lower initial concentration of RNT. Also, from Figure 5.2, it is observed that the degradation rate was highest for the initial concentration of 50 mg dm^{-3}, followed by 75 and 100 mg dm^{-3}, and lowest for 125 mg dm^{-3}, at 0.44 mg s^{-1} ozone flow rate. The lower degradation rate at a higher initial concentration of RNT may be due to the formation of more intermediates that consume more hydroxyl radicals. At a lower initial concentration of RNT, the concentration of the intermediates formed would be lower. Therefore, more hydroxyl radicals would be available for degradation, and thus a higher rate was observed.

This Figure is ommited due to copyright issue

Figure 5.2. Effect of initial concentration of RNT on the degradation of RNT at 0.44 mg s^{-1} ozone flow rate.

5.2.3. Effect of ozone dosage

The degradation of RNT and its reactivity towards ozone was assessed for three ozone dosages. A higher dosage of ozone in the reaction system increased the rate of formation of hydroxyl radical. Thus a higher degradation rate was observed [270]. The ozone supply was varied from 0.44 to 0.50 mg s^{-1}. This variation of ozone supply was studied on solutions having initial pH ranging from 4 to 9 (Figures 5.3a – 5.3f). For the ozone flow rate of 0.44 mg s^{-1}, the rate of degradation reached 90% in 50 min for pH 4, whereas no RNT was detected after 7 min of reaction at pH 9 when the ozone supply rate was increased to 0.50 mg s^{-1}. A higher dose of ozone favored the mineralization process. At the high ozone concentration, recalcitrant metabolites were also degraded, which increased the mineralization efficiency. The results demonstrate that the RNT can be degraded successfully even at a low ozone dose (i.e., 0.44 mg

s^{-1}). However, the reaction time would be higher than the case where the reaction is carried out with a high ozone dose.

This Figure is ommited due to copyright issue

Figure 5.3. Effect of ozone supply on RNT degradation at different pH: (a) pH 4, (b) pH 5, (c) pH 6, (d) pH 7, (e) pH 8, and (f) pH 9.

5.2.4. Effect of hydroxyl radical scavenger

This Figure is ommited due to copyright issue

Figure 5.4. Effect of hydroxyl radical scavenger for the ozone supply rate of 0.44 mg s^{-1}.

The degradation of RNT involves reactions with hydroxyl radicals, and in the process, the latter are consumed. To confirm the degradatic (b) hanism, a radical scavenger, i.e., isopropyl alcohol (IPA) was used at different concentrations (50, 100, and 150 mg dm^{-3}) for the ozone supply rate of 0.44 mg s^{-1} inasmuch as (d) as the ability to react with the hydroxyl radicals rapidly. The involvement of the hydroxyl radical and its effect on the degradation of RNT is shown in Figure 5.4. It can be seen that 85% of RNT was degraded within 30 min of ozonation without any isopropyl alcohol. On the other hand, 70, 59, and 43% degradation of RNT were achieved when the isopropyl alcohol concentrations were 50, 100, and 150 mg dm^{-3}, respectively. This indicates the presence of hydroxyl radicals in the reaction medium as isopropyl alcohol reacted with them, which resulted in a lower degradation rate.

5.2.5. Effect of H_2O_2 concentration

This Figure is ommited due to copyright issue

Figure 5.5. Effect of H_2O_2 concentration on the degradation of RNT.

The addition of H_2O_2 in the reaction system enhanced the degradation efficiency, as shown in Figure 5.5. When ozone was used as the oxidant alone, the removal efficiency was 87%. It increased by 17% when 0.088 mol dm^{-3} H_2O_2 was added to the system. Further increase in the H_2O_2 concertation led to the complete removal of RNT. The removal rate was found to be almost the same for the H_2O_2 concentrations of 0.176 and 0.246 mol dm^{-3}. H_2O_2 acted as a catalyst for ozone decomposition to produce more hydroxyl radicals [266]. An excess of H_2O_2 may consume the radicals in the competition with the target compounds and slow down the degradation rate [271]. The concertation of H_2O_2 should be optimized to maximize the removal rate. In the present case, the optimal concentration is 0.176 mol dm^{-3} because a similar trend was observed at the higher concentrations as well. Further increase in the H_2O_2 concentration may lead to a decrease in the removal rate.

5.2.6. Effect of water matrix

This Figure is ommited due to copyright issue

Figure 5.6. Effect of water matrix on the degradation of RNT.

An experiment was done separately using a real wastewater (COD = 50 – 55 mg dm^{-3}) spiked with RNT to compare the degradation efficiency in this system with that attained in ultrapure water (COD = 0 mg dm^{-3} and electrical resistivity = 0.0055 S cm^{-1}). The objective of this experiment was to investigate the influence of the water matrix. Based on the RNT concentration found in the water bodies, one run was performed with a lower RNT

concentration. The water matrix affected the ozonation efficiency to degrade RNT, and its effect is shown in Figure 5.6. The organic matter and inorganic substances found in real industrial wastewater hindered the ozonation of RNT to some extent. The RNT degradation was around 93% in the ultrapure water and only 67% in the real wastewater after 60 min of ozonation, which shows that the RNT degradation efficiency in the real wastewater was reduced by 26% as compared with the ultrapure water. Despite the reduced removal effectiveness, the reaction removed 67% of the RNT after 60 min. From the above observations, it is apparent that the chemicals and other organic matters present in the wastewater competed with RNT. They were responsible for consuming some fraction of the oxidants (i.e., hydroxyl radicals and ozone) present in the solution. As a result, the availability of oxidants for the RNT degradation process was reduced, leading to a lower removal rate. It is reasonable to predict that the additional pollutants and compounds compete for the oxidant and lower the extent of degradation of RNT. Thus, the removal efficiency achieved in the ultra-pure water would not be attained in the real wastewater.

5.2.7. Ozone concentration in the solution

Figure 5.7. Solubility profiles of ozone at 0.50 mg s^{-1} ozone supply rate in (a) pure water and (b) RNT solution.

The availability of ozone in the aqueous solution primarily controls the degradation rate of RNT. The degradation rate depends on the mass transfer of ozone from the gas phase to the aqueous phase, which depends on ozone decomposition and its dissolution rate in the aqueous phase [267]. Thus, the formation of hydroxyl radicals in the solution, which is required for the degradation process, depends on the availability of ozone. From Figure 5.7a, it can be seen that the ozone concentration in pure water went on increasing up to 3.1 mg dm^{-3} in 15 min when

the ozonation was conducted with the ozone flow rate of 0.50 mg s^{-1}. After that, it became constant with time. So, it is evident that after 15 min, the ozone concentration reached its saturation value of 3.1 mg dm^{-3} at the specified condition. When the RNT solution was ozonated, it was observed that the RNT concentration decreased with time while the ozone concentration in the solution initially started increasing slowly. From Figure 5.7b, it can be seen that the rate of increase of ozone concentration in the solution was much less than the rate of decrease of RNT concentration up to 11 min, indicating that most of the ozone in the solution was consumed to oxidize RNT. After 12 min, when 95% RNT was degraded, the rate of RNT concentration decreased almost to zero. In comparison, the ozone concentration in the solution increased at a higher rate from 0.2 mg dm^{-3} in 11 min to 1.6 mg dm^{-3} in 25 min, indicating that most of the ozone was available and unutilized in the solution, resulting in a sharp increase in its concentration.

5.2.8. Kinetics of degradation of RNT

The ozonation of wastewater comprises a series of gas–liquid reactions. In these reactions, the ozone transfer takes place from the gas to the liquid phase, where it reacts simultaneously with the other contaminants. Since molecular ozone (O_3) and hydroxyl free radicals $(HO\bullet)$ are responsible for the ability of oxidization of ozone, the reaction rate of degradation of RNT can be written as [272]

$$-\frac{dC(t)}{dt} = k_0[C(t)][O_3] + k_{HO\cdot}[C(t)][HO\bullet] \quad (5.6)$$

where $[C(t)]$ is the concentration of RNT in the solution, $[O_3]$ and $[HO\bullet]$ are the concentrations of ozone and hydroxyl radical, respectively, and k_0 and $k_{HO\cdot}$ are the rate constants of the reaction. Equation (5.6) can be rewritten as

$$-\frac{dC(t)}{dt} = \left(k_0[O_3] + k_{HO\cdot}[HO\bullet]\right)[C(t)] \tag{5.7}$$

Equation (5.7) can be expressed as the rate equation for a pseudo-first-order reaction as

$$-\frac{dC(t)}{dt} = \left(k_{app}\right)[C(t)] \tag{5.8}$$

where k_{app} is the apparent rate constant. Integration of Equation (5.8) with the initial condition that at $t = 0$, $C(t) = C_0$ yields

$$-\ln\left[\frac{C(t)}{C_0}\right] = k_{app}\, t \tag{5.9}$$

$$C(t) = C_0 \exp\left(-k_{app} t\right) \tag{5.10}$$

where C_0 is the initial concentration of RNT.

Equation (5.9) was fitted to the experimental data, and the slope of the plot of $-\ln[C(t)/C_0]$ versus t gave the value of k_{app} at different reaction conditions. One such plot is shown in Figure 5.8 for the ozone supply of 0.40 mg s^{-1}, C_0 = 50 mg dm^{-3}, and pH = 9. The value of R^2 was greater than 0.98, which clearly shows that the reaction followed the pseudo-first-order kinetics.

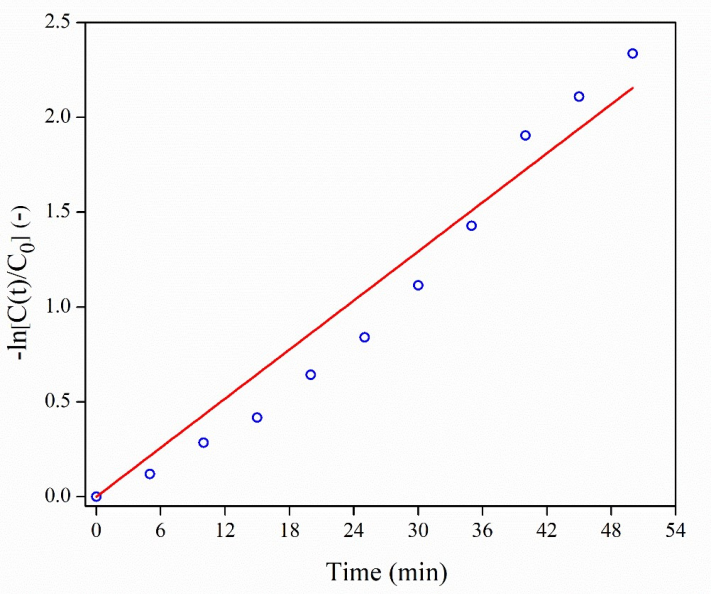

Figure 5.8. The plot of $-\ln\left[C(t)/C_0\right]$ versus t for the ozone supply rate of 0.44 mg s^{-1} (C_0 = 50 mg dm^{-3} and pH 9).

It was a complex and challenging task to measure the ozone concentration in the solution throughout the experiment. Therefore, the apparent rate constant $\left(k_{app}\right)$ was assumed to be related to the O_3 dosage [273]. Moreover, the apparent rate constant was also related to the initial concentration of RNT and temperature because these parameters could affect the degradation rate. An empirical relation (i.e., Equation 5.11) was developed [274].

$$k_{app} = A\exp\left(-\frac{E_a}{RT}\right)Q_{O_3}^{\alpha}C_0^{\beta} \tag{5.11}$$

Taking natural logarithm on both sides, we get

$$\ln k_{app} = \ln A - \frac{E_a}{RT} + \alpha \ln Q_{O_3} + \beta \ln C_0 \tag{5.12}$$

The term $\left(\frac{E_a}{RT}\right)$ in Equation (5.12) is a constant because the reaction was performed at a constant temperature. Also, the constants α and β were obtained by using the regression analysis between $\ln k_{app}$ vs $\ln Q_{O_3}$ and $\ln k_{app}$ vs $\ln C_0$.

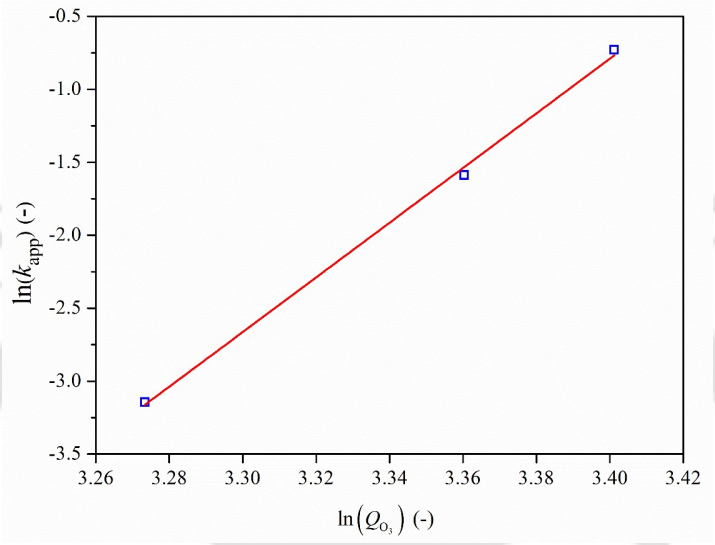

Figure 5.9. $\ln k_{app}$ vs. $\ln Q_{O_3}$ fitted curve.

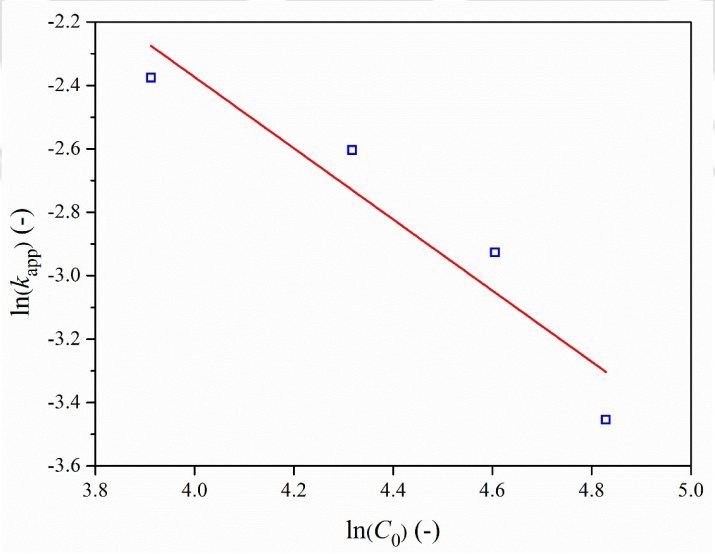

Figure 5.10. $\ln k_{app}$ vs. $\ln C_0$ fitted curve.

From Figure 5.9 and Figure 5.10, $\alpha = 18.73$ (from the slope of $\ln k_{app}$ vs. $\ln Q_{O_3}$, R^2 value greater than 0.99) and $\beta = -1.121$ (from the slope of $\ln k_{app}$ vs. $\ln C_0$, R^2 value greater than 0.96) respectively. Therefore Equation (5.13) can be rewritten as equation 8.

$$k_{app} = A\exp\left\{-\frac{E_a}{RT}\right\} Q_{O_3}^{18.73} C_0^{-1.121} \quad (5.13)$$

The experimental values were used and substituted in Equation (5.13), and the mean value of $A\exp\left\{-\frac{E_a}{RT}\right\}$ was evaluated. After performing the above procedure, the average value $A\exp\left\{-\frac{E_a}{RT}\right\}$ was equal to 1.9645 x 10^{-26}. Again, Equation (5.13) can finally be rewritten as Equation (5.14).

$$k_{app} = \left(1.9645 \times 10^{-26}\right) Q_{O_3}^{18.73} C_0^{-1.121} \quad (5.14)$$

By combining Equation (5.14) and (5.15), the final mathematical model for the degradation of RNT was proposed as

$$C(t) = C_0 \exp\left\{-(1.9645 \times 10^{-26}) Q_{O_3}^{18.73} C_0^{-1.121} t\right\} \quad (5.15)$$

5.2.9. Identification of the intermediates and the mechanism proposed

The potential degradation pathway for the ozonation of RNT was proposed by finding the varieties of the intermediates/products formed during ozonation. These intermediates and final products were identified and detected by using HR-LCMS (High Resolution Liquid Chromatography with Mass Spectrophotometry). With the help of the retention time and the *m*/*z* value of the precursor (i.e., the intermediates) and the product ions, the structures of the

products and intermediates were identified by comparing with the standards. The structures of the intermediate products for which the standards were not available were identified by comparing their *m*/*z* values with the literature. In order to identify the intermediates, an experiment was conducted separately, keeping the pH of the system at a fixed value with the ozone flow rate of 0.50 mg s^{-1} and H_2O_2 concentration of 42 mol dm^{-3}.

Based on the mass spectrum of HR–LCMS, it can be seen that the significant intermediates formed and detected had *m*/*z* 331 (hydroxylated/oxygenated), *m*/*z* 127 and 129 (C—S bond cleavage), and *m*/*z* 286 and 288 (oxygenated and C—N bond cleavage). The energy required to break the C—S and C—N bonds are 306 kJ mol^{-1} and 272 kJ mol^{-1}, respectively, which is considerably lower than those for the C—H, N—H, and C—C bonds [275]. The formation of the above intermediates validates that the reaction mechanism and degradation pathway were primarily driven by the addition of oxygen, hydroxylation, and cleavage of the C—S/C—N bonds [276]. The intermediate products with *m*/*z* 288, 286, and 331 were also detected in the previous studies during the ozonation/hydroxylation of RNT [198,277]. These three intermediates confirm that one of the transformation pathways was via the cleavage of the C—N bond, which also led to the formation of dimethylamine (DMA).

So, based on the intermediates formed, two primary degradation pathways of ozonation of RNT may be proposed. The first transformation pathway began with the dissociation of the C—S bond of RNT, leading to the formation of the intermediates designated as M6 (i.e., 2,5-furandimethanol, *m*/*z* 129) and M8 (*m*/*z* 127). The cleavage of the C—S bond first resulted in the rapid decomposition of RNT to a small amount of M5 (i.e., dimethyl-aminomethyl furfuryl alcohol, *m*/*z* 155) and M7 (i.e., thioethyl-N-methyl-2-nitroethene-1,1-diamine, *m*/*z* 175) degradation by-products [278]. The C—S bond cleavage during the ozonation occurred because of the attack of the hydroxyl radical at the carbon atom next to the sulfur atom of RNT [198].

Another attack of the HO• radical at the carbon atom next to the nitrogen atom of M5 led to the formation of the M6 (*m*/*z* 129) intermediate. Further oxidation by the abstraction of hydrogen at one of the alcoholic groups of M6 resulted in the formation of an aldehyde derivative intermediate, M8 (*m*/*z* 127). In the second pathway, the degradation of RNT started with the attachment of the oxygen atom to the nitrogen atom (i.e., M1, *m*/*z* 330). Further attack of the hydroxyl radical occurred at the carbon atom next to the nitrogen of the M1 intermediate, resulting in the dissociation of the C─N bond, and the intermediate, M2 (*m*/*z* 288) was formed with DMA as the by-product. Then, the alcoholic group of the M2 intermediate was oxidized to form another aldehyde derivative intermediate, M4 (*m*/*z* 286) in the presence of the HO• radicals and ozone. The intermediate, M3 (*m*/*z* 331) was also detected in the reaction medium as the intermediate, M1 with its N=O bond dissociated to form an alcohol derivative. The proposed reaction pathway for the ozonation of RNT is schematically shown in the Figure 5.11.

This Figure is ommited due to copyright issue

Figure 5.11. The proposed degradation pathway for the ozonation of RNT.

5.3. Conclusion

Ozonation was found to be highly effective for the removal of RNT from wastewater. RNT was completely removed within 7 min of reaction for the ozone supply rate of 0.50 mg s^{-1}. In the alkaline medium, 99% removal of RNT was observed, whereas the removal was 90 – 92% in the acidic medium. Higher ozone supply enhances the degradation rate. Time required for complete removal of RNT was reduced by 86% when ozone supply was increased by 13%. Higher availability of oxidants resulted higher mineralization efficiency. The pseudo-first-order rate constants were found to be in the range of 0.053 – 0.089 min^{-1} for the pH range 4 – 9. AT higher pH, reaction rate was found higher due to involvement of hydroxyl radicals in degradation process. Presence of IPA slowed down the degradation whereas hydrogen peroxide catalyzed it. The developed kinetic model suggests that the removal rate was susceptible to the ozone supply rate to the system. Total nine intermediates were identified after the ozonation. The mineralization process mainly consists of rupturing the C–N and C–S bonds of the RNT molecule. The formation of dimethylamine was also reported. However, the extent of formation was not determined.

Notations

Symbols

A	Pre-exponential factor in the Arrhenius equation (s^{-1})
E_a	Activation energy (kJ mol^{-1})
k_{app}	Pseudo-first-order rate constant for DCF ozonation (s^{-1})
$k_{\cdot OH}$	Rate constant for oxidation of DCF by ozone (mol^{-1} dm^3 s^{-1})
k_{O_3}	Rate constant for oxidation of DCF by hydroxyl radical (mol^{-1} dm^3 s^{-1})
Q_{O_3}	Ozone supply rate (mg s^{-1})
R	Universal gas constant (kJ mol^{-1} K^{-1})
T	Temperature (K)
t	Time (s)

Greek Letters

α	Coefficient in the correlation given by Equation (5.11) (-)
β	Coefficient in the correlation given by Equation (5.11) (-)

Abbreviations

AOP	Advanced oxidation process
COD	Chemical oxygen demand
IPA	Iso-propyl alcohol
PPCP	Pharmaceuticals and personal-care products
RNT	Ranitidine
UV	Ultra-violet

CHAPTER VI

TREATMENT OF A REAL PHARMACEUTICAL INDUSTRIAL EFFLUENT BY A HYBRID PROCESS OF ADVANCED OXIDATION AND ADSORPTION BY ACTIVATED CHAR

[1] S. Patel, S Mondal, S. K. Majumder, P. Ghosh, P. Das, Treatment of a pharmaceutical industrial effluent by a hybrid process of advanced oxidation and adsorption. ACS Omega. (2020), 5 (50), 32305-32317. DOI: 10.1021/acsomega.0c04139.

CHAPTER VI

Treatment of a Real Pharmaceutical Industrial Effluent by a Hybrid Process of Advanced Oxidation and Adsorption by Granular Activated Char (GAC)

This chapter presents the study on the degradation of a real pharmaceutical industrial effluent by a hybrid process of AOP and adsorption using ozone and granular activated char (GAC). Components of the effluent are identified and characterized. Removal of COD, ammonia, phenols, chloride, and BOD by the peroxone treatment are studied. The reaction kinetics of COD removal is also studied. COD removal by the adsorption by GAC is also studied, and the kinetics of adsorption is also determined.

6.1. Introduction

India has emerged as one of the top manufacturers of pharmaceuticals, producing 20% of generic medicines of the global market worth $19.14 billion in 2019 [282]. Most of the pharmaceutical industries are set up in the Indian cities of Ahmedabad, Bangalore, Hyderabad, and Mumbai. However, a relatively lenient regulatory for pharmaceutical waste disposal and irresponsible production have significantly affected the aquatic environment. The discharge from the pharmaceutical industries contains non-biodegradable recalcitrant organic substances, which have high toxicity towards aquatic and human life. 60 – 80% of the prescribed pharmaceuticals are excreted as unaltered, and they make their way to the sewage treatment plants and environment [5]. Several researchers [14–17] have detected pharmaceuticals in the

ground and surface water in the range of 15 – 1200 ng dm^{-3}. Recent studies have found traces of pharmaceuticals in the lakes, rivers, and wells in Hyderabad [263,283]. Although the amounts of pharmaceuticals were in the range of 90 – 31000 μg dm^{-3}, the chronic effects of these compounds are caused by their long-term exposure [18,19].

In the past three decades, the advanced oxidation processes (AOPs) have proven to be a perfect tool for removing refractory organic compounds such as pharmaceuticals [61,229,268,284,285] from synthetic wastewater. Most of the AOPs involve the generation of the hydroxyl radical as the primary oxidant. The possibility of a high degree of mineralization and the non-selective nature of the AOPs have rendered them attractive. However, the commercial application of the AOPs is still scarce due to their high cost. To overcome the high cost, the AOPs are often integrated with other techniques such as biodegradation, adsorption, electro-coagulation, and membrane separation. AOPs are used in the pretreatment stage to increase biodegradability and reduce the optimized integration cost for the highly contaminated industrial wastewaters [286].

This work deals with a real effluent collected from a pharmaceutical-manufacturing industry in India. Although a wide variety of literature is present for the pharmaceutical treatment by advanced oxidation processes from synthetic wastewater, very few studies have reported the treatment of real pharmaceutical industrial wastewater. The present study includes the complexities encountered for treating real wastewater, i.e., the presence of matrices and interference from other organic compounds. The pharmaceuticals present in the effluent were identified and classified. The presence of anti-cancer, antipsychotic, antidepressant, and antibiotic drugs was confirmed in the effluent. The effluent was treated with ozone in the presence of H_2O_2. The pretreated wastewater was passed through a bed of granular activated carbon (GAC) to reduce the COD further. The effects of pH, the concentration of H_2O_2, and

ozone feed rate were studied. The water quality parameters of the raw and treated wastewater were analyzed and discussed.

6.2. Results and discussion

6.2.1. Characterization of the effluent

The wastewater sample was qualitatively analyzed by HR-LCMS at the Sophisticated Analytical Instrument Facility (SAIF) of IIT Bombay (India). The chromatogram of wastewater is shown in Figure 6.1. The organic compounds identified are listed in Table 6.1.

Figure 6.1. Chromatogram of the industrial wastewater.

6.2.2. Peroxone treatment

The experiments were carried out at different pH (i.e., 5, 7.5, 9, and 11) for the ozone supply rate of 0.78 mg s^{-1}. The removal of COD, color, ammonia, chloride, and phenol was recorded with time for different pH. Figures 6.2a and 6.2b show the reduction in COD with time, and COD removal efficiency at different pH, respectively.

This Figure is ommited due to copyright issue

Figure 6.2. (a) Reduction of COD with respect to time, and (b) COD removal efficiency during reaction with peroxone at different pH (pH: 5 – 11, ozone flow rate: 0.78 mg s^{-1}, and $[H_2O_2]$: 0.176 mol dm^{-3}).

The COD removal was 75% (total COD removal = 1950 mg dm^{-3}) at pH 5, 85.3% (total COD removal = 2220 mg dm^{-3}) at pH 7.5, 86.5% (total COD removal = 2250 mg dm^{-3}) at pH 9, and 88.4% (total COD removal = 2300 mg dm^{-3}) at pH 11. At neutral and acidic conditions, molecular ozone reacts with the compounds. As the pH increases, the high rate of ozone decomposition leads to the generation of hydroxyl radicals vide equation (6.1) [287]. The non-selective hydroxyl radical is a better oxidant than ozone alone [288]. The initiation reactions for ozone decomposition in aqueous medium are expressed by the following equations [221]:

$$O_3 + OH^- \rightarrow O_2^{\bullet -} + HO_2^{\bullet} \quad (6.1)$$

$$O_3 + H_2O \rightarrow 2HO\bullet + O_2 \quad (6.2)$$

$$O_3 + HO\bullet \rightarrow HO_2^{\bullet} + O_2 \quad (6.3)$$

As the organic compounds present in the aqueous medium degrade, the concentration of carbonates and bicarbonates increases. The scavenging nature of these ions for the hydroxyl

radicals has been established in previous studies [221,289]. Carbonates and bicarbonates not only obstruct the generation of the accelerating agents for O_3 decomposition such as $O_2^{\bullet -}$, HO_2^-, and O_3^-, but also scavenge the HO• rapidly. The presence of these inhibitors also increases the stability of ozone and its exposure. After 100 min of reaction, the increase in the concentration of these scavengers slows down the reaction considerably. Beyond that, the ozone supply dosage does not significantly affect the mineralization efficiency. Therefore, it is concluded that the alkaline medium favors the mineralization, but the ozone concentration or its exposure for a longer duration does not accelerate the mineralization appreciably.

The reaction rate equation can be written in terms of COD and ozone concentrations present in the solution as follows:

$$\frac{-d[\mathrm{COD}]}{dt} = k'[\mathrm{COD}][\mathrm{O_3}] \tag{6.4}$$

The reaction kinetics can be considered as pseudo-first-order [290], inasmuch as the ozone supply rate was constant throughout the process for the first 120 min. The rate equation can be written as

$$\frac{-d[\mathrm{COD}]}{dt} = k[\mathrm{COD}] \tag{6.5}$$

As the processing time increased, the ozone concentration began to increase due to the lower ozone decomposition rate. Therefore, after 120 min of reaction, the ozone concentration cannot be considered to remain constant.

Integrating equation (6.5), we get

$$\ln \frac{[\mathrm{COD}]_0}{[\mathrm{COD}]_t} = kt \qquad (6.6)$$

where k is the pseudo-first-order rate constant, which is calculated by plotting $\ln \frac{[\mathrm{COD}]_0}{[\mathrm{COD}]_t}$ versus t. The effect of pH on k is shown in Figure 6.3. The value of k increased with increasing pH because the generation of hydroxyl radical was increased at the higher pH [291].

This Figure is ommited due to copyright issue

Figure 6.3. Effect of pH on the pseudo-first-order rate constant (k).

The raw wastewater had a dark-yellow color. On the application of peroxone, decolorization took place rapidly. The variation in pH favored decolorization in the same way as the COD removal. Although the molecular ozone also decolorizes the wastewater effectively despite its selective attacking nature, the color removal rate at the alkaline pH was higher than that in the acidic pH. Figure 6.4 shows the effect of pH on color removal. The effect of the concentration of H_2O_2 in the peroxone process is well known [292].

This Figure is ommited due to copyright issue

Figure 6.4. Effect of pH on the color removal with respect to time (ozone flow rate: 0.78 mg s^{-1}, and $[H_2O_2]$: 0.176 mol dm^{-3}).

It was observed that the water was dark yellow initially. After the peroxone treatment, the water started to decolorize rapidly, and after 180 min, the water turned into a clear liquid, as shown in Figure 6.5. Initially, the color disappeared rapidly, and after the final stage of reaction, the removal rate of the color was slower. This behavior was observed probably due to the nature of the products formed during the reaction. For example, during ozonation, initially, aromatic

compounds are converted into phenols and aromatic acids rapidly, then further reaction leads to aldehydes and acids, which have slower reactivity towards ozonation [293].

Figure 6.5. Decolorization of the pharmaceutical wastewater with respect to time: (a). t = 0, (b). t = 30, (c). t = 60, (d). t = 120, and (e). t = 180 min.

The concentration of the phenolic compounds present in the effluent decreased with time, as shown in Figure 6.6. The degradation of phenolic compounds followed the same trend as the COD and color.

Figure 6.6. Degradation of phenolic compounds present in wastewater at different pH (ozone flow rate: 0.78 mg s^{-1} and $[H_2O_2]$: 0.176 mol dm^{-3}).

The alkaline pH favored the removal due to the presence of the hydroxyl radicals generated *in situ*. At acidic pH, the removal was found to be 87.5%. At pH 7.5 – 11, phenol was not detected after the treatment. It was observed that the decrease in the removal rate was not commensurate with the COD removal. From Figure 6.6, it is observed that the values of phenol concentration at pH 7.5 and 9 are very close to each other, whereas the slow ozone decomposition at the neutral pH is already known [294]. It has also been reported that the presence of the phenolate ions promotes the generation of hydroxyl radical, which agrees with present behavior [294]. However, the degradation increased with the system pH, and the phenolic compounds were below the detectable range after the treatment.

Figure 6.7. Removal of ammonia during the peroxone process at different pH (ozone flow rate: 0.78 mg s^{-1}, and $[H_2O_2]$: 0.176 mol dm^{-3}).

The removal of ammonia by the peroxone process was also studied (see Figure 6.7). The ammonia present in the effluent was converted into nitrate by ozone and hydroxyl radical as follows [295,296]:

$$NH_3 + 4O_3 \rightarrow NO_3^- + 4O_2 + H_2O + H^+ \quad (6.7)$$

$$NH_3 + HO\bullet \rightarrow NH_2^\bullet + H_2O \quad (6.8)$$

$$NH_2^\bullet + 2O_3 \rightarrow NO_3^- + H_2O + O_2 \quad (6.9)$$

The removal of ammonia was found to be dependent on pH. Negligible removal of ammonia was observed at acidic pH due to the conversion of ammonia into ammonium, which is recalcitrant towards the oxidants [297]. At pH < 9, less availability of free ammonia and the predominance of ozone as oxidant slow down the removal of ammonia. The generation of bicarbonate ions may increase the removal by suppressing the radical reaction and accelerating the decomposition of ozone [298]. At pH > 9, the hydroxyl radicals take over the removal process and react with free ammonia. Further increase in the pH did not accelerate the removal significantly, although the removal by the peroxone process (>96%) was found to be more effective than ozone alone [297].

The concentration of the chloride ions was found to decrease by the peroxone process, as shown in Figure 6.8.

Figure 6.8. The concentration of chloride during the peroxone process at different pH (ozone flow rate: 0.78 mg s^{-1} and $[H_2O_2]$: 0.176 mol dm^{-3}).

It was mentioned in Section 6.2.2 that molecular ozone dominates as the main oxidant at the acidic pH and the hydroxyl radical plays the role of the dominant oxidant at the alkaline pH [298]. The reactions between the chloride ion and molecular ozone are as follows:

$$Cl^- + O_3 \rightarrow ClO^- + O_2 \quad (6.10)$$

$$ClO^- + O_3 \rightarrow ClO_2 + O_2 \quad (6.11)$$

$$ClO_2^- + O_3 \rightarrow ClO_2^{\bullet} + O_3^- \quad (6.12)$$

$$ClO_2^{\bullet} + O_3^- \rightarrow ClO_3 + O_3^- \quad (6.13)$$

Chloride ions are well known for their property of scavenging the hydroxyl radicals [299]. The reactions between the chloride ion and the hydroxyl radical are as follows [300–302]:

$$HO\bullet + Cl^- \rightarrow HOCl^{\bullet -} \quad (6.14)$$

$$HOCl^{\bullet -} + H^+ \rightarrow Cl\bullet + H_2O \quad (6.15)$$

$$Cl\bullet + OH^- \rightarrow HOCl^{\bullet -} \quad (6.16)$$

$$Cl\bullet + Cl^- \rightarrow Cl_2^{\bullet -} \quad (6.17)$$

$$Cl_2^{\bullet -} + Cl_2^{\bullet -} \rightarrow Cl_2 + 2Cl^- \quad (6.18)$$

It can be concluded that the gaseous chlorine would be formed at the alkaline pH during the reaction, but the chlorate ions are formed at the acidic pH. The chloride ion removal efficiency was found to have a moderate dependency on the pH.

6.2.3. Effect of H_2O_2 concentration

The positive effect of the presence of H_2O_2 on the ozonation process has been well-documented and extensively studied [120,303]. The presence of H_2O_2 triggers ozone decomposition at a faster rate [223]. Previous studies have suggested that higher H_2O_2 concentrations may scavenge hydroxyl radicals [120,303]. H_2O_2 can act as an inhibitor to ozone decomposition by triggering the free radical reactions at elevated concentrations, whereas it accelerates the production of hydroxyl radical at the optimal concentration. Present study also suggests the same behavior inasmuch as the COD removal decreased to 75% for 0.264 mol dm^{-3} of H_2O_2 whereas, for the H_2O_2 concentration of 0.176 mol dm^{-3}, the removal was 85%. It is concluded that the COD removal was dropped by 11.8% when the H_2O_2 dose was increased by 50%. However, the generation of the superoxide ions may prevent the scavenging of hydroxyl radicals via equation (6.19).

$$H_2O_2 + HO\bullet \rightarrow O_2^- + H_2O + H^+ \qquad (6.19)$$

The optimal concentration of H_2O_2 was 0.176 mol dm^{-3} because the maximum removal (i.e., 85%) was recorded at this concentration. Figure 6.9 shows the enhancement in the COD removal efficiency with increasing H_2O_2 concentration.

This Figure is ommited due to copyright issue

Figure 6.9. Effect of concentration of H_2O_2 on COD removal at pH 7.5 for the ozone flow rate of 0.78 mg s^{-1}.

For the H_2O_2 concentrations of 0, 0.088, 0.176, and 0.264 mol dm^{-3}, the COD removal efficiencies were 61.5, 73.8, 85.4, and 75%, respectively, for same initial pH. Hence, the COD removal efficiency increased with the increasing H_2O_2 concentration till the optimal H_2O_2 concentration, which corroborated the results reported [34,38].

This Figure is ommited due to copyright issue

Figure 6.10. Effect of concentration of H_2O_2 on biodegradability at pH 7.5 for the ozone flow rate of 0.78 mg s^{-1}.

Biodegradability is considered an essential factor for wastewater treatment. Figure 6.10 shows that the low biodegradability (BOD_5/COD = 0.1) of the effluent was enhanced after treatment to 0.55 for the 0.176 mol dm^{-3} H_2O_2. Several previous studies have also reported that the ozone-based processes generate more biodegradable products on degradation, and hence enhanced biodegradability can be achieved [293,305–308]. Ozone-based treatments reduce aromaticity, resulting in improved biodegradability [309,310]. The presence of H_2O_2 accelerates the production of hydroxyl radical, thereby generating more biodegradable metabolites than ozone alone due to its non-selective nature. At the optimal H_2O_2 concentration, the BOD_5/COD was increased by 5.5 folds, whereas it increased by three folds at 0.264 mol dm^{-3} H_2O_2 due to the less availability of the hydroxyl radical. It can be concluded that the peroxone treatment increases biodegradability and the H_2O_2 concentration plays an important role.

6.2.4. Treatment of the ozonated wastewater by adsorption

After ozonation, the wastewater was subjected to adsorption by GAC. The adsorption on GAC was effective for removing the COD further. The samples obtained from the peroxone process

were directly used for the adsorption studies without any further modification. The initial CODs considerably varied with pH (as shown in Figure 6.11).

This Figure is ommited due to copyright issue

Figure 6.11. Removal of COD during the adsorption on GAC (adsorbent dose: 4 g, temperature: 297 K).

All adsorption experiments were performed at 297 K. During adsorption, the residual COD decreased with time, and after a specific time, the residual COD was constant. It was assumed that the amount of adsorption and desorption of the metabolites were in a dynamic equilibrium at this point. The residual COD and time were termed as equilibrium COD and equilibrium time, respectively.

The kinetic data for the adsorption were analyzed using the pseudo-first-order, pseudo-second-order, and Elovich models at pH 5, 7.5, 9, and 11. The linearized forms of the pseudo-first-order and pseudo-second-order models can be expressed as

$$\ln\left(q_e - q_t\right) = \ln q_e - k_1 t \tag{6.20}$$

$$\frac{t}{q_t} = \frac{1}{k_2 q_e^{\,2}} + \frac{t}{q_e} \tag{6.21}$$

where q_e and q_t are the residual COD values at equilibrium and at time *t*, respectively. Both of these quantities are expressed in mg g^{-1}. The pseudo-first-order and pseudo-second-order rate constants, i.e., k_1 (min^{-1}) and k_2 (g mg^{-1} min^{-1}), respectively, were obtained from the linear plots of $\ln\left(q_e - q_t\right)$ versus *t* and t/q_t versus *t*, respectively. These plots are shown

in Figures 6.12a and 6.12b. The chemisorption process is best described by the Elovich model [311], as follows:

$$q_t = \frac{1}{b_e}\ln(a_e b_e) + \frac{1}{b_e}\ln t \qquad (6.22)$$

where a_e and b_e are the initial adsorption rate (mg g^{-1} min^{-1}) and extent of surface utilization (g mg^{-1}), respectively. The values of these two kinetic parameters can be obtained from the plot of q_t versus $\ln t$ (see Figure 6.12c).

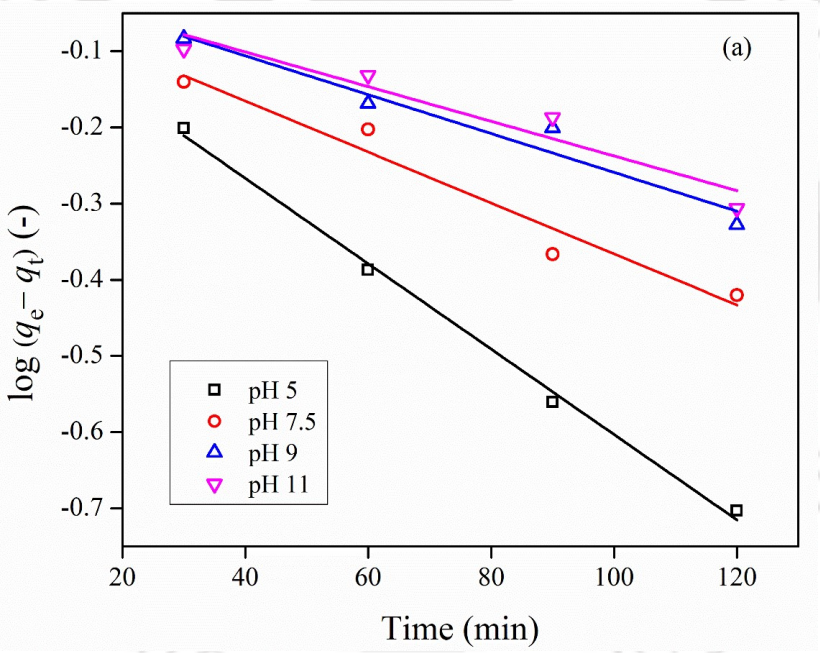

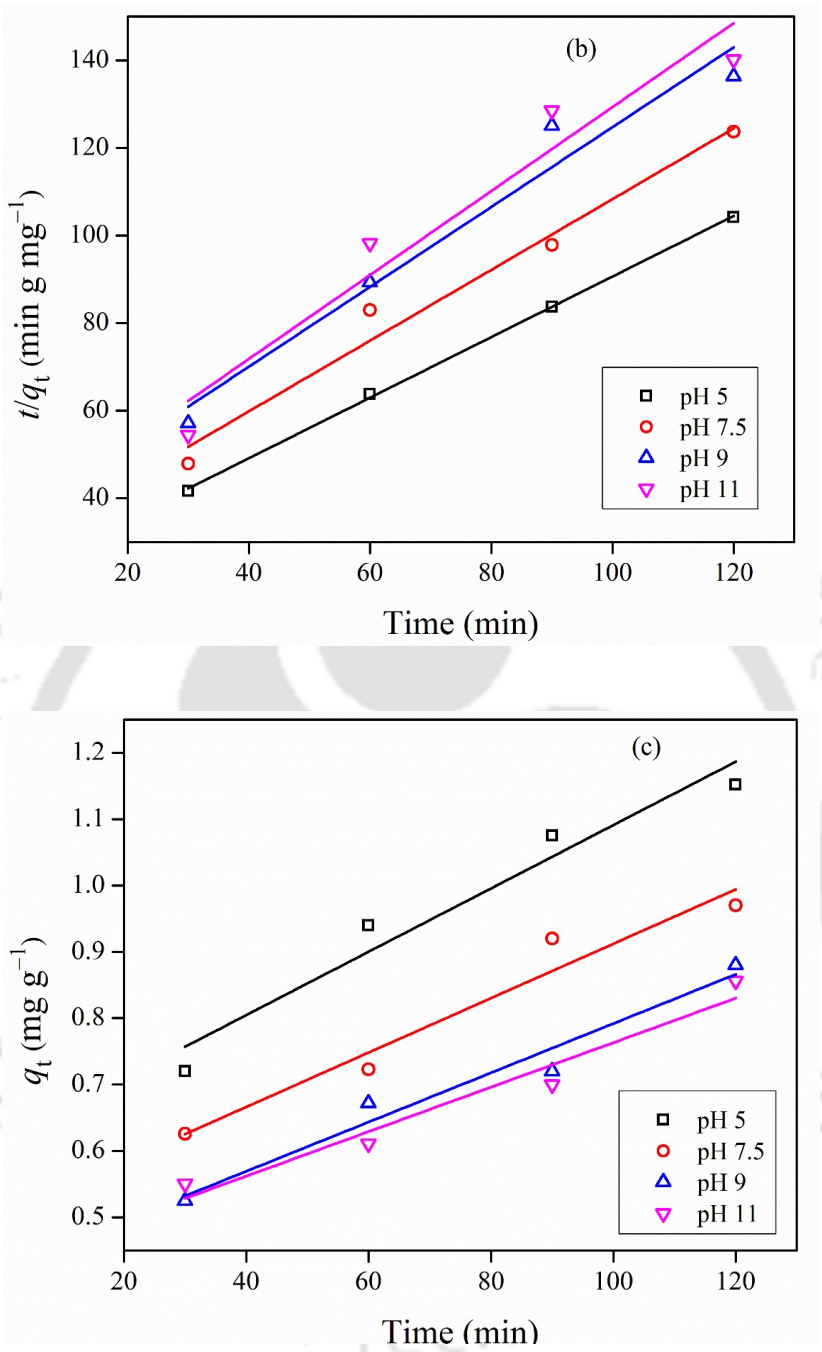

Figure 6.12. Adsorption kinetics for the removal of COD by GAC, (a) pseudo-first-order, (b) pseudo-second-order, and (c) Elovich model.

The deviation of the values obtained from the model and the experimental data were calculated in terms of the average relative error (ARE) as follows:

$$\mathrm{ARE}(\%) = \frac{100}{N}\sum_{i=1}^{N}\left|\frac{q_i^{\mathrm{cal}} - q_i^{\mathrm{exp}}}{q_i^{\mathrm{exp}}}\right| \tag{6.23}$$

where q^{cal} and q^{exp} (mg g^{-1}) denote the calculated and experimental adsorption capacities, respectively, and N represents the number of data points. The kinetics parameters calculated from the models are given in Table 6.3.

Table 6.3. Kinetic parameters for the adsorption on GAC (initial COD: 650 mg dm^{-3}, adsorbent dose: 4 g, sample volume: 20 cm^3, temperature: 297 K, and contact time: 160 min)

Kinetic Models	**pH**	**Kinetic Parameters**		**R^2**	**ARE (%)**
Pseudo-first-order		q_e (mg g^{-1})	k_1 (min^{-1})		
	5	0.9066	0.0129	0.9965	46.95
	7.5	0.9300	0.0076	0.9572	53.80
	9	0.9908	0.0058	0.9489	53.79
	11	0.9777	0.0053	0.9248	55.92
Pseudo-second-order		q_e (mg g^{-1})	k_2 (g mg^{-1} min^{-1})		
	5	1.4465	0.0222	0.9995	4.64
	7.5	1.2387	0.0236	0.9767	7.26

	9	1.0973	0.0247	0.9622	13.19
	11	1.0436	0.0274	0.9411	17.78
Elovich		a_e (mg g^{-1} min^{-1})	b_e (g mg^{-1})		
	5	0.1039	3.1766	0.9991	0.37
	7.5	0.0874	3.8285	0.9345	4.01
	9	0.0695	4.2608	0.9303	3.66
		0.0869	4.9285	0.8445	6.54

The coefficient of determination $\left(R^2\right)$ was closer to unity for the fits of the pseudo-second-order model, and the values of ARE were lower too, as compared to the pseudo-first-order model, for all pH. The point of zero charges (pH_{pzc}) of the GAC was in the range of 7.22 – 8 [312–314]. pH_{pzc} plays an important role in the adsorption at different pH. In the present study, the adsorption rate was higher in the acidic medium than in the alkaline medium. At pH < pH_{pzc}, the surface was positively charged, but at pH > pH_{pzc}, the surface was negatively charged. At pH < pH_{pzc} (i.e., pH = 5), the removal of COD by adsorption was maximum (i.e., 85%). At pH > pH_{pzc}, the adsorption efficiency ranged from 65 – 71%. The good fit of the pseudo-second-order kinetics to the experimental data indicates that the rate-limiting step was chemisorption or ion exchange [149,315,316]. The values of k_2 ranged from 0.0222 to 0.0274 g mg^{-1} min^{-1} for the pH range 5 – 11. At pH 5, the value of k_2 was minimum, i.e., 0.0222, which indicates that low pH favored the adsorption.

6.3. Conclusion

The present study demonstrates a hybrid approach for treating a real industrial effluent obtained from a pharmaceutical manufacturer. The pharmaceuticals identified in the effluent were mainly anti-cancer drugs, antipsychotics, anesthetics, and mild pain killers. A combination of ozone and H_2O_2 was effective in treating the wastewater. The COD removal of wastewater during the peroxone process was in the range of 75 – 88.5% for pH 5 – 11. All other parameters (i.e., color and the concentration of phenolic compounds, chloride, and ammonia) also decreased significantly. High pH and ozone supply rate accelerated the degradation process. The increasing concentration of H_2O_2 was also effective. The COD removal was increased by 50.4% when the H_2O_2 concentration was varied from 0 to 0.264 mol dm^{-3}. BOD_0/COD was also improved from 0.1 to 0.55 at 0.176 mol dm^{-3} H_2O_2. The ozonation followed the pseudo-first-order kinetics, and the rate constants were in the range of 1.42×10^{-4} – 3.35×10^{-4} s^{-1}.

Application of adsorption by GAC as a post-treatment after the peroxone treatment was effective. After adsorption, the COD value was further decreased by 34.5 – 41.2 %. The minimum COD achieved from the hybrid process was 190 mg dm^{-3} at pH 11 at the ozone flow rate of 0.78 mg s^{-1}, H_2O_2 concentration of 0.176 mol dm^{-3}, and an adsorbent dose of 4 g. The parameters for the adsorption kinetics for the pseudo-first-order, pseudo-second-order, and Elovich models were determined. The fit of the pseudo-second-order model was the best. The kinetic parameters for this model ranged from 2.22×10^{-2} to 2.74×10^{-2} g mg^{-1} min^{-1}. The removal of total COD by combining both the processes was in the range of 85.4 – 92.7%.

The results obtained from the present work demonstrate that a hybrid process of peroxone and adsorption can be applied to treat real industrial pharmaceutical wastewater containing complex organic compounds. A selective oxidant, i.e., ozone, was partially effective

for treating the complex wastewater, whereas the presence of a non-selective and stronger oxidizing species, i.e., HO• accelerated the degradation rapidly. Adsorption can be applied for the post-treatment of the ozonated wastewater for the removal of metabolites produced from ozonation. Further studies involving surface modification of the GAC and different adsorbent dosages may be carried out to understand the isotherms and kinetic behavior better.

Notations

Symbols

a_e	Initial rate of adsorption for the Elovich model (mg g^{-1} min^{-1})
b_e	Extent of surface coverage for chemisorption for the Elovich model (g mg^{-1})
N	Number of data points (-)
k	Rate constant for the pseudo-first-order reaction (min^{-1})
k'	Rate constant for the second-order reaction (dm^3 mol^{-1} s^{-1})
k_1	Pseudo-first-order rate constant for the adsorption kinetics (min^{-1})
k_2	Pseudo-second-order rate constant for the adsorption kinetics (g mg^{-1} min^{-1})
q_{cal}	Equilibrium values calculated from the kinetic model of adsorption (mg g^{-1})
q_e	Equilibrium adsorption capacity (mg g^{-1})
q_{exp}	Equilibrium values obtained from the adsorption experiments (mg g^{-1})
q_t	Adsorption capacity at time t (mg g^{-1})
t	Time (s)

Abbreviations

AOP	Advanced oxidation process
ARE	Average relative error
BOD	Biological oxygen demand
COD	Chemical oxygen demand
GAC	Granular activated char
HR-LCMS	High-resolution liquid chromatography
SAIF	Sophisticated analytical instrument facility

CHAPTER VII

TREATMENT OF A MIXTURE OF REAL PHARMACEUTICAL INDUSTRIAL EFFLUENTS BY COAGULATION AND PEROZONATION

CHAPTER VII

Treatment of a Mixture of Real Pharmaceutical Industrial Effluents with a Combination of Coagulation and Perozoznation

This chapter presents the study of the treatment of a mixture of two pharmaceutical effluents with a hybrid technology of coagulation by $FeCl_3$ and oxidation by O_3 and H_2O_2. This study aims for the higher removal of TOC, COD, and toxicity of the effluent. In the pre-treatment process, coagulation has been performed by $FeCl_3.6H_2O$ to reduce the TSS. The effects of the pH of the medium pH and the dose of the coagulant on COD removal have been studied during the coagulation treatment. Ozonation was applied after coagulation and the effect of operational parameters is analyzed. Toxicity analysis is also performed to ensure toxicity removal.

7.1. Introduction

Advances in lifestyle and disease profiling have resulted in a shift in the pattern of using medicines. In 2020, the worldwide pharmaceutical industry was valued at USD 1265.2 billion, with a projected growth rate of 3–6% by 2024 (USD 1420.0 billion) [1–3]. An increased sale of antibiotics was also recorded due to the ongoing breakout of coronavirus. 216 million excess doses of antibiotics were sold between June to September 2020 in India alone [4]. The discharged water from the pharmaceutical industries contains non-biodegradable recalcitrant organic substances, which have high toxicity towards the aquatic and human life.

Pharmaceuticals and their metabolites are frequently detected in ground and surface water bodies [10–13]. Pharmaceuticals were first detected as a pollutant in the aquatic system in 1970 [9]. Villages adjacent to the pharmaceutical industries are in alarming condition due to the highly contaminated groundwater, which leads to serious health problems such as cancer, miscarriage, and skin disorders [20].

Effluents from more specialized sources, such as pharmaceutical manufacturing plants, have received significantly less attention [317]. The dynamic and complex nature of the pharmaceutical effluents makes it difficult to anticipate their eco-toxicological risks [317]. Raw materials used in the pharmaceutical industries are mainly organic solvents, organic materials, inorganic and organic additives, catalysts, and distilled water. In turn, a large amount of effluent with a high loading of organics is produced [318]. Most of the pharmaceutical industries still rely on biological treatment. However, the inefficiency of biological treatments is already an established fact [227]. Most of the pharmaceuticals present in the effluent may exhibit recalcitrant behavior towards the conventional processes [318]. Pharmaceuticals and their metabolites make their way into the surface and potable water from various sources, i.e., excretion and improper disposal of medicines [319,320]. The emerging presence of APIs in the treated effluents is a matter of concern as their exposure poses a risk of developing resistance in biological organisms [319,321]. Non-biological treatments such as membrane separation, adsorptive removal, and electro-coagulation have been found to be effective for a few synthetic wastewaters. However, the unreasonably high operating cost and unfeasible maintenance operations restrict their use at the industrial level for effluent treatment.

Advanced oxidation processes (AOPs) have been applied to refractory organic contaminants found in surface water, groundwater, and industrial wastewater over the last two decades in order to improve the biodegradability and treatment efficacy [322,323]. These processes are based on generation of hydroxyl radicals *in-situ*, which are highly reactive and

non-selective in nature for the organic contaminants [324]. Various AOPs have been used for pharmaceutical wastewater treatments, i.e., Fenton and Fenton-like techniques [325,326], electro-oxidation [327], and ozonation [120]. Among these ozone and ozone-based, AOPs are the most famous and efficient. Ozone has the capability of generating hydroxyl radicals at alkaline pH and with a combination of H_2O_2 [211]. Most of the researchers have conducted their studies on pharmaceutical removal from synthetic wastewater by employing various AOPs [328–330]. However, the study on the removal of real pharmaceutical industrial effluent is still scarce in the literature [331–333].

In the light of the aforementioned facts, the present study investigates the degradation of a mixture of two real industrial pharmaceutical effluents with a hybrid coagulation process (i.e., alum) and AOP (i.e., O3/H2O2) The main objective of this study is to investigate the effect of the parameters of the peroxone process and coagulation on chemical oxygen demand (COD). The toxicity after the treatment was also assessed.

7.2. Results and discussion

7.2.1. Effluent characterization

The wastewater was qualitatively analyzed by HR-LCMS at the Sophisticated Analytical Instrument Facility (SAIF) of IIT Bombay (India). The chromatogram of wastewater is shown in Figure 7.1. The characteristics of raw effluent are listed in Table 7.1.

7.2.2. Coagulation studies

7.2.2.1. Effect of system pH on TSS and COD removal

To assess the effect of system pH on COD and TSS removal, the pH was varied in the range of 4−11. It was observed that the highest COD and TSS removal were 10.4 and 63%, respectively, at pH 6. Figures 7.2a and 7.2b exhibit the final COD and TSS removal, respectively, for different pH.

Figure 7.2. Effect of system pH on (a) COD value and (b) TSS removal of pharmaceutical effluent. Coagulant dose was 1250 mg dm^{-3} $FeCl_3.6H_2O$.

In Figures 7.2a and 7.2b, it can be observed that the highest TSS removal (i.e., 63%) and lowest COD (i.e., 1550 mg dm^{-3}) were achieved at pH 6. The removal of color was not studied as the same was performed by ozonation. A higher coagulant dose also affected the color of the effluent.

In the acidic medium, Fe^{2+} and Fe^{3+} are converted into $Fe(OH)_2^+$, which neutralizes the negatively charged particles, i.e., organic compounds and suspended particles. The formation of $Fe(OH)_2^+$ took place due to the interaction between the ferric and hydroxide ions present in the water. Generally, the pharmaceutical effluents are found to be rich in organic compounds. The maximum removal of COD and TSS at acidic pH also suggests the same. However, the formation of $Fe(OH)_3$, which is hydrophobic in nature, occurs in the alkaline medium. It can remove pollutants by surface interactions. At pH 6, mainly $Fe(OH)_2^+$ takes part in the removal process. However, the presence of $Fe(OH)_3$ also promotes the precipitation.

7.2.2.2. Effect of $FeCl_3$ dosage

By the study of pH effect, it was observed that at pH 6 the maximum removal of COD and TSS was achieved. To find the effect of coagulant dose, $FeCl_3$ concentration was varied 500 mg

dm^{-3} to 1500 mg dm^{-3}. It was seen that the maximum COD removal (10.4 %) was achieved at 1250 mg dm^{-3} dose. For $FeCl_3$ doses of 500, 750, and 1000 mg dm^{-3}, COD removal rates achieved were 1.7, 4.6, and 6.9 %, respectively. When $FeCl_3$ dose was further increased to 1500 mg dm^{-3}, COD removal efficiency witnessed a significant drop. For high dose of $FeCl_3$, color of sample was started to change from yellow to red as content of oxidized was increased. It can be concluded that the optimum pH and dose for coagulation for maximum COD removal were 6 and 1250 mg dm^{-3}, respectively.

7.2.3. Ozonation experiments

7.2.3.1. Effect of pH

Ozonation experiments were conducted for various pH (5–11) in the presence of H_2O_2 to analyze the effect of system pH on COD removal. It was observed from Figure 7.3 that the basic system pH favored the COD removal rate. At pH 11, the COD removal achieved was 91.6 %. Although at pH 13, a decrease in COD removal was witnessed. It was also concluded that the COD removal efficiency also improved significantly as pH increased. At acidic pH, the COD removal recorded was 68.4 %.

It is already an established fact that molecular ozone is present as an oxidizing agent at acidic pH whereas hydroxyl radicals dominate at basic pH [334–336]. The amount of ozone dissolved in water is determined by two contradictory mechanisms, i.e., dissociation of ozone by OH^- (> 48 mol^{-1} dm^3 s^{-1}) and supply of ozone by gas to liquid mass transfer [337]. When availability is limited (acidic medium), ozone depletion slows down to allow the accumulation of molecular ozone. An abundant amount of OH^- promotes ozone depletion to generate the hydroxyl radicals and prohibit ozone accumulation. Thus, the compounds vulnerable to electrophilic attack of molecular ozone are easily degradable at low pH. On the contrary,

compounds resistant to ozone degradation undergo rapid degradation at alkaline pH. It was observed that the COD rates were higher at alkali than acidic medium, which indicates the presence of ozone resistance compound in the effluent. Decomposition steps of ozone are basic medium are described below [338]

$$O_3 + OH^- \rightarrow O_2^{\bullet -} + HO_2^{\bullet} \qquad (k_1 = 70\ mol^{-1}\ dm^3\ s^{-1}) \qquad (7.1)$$

$$HO_2^{\bullet} \Leftrightarrow O_2^{\bullet -} + H^+ \qquad (pK = 4.8) \qquad (7.2)$$

$$O_2^{\bullet -} + O_3 \rightarrow O_3^{\bullet -} + O_2 \qquad (k_2 = 2\times10^{-9}\ mol^{-1}\ dm^3\ s^{-1}) \qquad (7.3)$$

$$O_3^{\bullet -} + H^+ \rightarrow HO_3^{\bullet} \qquad (k_3 = 5\times10^{10}\ mol^{-1}\ dm^3\ s^{-1}) \qquad (7.4)$$

$$HO_3^{\bullet} \rightarrow HO\bullet + O_2 \qquad (k_4 = 1.4\times10^{5}\ s^{-1}) \qquad (7.5)$$

$$HO\bullet + O_3 \rightarrow HO_2^{\bullet} + O_2 \qquad (k_5 = 2.8\times10^{9}\ mol^{-1}\ dm^3\ s^{-1}) \qquad (7.6)$$

This Figure is ommited due to copyright issue

Figure 7.3. Effect system pH on COD removal of effluent.

7.2.3.2. Effect of ozone supply

Figure 7.4 shows the system's COD removal efficiencies for three different ozone supplies (0.65, 0.67, and 0.78 mg s^{-1}). It was witnessed that the COD removal rate was constantly increasing the ozone supply. When ozone supply was increased from 0.65 to 0.67 mg s^{-1}

(increased by 3 %), COD removal was increased by 12 %. However, when ozone supply was further increased by 16 %, COD removal efficiency was increased by 15 % only.

The two-film theory might explain the increase in COD removal with increasing ozone supply [238,339]. According to two-film theory, mass transfer of ozone into the aqueous phase involves several stages, i.e., ozone diffusion in the gas phase to the gas-liquid interface, interface transfer of gas into the aqueous phase, and transfer across bulk liquid phase. Due to this, ozone availability for COD removal and to generate hydroxyl radical is enhanced, which explains the higher COD removal efficiency at high ozone supply. However, when the ozone concentration in the liquid phase hits its maximum value, the rate of chemical reaction will become increasingly important in controlling the process. Further increment in ozone supply will have no beneficial effect on degradation rate.

On the other hand, an increase in ozone supply and ozonation time reduce the ozone utilization and more than 50 % ozone would escape from the reactor. Therefore, optimizing the ozone supply and ozonation time is necessary for efficient process.

This Figure is ommited due to copyright issue

Figure 7.4. Effect of ozone supply on COD removal rate.

7.2.3.3. Effect of H_2O_2 concentration

Ozone in the presence of H_2O_2 generates hydroxyl radical, which is a non-selective more potent oxidant than ozone alone [108]. The yield of hydroxyl radicals depends on concentration of H_2O_2 decomposition.

Reaction of ozone with hydrogen peroxide is given in Equation (7.7)

$$O_3 + H_2O_2 \rightarrow 2HO\bullet + 3O_2 \qquad (7.7)$$

Figure 7.5 shows the COD removal efficiencies for initial H_2O_2 in the range of 0 – 0.25 mol dm^{-3}. In the absence of H_2O_2, only 45 % of the total COD was removed. A small quantity of H_2O_2 (0.08 mol dm^{-3}) accelerates the COD removal by 11 %. With the increasing quantity of H_2O_2, elevation in COD removal efficiency was observed. Although, there was no significant increase in COD removal was observed, when H_2O_2 concentration was increased above 0.25 mol dm^{-3}. Thus, it can be concluded that the maximum COD removal achieved was 75.5 % at 0.25 mol dm^{-3} of H_2O_2. Various studies [340–343] reported that the excess of H_2O_2 may consume the $HO\bullet$ (Equation (7.8)) The rate constant of $HO\bullet$ consumption by H_2O_2 is reported very high [338].

$$H_2O_2 + HO\bullet \rightarrow +O_2^{\bullet -} + H^+ + H_2O \qquad (k_6 = 2.7\times10^7\ mol^{-1}\ dm^3\ s^{-1}) \quad (7.8)$$

$$H_2O_2 + HO\bullet \rightarrow H_2O + HO_2^{\bullet} \qquad (7.9)$$

$HO\bullet$ may undergo various series of reaction [344,345]

$$2HO_2^{\bullet} \rightarrow H_2O_2 + O_2 \qquad (k_7 = 3.4\times10^7\ mol^{-1}\ dm^3\ s^{-1}) \quad (7.10)$$

$$H_2O_2 + HO_2^{\bullet} \rightarrow HO\bullet + O_2 + H_2O \qquad (7.11)$$

This Figure is ommited due to copyright issue

Figure 7.5. Variation in COD removal with increasing concentration of H_2O_2.

7.2.3.4. TOC removal during ozonation

The carbon content of the effluent was reduced during ozonation. Effect of pH and ozone supply rate was analyzed on TOC removal as shown in Figures 7.6a and 7.6b. In acidic pH, the removal achieved was 21%, whereas the TOC removal increased to 36% in alkaline pH. For

pH 9 and 11, the TOC removal was almost the same. Thus, further increase in pH did not contribute to TOC removal. A plateau was observed after 80 min of ozonation in TOC removal graphs. Constant values of TOC were indicated at the formation of recalcitrant compounds. Ozone supply was varied in the range of 0.65 – 0.78 mg s^{-1}. At lower ozone supply (0.65 and 0.67 mg s^{-1}), mineralization efficiency was found to be very low (10%) even at higher reaction time. This confirmed that the metabolites formed during ozonation required high ozone availability to be fully mineralized. When ozone supply was increased to 0.78 mg s^{-1}, mineralization efficiency was increased by 3 folds at pH 7. Maximum mineralization achieved was 36% at pH 9 – 11 at ozone supply of 0.78 mg s^{-1}.

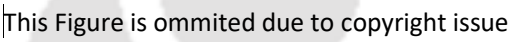

Figure 7.6. TOC removal during ozonation for (a) pH 5 – 11 and (b) ozone flow rate of 0.65 – 0.78 mg s^{-1}.

7.2.3.5. Color removal

Color of the raw effluent was found yellowish brown. Color of the effluent was completely removed for all system pH. Although in case of alkaline pH, the removal rate was faster than in acidic medium (See Figure 7.7). After performing ozonation experiments, color of the samples was measured immediately. Then samples were kept in dark to insure that the color was not reappearing. Complete removal of color was achieved in 40 min for alkaline medium whereas in case acidic medium time required it was increased by 50%.

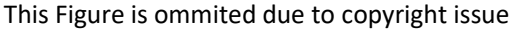

Figure 7.7. Removal of effluent color during ozonation for pH 5 – 11 for ozone supply of 0.78 mg s^{-1}.

7.2.3.6. Toxicity removal

Toxicity removal was assessed by using *E. coli*. and *S. Aureus*. Effluent before treatment exhibited the zone of inhibition for both the bacteria in the range of 16 – 19 mm. After treatment of 60 min reduced the diameter of the zone of inhibition by 25 – 26 %. The formation of zone of inhibition confirmed the presence of antibiotics in effluent in sufficient amount to kill the bacteria. After treatment the zone of inhibitions were completely disappeared as shown in Figure 7.8. Thus, it can be concluded that the antibiotics present in effluent were degraded efficiently.

This Figure is ommited due to copyright issue

Figure 7.8. Zone of inhibitions by raw and treated effluents for *E. Coli* and *S. Aureus*.

7.3. Conclusions

A real pharmaceutical industrial effluent was efficiently treated by a hybrid process of coagulation by $FeCl_3.6H_2O$ and ozonation. The optimum condition for coagulation was pH 6 and a coagulant dose of 1250 mg dm^{-3}. Total 10% COD and 63% TSS are removed by coagulation by $FeCl_3.6H_2O$ under the optimal conditions. Next, advanced oxidation has been performed by using O_3/H_2O_2. Maximum COD removal by $O_3 + H_2O_2$ is 91.6% at pH 11 and ozone supply of 0.78 mg s^{-1}. The COD removal efficiency drops to 45% in the absence of H_2O_2. Contribution of hydroxyl radicals in COD removal was also confirmed. Maximum mineralization efficiency achieved was 36% at optimum conditions. Toxicity analysis with the help of *S. Aureus* and *E. coli* has also been performed to assess the removal of the same. The effluent is found non-toxic after the treatment as no zone of inhibition is observed.

Notations

Abbreviations

AOP	Advanced oxidation process
API	Average relative error
COD	Chemical oxygen demand
HR-LCMS	High-resolution liquid chromatography
IIT	Indian Institute of technology
SAIF	Sophisticated analytical instrument facility
TOC	Total organic carbon
TSS	Total suspended solids
USD	United States Doller

CHAPTER VIII

CONCLUSIONS AND FUTURE SCOPE

CHAPTER VIII

Conclusions and Future Scope

This chapter summarizes the main conclusions drawn from this work and offers suggestions for future research.

8.1. Conclusions

This work dealt with degradation of pharmaceuticals in synthetic and real industrial effluents by ozonation and ozonation based hybrid processes. Promising results were observed during the treatment process. Three of the best-selling drugs were used to analyze the efficiency of ozonation process. Synthetic pharmaceutical wastewater spiked with NPX, DCF, and RNT have been successfully degraded by a combination of O_3 and H_2O_2. Alkaline medium and high ozone supply are found more efficient than the acidic medium. Complete removal has been achieved within 10 min for all three pharmaceuticals at various operating conditions. The presence of hydroxyl radicals in the reaction system considerably influenced the degradation process, which explains the increased removal efficiencies in the alkaline medium. According to the model, the concentration of ozone in the aqueous phase became constant within a min, indicating that the ozone concentration was constant throughout the reaction when compared to the drug concentration. Mass transfer study for ozone suggested that the alkaline pH and high ozone supply favored the mass transfer. However, it was also found that the high pH promotes the ozone dissociation to form hydroxyl radicals. Presence of hydroxyl radicals enhanced the degradation process. Degradation of drug followed the pseudo-first-order reaction for all drugs. The decarboxylation of NPX resulted in the formation of three

intermediates during ozonation whereas in DCF system total 13 intermediates were identified. Process were found effective in presence of other water matrix.

Ozonation based techniques were found efficient for the degradation of two different industrial effluents. In case of the first real industrial pharmaceutical effluent, maximum COD removal is 88.5% by $O_3 + H_2O_2$. Post-treatment, i.e., adsorptive removal by granular activated char has been performed on the first effluent inasmuch as after 3 h of AOP, COD values become constant. COD removal efficiencies are in the range of 75 – 88.5% in 3 h by $O_3 + H_2O_2$. Alkaline pH favors the degradation by AOP, whereas COD removal is higher in the acidic medium when the adsorption is carried out. The lowest COD for the hybrid process is 190 mg dm^{-3}. For the second effluent, pre-treatment was performed to remove TSS as a high amount of it has been observed. 10% COD and 63% TSS have been removed by coagulation by $FeCl_3.6H_2O$ at the optimal conditions. Maximum COD removal by $O_3 + H_2O_2$ is 91.6% at pH 11, and it reduces to 68.4% in the acidic medium. No toxicity has been found in both effluents after the treatments.

The results demonstrated that the ozonation technique can be used for the treatment of high strength real pharmaceutical industrial effluents as post or pre-treatment.

8.2. Future scope

The findings from the present work provide insight into the future scope for upgraded treatment techniques for the industrial pharmaceuticals effluents.

- AOPs can be used for pre-treatment to enhance the biodegradability of pharmaceutical effluents. Application of bio-treatment after the pre-treatment would be efficient and cost-effective.
- In the case of highly recalcitrant effluents, the hybrid process consists of the AOPs followed

by the adsorptive removal by a low-cost adsorbent.

A low-cost adsorbent for the post-treatment can be synthesized to remove the organic metabolites.

REFERENCES

References

[1] M. Mikulic, Global pharmaceutical market size 2001-2019 | Statista, Statista. (2020). https://www.statista.com/statistics/263102/pharmaceutical-market-worldwide-revenue-since-2001/ (accessed July 29, 2021).

[2] Global Pharmaceuticals Market Report, (2020). https://www.globenewswire.com/en/news-release/2021/03/31/2202135/28124/en/Global-Pharmaceuticals-Market-Report-2021-Market-is-Expected-to-Grow-from-1228-45-Billion-in-2020-to-1250-24-Billion-in-2021-Long-term-Forecast-to-2025-2030.html (accessed July 27, 2021).

[3] Global Pharmaceutical Industry | Market 2021 - FirmsWorld, (2021). https://firmsworld.com/global-pharmaceutical-industry-market-2021/ (accessed July 29, 2021).

[4] G. Sulis, B. Batomen, A. Kotwani, M. Pai, S. Gandra, Sales of antibiotics and hydroxychloroquine in India during the COVID-19 epidemic: An interrupted time series analysis, PLOS Med. 18 (2021) e1003682. DOI: 10.1371/JOURNAL.PMED.1003682.

[5] T. Heberer, Occurrence, fate, and removal of pharmaceutical residues in the aquatic environment: A review of recent research data, Toxicol. Lett. 131 (2002) 5–17. DOI: 10.1016/S0378-4274(02)00041-3.

[6] A. Pal, K.Y.H. Gin, A.Y.C. Lin, M. Reinhard, Impacts of emerging organic contaminants on freshwater resources: Review of recent occurrences, sources, fate and effects, Sci. Total Environ. 408 (2010) 6062–6069. DOI: 10.1016/j.scitotenv.2010.09.026.

[7] V.L. Cunningham, M. Buzby, T. Hutchinson, F. Mastrocco, N. Parke, N. Roden, Effects

of human pharmaceuticals on aquatic life: Next steps, Environ. Sci. Technol. 40 (2006) 3456–3462. DOI: 10.1021/es063017b.

[8] World Health Organisation, New report calls for urgent action to avert antimicrobial resistance crisis, Jt. News Release. 29 (2019) 2019–2022. https://www.who.int/news/item/29-04-2019-new-report-calls-for-urgent-action-to-avert-antimicrobial-resistance-crisis (accessed July 28, 2021).

[9] H.H. Tabak, R.L. Bunch, Steroid hormones as water pollutants. I. Metabolism of natural and synthetic ovulation-inhibiting hormones by microorganisms of activated sludge and primary settled sewage, Dev. Ind. Microbiol. 11 (1970) 367–376.

[10] A.M. Veach, M.J. Bernot, Temporal variation of pharmaceuticals in an urban and agriculturally influenced stream, Sci. Total Environ. 409 (2011) 4553–4563. DOI: 10.1016/J.SCITOTENV.2011.07.022.

[11] M.D. Camacho-Muñoz, J.L. Santos, I. Aparicio, E. Alonso, Presence of pharmaceutically active compounds in Doñana Park (Spain) main watersheds, J. Hazard. Mater. 177 (2010) 1159–1162. DOI: 10.1016/j.jhazmat.2010.01.030.

[12] K.K. Barnes, D.W. Kolpin, E.T. Furlong, S.D. Zaugg, M.T. Meyer, L.B. Barber, A national reconnaissance of pharmaceuticals and other organic wastewater contaminants in the United States - I) Groundwater, Sci. Total Environ. 402 (2008) 192–200. DOI: 10.1016/j.scitotenv.2008.04.028.

[13] A. Daneshvar, J. Svanfelt, L. Kronberg, G.A. Weyhenmeyer, Winter accumulation of acidic pharmaceuticals in a Swedish river, Environ. Sci. Pollut. Res. 17 (2010) 908–916. DOI: 10.1007/s11356-009-0261-y.

[14] M.J. Focazio, D.W. Kolpin, K.K. Barnes, E.T. Furlong, M.T. Meyer, S.D. Zaugg, L.B.

Barber, M.E. Thurman, A national reconnaissance for pharmaceuticals and other organic wastewater contaminants in the United States - II) Untreated drinking water sources, Sci. Total Environ. 402 (2008) 201–216. DOI: 10.1016/j.scitotenv.2008.02.021.

[15] T. V. Madureira, M.J. Rocha, Q.B. Cass, M.E. Tiritan, Development and optimization of a HPLC-DAD method for the determination of diverse pharmaceuticals in estuarine surface waters, J. Chromatogr. Sci. 48 (2010) 176–182. DOI: 10.1093/chromsci/48.3.176.

[16] J.W. Kim, H.S. Jang, J.G. Kim, H. Ishibashi, M. Hirano, K. Nasu, N. Ichikawa, Y. Takao, R. Shinohara, K. Arizono, Occurrence of pharmaceutical and personal care products (PPCPs) in surface water from Mankyung River, South Korea, J. Heal. Sci. 55 (2009) 249–258. DOI: 10.1248/jhs.55.249.

[17] M.S. Fram, K. Belitz, Occurrence and concentrations of pharmaceutical compounds in groundwater used for public drinking-water supply in California, Sci. Total Environ. 409 (2011) 3409–3417. DOI: 10.1016/j.scitotenv.2011.05.053.

[18] M.D. Hernando, M. Mezcua, A.R. Fernández-Alba, D. Barceló, Environmental risk assessment of pharmaceutical residues in wastewater effluents, surface waters and sediments, Talanta 69 (2006) 334–342. DOI: 10.1016/j.talanta.2005.09.037.

[19] W. Sanchez, W. Sremski, B. Piccini, O. Palluel, E. Maillot-Maréchal, S. Betoulle, A. Jaffal, S. Aït-Aïssa, F. Brion, E. Thybaud, N. Hinfray, J.M. Porcher, Adverse effects in wild fish living downstream from pharmaceutical manufacture discharges, Environ. Int. 37 (2011) 1342–1348. DOI: 10.1016/j.envint.2011.06.002.

[20] Nordea, Impacts of pharmaceutical pollution on communities and environment in India Impacts of pharmaceutical pollution on communities and environment in India, Nord.

Asset Manag. (2016) 1–33. http://changingmarkets.org/wp-content/uploads/2016/12/Impacts-of-pharmaceutical-pollution-on-communities-and-environment-in-India-WEB-light.pdf%0Ahttp://changingmarkets.org/wp-content/uploads/2017/07/2016-04_pharma-pollution-in-India_small_web_spread.pdf.

[21] R.S. Rana, P. Singh, V. Kandari, R. Singh, R. Dobhal, S. Gupta, A review on characterization and bioremediation of pharmaceutical industries' wastewater: An Indian perspective, Appl. Water Sci. 7 (2017) 1–12. DOI: 10.1007/s13201-014-0225-3.

[22] K. Kümmerer, Antibiotics in the aquatic environment – A review – Part I, Chemosphere. 75 (2009) 417–434. DOI: 10.1016/J.CHEMOSPHERE.2008.11.086.

[23] R.P. Wenzel, T.F. Brewer,J.P. Butzler, A guide to infection control in the hospital. Elsevier (2002). PMPH-USA.

[24] WHO | World Health Organization, (n.d.). https://www.who.int/ (accessed August 4, 2021).

[25] M. Qadir, D. Wichelns, L. Raschid-Sally, P.G. McCornick, P. Drechsel, A. Bahri, P.S. Minhas, The challenges of wastewater irrigation in developing countries, Agric. Water Manag. 97 (2010) 561–568. DOI: 10.1016/J.AGWAT.2008.11.004.

[26] K. Kümmerer, Resistance in the environment, J. Antimicrob. Chemother. 54 (2004) 311–320. DOI: 10.1093/jac/dkh325.

[27] Environment Screening report Iceland Chapter 27-Environment Date of screening meetings, 2011.

[28] Council of the European Communities, Directive 2013/39/EU of the European Parliament and of the Council of 12 August 2013 amending Directives 2000/60/EC and 2008/105/EC as regards priority substances in the field of water policy, 2013. https://eur-

lex.europa.eu/legal-content/EN/ALL/?uri=celex:32013L0039 (accessed August 3, 2021).

[29] A. Gogoi, P. Mazumder, V.K. Tyagi, G.G. Tushara Chaminda, A.K. An, M. Kumar, Occurrence and fate of emerging contaminants in water environment: A review, Groundw. Sustain. Dev. 6 (2018) 169–180. DOI: 10.1016/j.gsd.2017.12.009.

[30] Z. Barnes, M. Caudwell, P. Chadwick, Tool for risk management of water utility assets. Water Research Foundation (2009).

[31] R. López-Serna, M. Petrović, D. Barceló, Occurrence and distribution of multi-class pharmaceuticals and their active metabolites and transformation products in the Ebro River basin (NE Spain), Sci. Total Environ. 440 (2012) 280–289. DOI: 10.1016/j.scitotenv.2012.06.027.

[32] M. Gros, S. Rodríguez-Mozaz, D. Barceló, Fast and comprehensive multi-residue analysis of a broad range of human and veterinary pharmaceuticals and some of their metabolites in surface and treated waters by ultra-high-performance liquid chromatography coupled to quadrupole-linear ion trap tandem, J. Chromatogr. A. 1248 (2012) 104–121. DOI: 10.1016/j.chroma.2012.05.084.

[33] R. López-Serna, M. Petrović, D. Barceló, Development of a fast instrumental method for the analysis of pharmaceuticals in environmental and wastewaters based on ultra high performance liquid chromatography (UHPLC)-tandem mass spectrometry (MS/MS), Chemosphere. 85 (2011) 1390–1399. DOI: 10.1016/j.chemosphere.2011.07.071.

[34] R. López-Serna, S. Pérez, A. Ginebreda, M. Petrović, D. Barceló, Fully automated determination of 74 pharmaceuticals in environmental and waste waters by online solid

phase extraction-liquid chromatography-electrospray-tandem mass spectrometry, Talanta. 83 (2010) 410–424. DOI: 10.1016/j.talanta.2010.09.046.

[35] M.R. Boleda, M.T. Galceran, F. Ventura, Validation and uncertainty estimation of a multiresidue method for pharmaceuticals in surface and treated waters by liquid chromatography-tandem mass spectrometry, J. Chromatogr. A. 1286 (2013) 146–158. DOI: 10.1016/j.chroma.2013.02.077.

[36] P. Paíga, L.H.M.L.M. Santos, S. Ramos, S. Jorge, J.G. Silva, C. Delerue-Matos, Presence of pharmaceuticals in the Lis river (Portugal): Sources, fate and seasonal variation, Sci. Total Environ. 573 (2016) 164–177. DOI: 10.1016/j.scitotenv.2016.08.089.

[37] T. Radović, S. Grujić, A. Petković, M. Dimkić, M. Laušević, Determination of pharmaceuticals and pesticides in river sediments and corresponding surface and ground water in the Danube River and tributaries in Serbia, Environ. Monit. Assess. 187 (2015) 1–17. DOI: 10.1007/s10661-014-4092-z.

[38] B. Morasch, Occurrence and dynamics of micropollutants in a karst aquifer, Environ. Pollut. 173 (2013) 133–137. DOI: 10.1016/j.envpol.2012.10.014.

[39] R. López-Serna, A. Jurado, E. Vázquez-Suñé, J. Carrera, M. Petrović, D. Barceló, Occurrence of 95 pharmaceuticals and transformation products in urban groundwaters underlying the metropolis of Barcelona, Spain, Environ. Pollut. 174 (2013) 305–315. DOI: 10.1016/j.envpol.2012.11.022.

[40] L. Tong, S. Huang, Y. Wang, H. Liu, M. Li, Occurrence of antibiotics in the aquatic environment of Jianghan Plain, central China, Sci. Total Environ. 497–498 (2014) 180–187. DOI: 10.1016/j.scitotenv.2014.07.068.

[41] A. Chiffre, F. Degiorgi, A. Buleté, L. Spinner, P.M. Badot, Occurrence of pharmaceuticals in WWTP effluents and their impact in a karstic rural catchment of Eastern France, Environ. Sci. Pollut. Res. 23 (2016) 25427–25441. DOI: 10.1007/s11356-016-7751-5.

[42] S. Lardy-Fontan, V. Brieudes, B. Lalere, P. Candido, G. Couturier, H. Budzinski, G. Lavison-Bompard, For more reliable measurements of pharmaceuticals in the environment: Overall measurement uncertainty estimation, QA/QC implementation and metrological considerations. A case study on the Seine River, Trends Anal. Chem. 77 (2016) 76–86. DOI: 10.1016/j.trac.2015.12.011.

[43] C.E. Chen, H. Zhang, K.C. Jones, A novel passive water sampler for in situ sampling of antibiotics, J. Environ. Monit. 14 (2012) 1523–1530. DOI: 10.1039/c2em30091e.

[44] L.A. Schaider, R.A. Rudel, J.M. Ackerman, S.C. Dunagan, J.G. Brody, Pharmaceuticals, perfluorosurfactants, and other organic wastewater compounds in public drinking water wells in a shallow sand and gravel aquifer, Sci. Total Environ. 468–469 (2014) 384–393. DOI: 10.1016/j.scitotenv.2013.08.067.

[45] F. Riva, E. Zuccato, S. Castiglioni, Prioritization and analysis of pharmaceuticals for human use contaminating the aquatic ecosystem in Italy, J. Pharm. Biomed. Anal. 106 (2015) 71–78. DOI: 10.1016/j.jpba.2014.10.003.

[46] G.A. Khan, R. Lindberg, R. Grabic, J. Fick, The development and application of a system for simultaneously determining anti-infectives and nasal decongestants using on-line solid-phase extraction and liquid chromatography-tandem mass spectrometry, J. Pharm. Biomed. Anal. 66 (2012) 24–32. DOI: 10.1016/j.jpba.2012.02.011.

[47] P. Vazquez-Roig, V. Andreu, C. Blasco, F. Morillas, Y. Picó, Spatial distribution of

illicit drugs in surface waters of the natural park of Pego-Oliva Marsh (Valencia, Spain), Environ. Sci. Pollut. Res. 19 (2012) 971–982. DOI: 10.1007/s11356-011-0617-y.

[48] J. Fick, H. Söderström, R.H. Lindberg, C. Phan, M. Tysklind, D.G.J. Larsson, Contamination of surface, ground, and drinking water from pharmaceutical production, Environ. Toxicol. Chem. 28 (2009) 2522–2527. DOI: 10.1897/09-073.1.

[49] B.R. Ramaswamy, G. Shanmugam, G. Velu, B. Rengarajan, D.G.J. Larsson, GC-MS analysis and ecotoxicological risk assessment of triclosan, carbamazepine and parabens in Indian rivers, J. Hazard. Mater. 186 (2011) 1586–1593. DOI: 10.1016/j.jhazmat.2010.12.037.

[50] L. Wolf, C. Zwiener, M. Zemann, Tracking artificial sweeteners and pharmaceuticals introduced into urban groundwater by leaking sewer networks, Sci. Total Environ. 430 (2012) 8–19. DOI: 10.1016/j.scitotenv.2012.04.059.

[51] N. Gottschall, E. Topp, C. Metcalfe, M. Edwards, M. Payne, S. Kleywegt, P. Russell, D.R. Lapen, Pharmaceutical and personal care products in groundwater, subsurface drainage, soil, and wheat grain, following a high single application of municipal biosolids to a field, Chemosphere. 87 (2012) 194–203. DOI: 10.1016/j.chemosphere.2011.12.018.

[52] M. Petrović, B. Škrbić, J. Živančev, L. Ferrando-Climent, D. Barcelo, Determination of 81 pharmaceutical drugs by high performance liquid chromatography coupled to mass spectrometry with hybrid triple quadrupole-linear ion trap in different types of water in Serbia, Sci. Total Environ. 468–469 (2014) 415–428. DOI: 10.1016/j.scitotenv.2013.08.079.

[53] N.H. Tran, J. Li, J. Hu, S.L. Ong, Occurrence and suitability of pharmaceuticals and

personal care products as molecular markers for raw wastewater contamination in surface water and groundwater, Environ. Sci. Pollut. Res. 21 (2014) 4727–4740. DOI: 10.1007/s11356-013-2428-9.

[54] J. Giebułtowicz, A. Stankiewicz, P. Wroczyński, G. Nałęcz-Jawecki, Occurrence of cardiovascular drugs in the sewage-impacted Vistula River and in tap water in the Warsaw region (Poland), Environ. Sci. Pollut. Res. 23 (2016) 24337–24349. DOI: 10.1007/s11356-016-7668-z.

[55] P. Grenni, L. Patrolecco, N. Ademollo, A. Tolomei, A. Barra Caracciolo, Degradation of Gemfibrozil and Naproxen in a river water ecosystem, Microchem. J. 107 (2013) 158–164. DOI: 10.1016/j.microc.2012.06.008.

[56] C. Valhondo, J. Carrera, C. Ayora, I. Tubau, L. Martinez-Landa, K. Nödler, T. Licha, Characterizing redox conditions and monitoring attenuation of selected pharmaceuticals during artificial recharge through a reactive layer, Sci. Total Environ. 512–513 (2015) 240–250. DOI: 10.1016/j.scitotenv.2015.01.030.

[57] M. Zemann, L. Wolf, F. Grimmeisen, A. Tiehm, J. Klinger, H. Hötzl, N. Goldscheider, Tracking changing X-ray contrast media application to an urban-influenced karst aquifer in the Wadi Shueib, Jordan, Environ. Pollut. 198 (2015) 133–143. DOI: 10.1016/J.ENVPOL.2014.11.033.

[58] V. Matamoros, C.A. Arias, L.X. Nguyen, V. Salvadó, H. Brix, Occurrence and behavior of emerging contaminants in surface water and a restored wetland, Chemosphere. 88 (2012) 1083–1089. DOI: 10.1016/j.chemosphere.2012.04.048.

[59] V. Brieudes, S. Lardy-Fontan, B. Lalere, S. Vaslin-Reimann, H. Budzinski, Validation and uncertainties evaluation of an isotope dilution-SPE-LC-MS/MS for the

quantification of drug residues in surface waters, Talanta. 146 (2016) 138–147. DOI: 10.1016/j.talanta.2015.06.073.

[60] D.R. Baker, B. Kasprzyk-Hordern, Spatial and temporal occurrence of pharmaceuticals and illicit drugs in the aqueous environment and during wastewater treatment: New developments, Sci. Total Environ. 454–455 (2013) 442–456. DOI: 10.1016/j.scitotenv.2013.03.043.

[61] A.M. Deegan, B. Shaik, K. Nolan, K. Urell, M. Oelgemöller, J. Tobin, A. Morrissey, Treatment options for wastewater effluents from pharmaceutical companies, Int. J. Environ. Sci. Technol. 8 (2011) 649–666. DOI: 10.1007/BF03326250.

[62] S. Rezania, J. Park, M.F. Md Din, S. Mat Taib, A. Talaiekhozani, K. Kumar Yadav, H. Kamyab, Microplastics pollution in different aquatic environments and biota: A review of recent studies, Mar. Pollut. Bull. 133 (2018) 191–208. DOI: 10.1016/j.marpolbul.2018.05.022.

[63] Y.A. Oktem, O. Ince, P. Sallis, T. Donnelly, B.K. Ince, Anaerobic treatment of a chemical synthesis-based pharmaceutical wastewater in a hybrid upflow anaerobic sludge blanket reactor, Bioresour. Technol. 99 (2008) 1089–1096. DOI: 10.1016/j.biortech.2007.02.036.

[64] A.H. Khan, H.A. Aziz, N.A. Khan, M.A. Hasan, S. Ahmed, I.H. Farooqi, A. Dhingra, V. Vambol, F. Changani, M. Yousefi, S. Islam, N. Mozaffari, M.S. Mahtab, Impact, disease outbreak and the eco-hazards associated with pharmaceutical residues: A Critical review, Int. J. Environ. Sci. Technol. (2021) 1–12. DOI: 10.1007/s13762-021-03158-9.

[65] A.B.A. Boxall, M.A. Rudd, B.W. Brooks, D.J. Caldwell, K. Choi, S. Hickmann, E.

Innes, K. Ostapyk, J.P. Staveley, T. Verslycke, G.T. Ankley, K.F. Beazley, S.E. Belanger, J.P. Berninger, P. Carriquiriborde, A. Coors, P.C. DeLeo, S.D. Dyer, J.F. Ericson, F. Gagné, J.P. Giesy, T. Gouin, L. Hallstrom, M. V. Karlsson, D.G. Joakim Larsson, J.M. Lazorchak, F. Mastrocco, A. McLaughlin, M.E. McMaster, R.D. Meyerhoff, R. Moore, J.L. Parrott, J.R. Snape, R. Murray-Smith, M.R. Servos, P.K. Sibley, J.O. Straub, N.D. Szabo, E. Topp, G.R. Tetreault, V.L. Trudeau, G. Van Der Kraak, Pharmaceuticals and personal care products in the environment: What are the big questions?, Environ. Health Perspect. 120 (2012) 1221–1229. DOI: 10.1289/ehp.1104477.

[66] J. Garric, Emerging Issues in Ecotoxicology: Pharmaceuticals and Personal Care Products (PPCPs), Encycl. Aquat. Ecotoxicol. (2013) 407–428. DOI: 10.1007/978-94-007-5704-2_39.

[67] A. Majumder, B. Gupta, A.K. Gupta, Pharmaceutically active compounds in aqueous environment: A status, toxicity and insights of remediation, Environ. Res. 176 (2019) 108542. DOI: 10.1016/j.envres.2019.108542.

[68] S.A. Snyder, Occurrence, treatment, and toxicological relevance of EDCs and pharmaceuticals in water, Ozone Sci. Eng. 30 (2008) 65–69. DOI: 10.1080/01919510701799278.

[69] N.H. Tran, M. Reinhard, K.Y.H. Gin, Occurrence and fate of emerging contaminants in municipal wastewater treatment plants from different geographical regions-a review, Water Res. 133 (2018) 182–207. DOI: 10.1016/j.watres.2017.12.029.

[70] A. Harada, K. Komori, N. Nakada, K. Kitamura, Y. Suzuki, Biological effects of PPCPs on aquatic lives and evaluation of river waters affected by different wastewater treatment levels, Water Sci. Technol. 58 (2008) 1541–1546. DOI: 10.2166/wst.2008.742.

[71] N.K. Haro, P. Del Vecchio, N.R. Marcilio, L.A. Féris, Removal of atenolol by adsorption – Study of kinetics and equilibrium, J. Clean. Prod. 154 (2017) 214–219. DOI: 10.1016/j.jclepro.2017.03.217.

[72] V. de Jesus Gaffney, C.M.M. Almeida, A. Rodrigues, E. Ferreira, M.J. Benoliel, V.V. Cardoso, Occurrence of pharmaceuticals in a water supply system and related human health risk assessment, Water Res. 72 (2015) 199–208. DOI: 10.1016/j.watres.2014.10.027.

[73] S. Rodriguez-Mozaz, S. Chamorro, E. Marti, B. Huerta, M. Gros, A. Sànchez-Melsió, C.M. Borrego, D. Barceló, J.L. Balcázar, Occurrence of antibiotics and antibiotic resistance genes in hospital and urban wastewaters and their impact on the receiving river, Water Res. 69 (2015) 234–242. DOI: 10.1016/j.watres.2014.11.021.

[74] N.A. Khan, S.U. Khan, S. Ahmed, I.H. Farooqi, M. Yousefi, A.A. Mohammadi, F. Changani, Recent trends in disposal and treatment technologies of emerging-pollutants-A critical review, Trends Anal. Chem. 122 (2020) 115744. DOI: 10.1016/j.trac.2019.115744.

[75] S. Castiglioni, R. Bagnati, R. Fanelli, F. Pomati, D. Calamari, E. Zuccato, Removal of pharmaceuticals in sewage treatment plants in Italy, Environ. Sci. Technol. 40 (2006) 357–363. DOI: 10.1021/es050991m.

[76] N.A. Oz, O. Ince, B.K. Ince, Effect of wastewater composition on methanogenic activity in an anaerobic reactor, J. Environ. Sci. Heal. - Part A Toxic/Hazardous Subst. Environ. Eng. 39 (2004) 2941–2953. DOI: 10.1081/LESA-200034284.

[77] M. Kim, P. Guerra, A. Shah, M. Parsa, M. Alaee, S.A. Smyth, Removal of pharmaceuticals and personal care products in a membrane bioreactor wastewater

treatment plant, Water Sci. Technol. 69 (2014) 2221–2229. DOI: 10.2166/wst.2014.145.

[78] M. Zupanc, T. Kosjek, M. Petkovšek, M. Dular, B. Kompare, B. Širok, Ž. Blažeka, E. Heath, Removal of pharmaceuticals from wastewater by biological processes, hydrodynamic cavitation and UV treatment, Ultrason. Sonochem. 20 (2013) 1104–1112. DOI: 10.1016/j.ultsonch.2012.12.003.

[79] P.G.Patil , G.S. Kulkarni, Aerobic sequencing batch reactor for wastewater treatment: A review, Int. J. Eng. Res. Technol. 10 (2013) 534–550.

[80] N.H. Tran, H. Chen, M. Reinhard, F. Mao, K.Y.H. Gin, Occurrence and removal of multiple classes of antibiotics and antimicrobial agents in biological wastewater treatment processes, Water Res. 104 (2016) 461–472. DOI: 10.1016/j.watres.2016.08.040.

[81] A. Langenhoff, N. Inderfurth, T. Veuskens, G. Schraa, M. Blokland, K. Kujawa-Roeleveld, H. Rijnaarts, Microbial removal of the pharmaceutical compounds ibuprofen and diclofenac from wastewater, Biomed Res. Int. 2013 (2013). DOI: 10.1155/2013/325806.

[82] J. Rodriguez, S. Stopić, G. Krause, B. Friedrich, Feasibility assessment of electrocoagulation towards a new sustainable wastewater treatment, Environ. Sci. Pollut. Res. 14 (2007) 477–482. DOI: 10.1065/espr2007.05.424.

[83] O. Sahu, B. Mazumdar, P.K. Chaudhari, Treatment of wastewater by electrocoagulation: A review, Environ. Sci. Pollut. Res. 21 (2014) 2397–2413. DOI: 10.1007/s11356-013-2208-6.

[84] S. Garcia-Segura, M.M.S.G. Eiband, J.V. de Melo, C.A. Martínez-Huitle, Electrocoagulation and advanced electrocoagulation processes: A general review about

the fundamentals, emerging applications and its association with other technologies, J. Electroanal. Chem. 801 (2017) 267–299. DOI: 10.1016/j.jelechem.2017.07.047.

[85] P.K. Holt, G.W. Barton, M. Wark, C.A. Mitchell, A quantitative comparison between chemical dosing and electrocoagulation, Colloids Surfaces A Physicochem. Eng. Asp. 211 (2002) 233–248. DOI: 10.1016/S0927-7757(02)00285-6.

[86] S. Mahesh, B. Prasad, I.D. Mall, I.M. Mishra, Electrochemical degradation of pulp and paper mill wastewater. Part 1. COD and color removal, Ind. Eng. Chem. Res. 45 (2006) 42830–2839 DOI: 10.1021/ie0514096.

[87] A.H. Essadki, M. Bennajah, B. Gourich, C. Vial, M. Azzi, H. Delmas, Electrocoagulation/electroflotation in an external-loop airlift reactor—Application to the decolorization of textile dye wastewater: A case study, Chem. Eng. Process. Process Intensif. 47 (2008) 1211–1223. DOI: 10.1016/J.CEP.2007.03.013.

[88] B.H. Diya'Uddeen, W.M.A.W. Daud, A.R. Abdul Aziz, Treatment technologies for petroleum refinery effluents: A review, Process Saf. Environ. Prot. 89 (2011) 95–105. DOI: 10.1016/J.PSEP.2010.11.003.

[89] I. Linares-Hernández, C. Barrera-Díaz, P.C. Juárez-GarcíaRojas, G. Roa-Morales, F. Ureña, Industrial wastewater treatment by electrocoagulation-direct anodic oxidation system, ECS Trans. 20 (2019) 301–311. DOI: 10.1149/1.3268398.

[90] M.H. El-Naas, S. Al-Zuhair, A. Al-Lobaney, S. Makhlouf, Assessment of electrocoagulation for the treatment of petroleum refinery wastewater, J. Environ. Manage. 91 (2009) 180–185. DOI: 10.1016/j.jenvman.2009.08.003.

[91] S. Zaidi, T. Chaabane, V. Sivasankar, A. Darchen, R. Maachi, T.A.M. Msagati, Electro-coagulation coupled electro-flotation process: Feasible choice in doxycycline removal

from pharmaceutical effluents, Arab. J. Chem. 12 (2019) 2798–2809. DOI: 10.1016/j.arabjc.2015.06.009.

[92] K. Govindan, A. Angelin, M. Kalpana, M. Rangarajan, P. Shankar, A. Jang, Electrocoagulants characteristics and application of electrocoagulation for micropollutant removal and transformation mechanism, ACS Appl. Mater. Interfaces. 12 (2020) 1775–1788. DOI: 10.1021/acsami.9b16559.

[93] M. Ek, C. Baresel, J. Magnér, R. Bergstrom̈, M. Harding, Activated carbon for the removal of pharmaceutical residues from treated wastewater, Water Sci. Technol. 69 (2014) 2372–2380. DOI: 10.2166/wst.2014.172.

[94] A. Alahabadi, A. Hosseini-Bandegharaei, G. Moussavi, B. Amin, A. Rastegar, H. Karimi-Sani, M. Fattahi, M. Miri, Comparing adsorption properties of NH_4Cl-modified activated carbon towards chlortetracycline antibiotic with those of commercial activated carbon, J. Mol. Liq. 232 (2017) 367–381. DOI: 10.1016/J.MOLLIQ.2017.02.077.

[95] L. Nielsen, M.J. Biggs, W. Skinner, T.J. Bandosz, The effects of activated carbon surface features on the reactive adsorption of carbamazepine and sulfamethoxazole, Carbon 80 (2014) 419–432. DOI: 10.1016/j.carbon.2014.08.081.

[96] E. V. Liakos, K. Rekos, D.A. Giannakoudakis, A.C. Mitropoulos, J. Fu, G.Z. Kyzas, Activated porous carbon derived from tea and plane tree leaves biomass for the removal of pharmaceutical compounds from wastewaters, Antibiotics. 10 (2021) 1–16. DOI: 10.3390/antibiotics10010065.

[97] V. Calisto, G. Jaria, C.P. Silva, C.I.A. Ferreira, M. Otero, V.I. Esteves, Single and multi-component adsorption of psychiatric pharmaceuticals onto alternative and commercial carbons, J. Environ. Manage. 192 (2017) 15–24. DOI: 10.1016/j.jenvman.2017.01.029.

[98] D. Simazaki, J. Fujiwara, S. Manabe, M. Matsuda, M. Asami, S. Kunikane, Removal of selected pharmaceuticals by chlorination, coagulation-sedimentation and powdered activated carbon treatment, Water Sci. Technol. 58 (2008) 1129–1135. DOI: 10.2166/wst.2008.472.

[99] J. Rivera-Utrilla, G. Prados-Joya, M. Sánchez-Polo, M.A. Ferro-García, I. Bautista-Toledo, Removal of nitroimidazole antibiotics from aqueous solution by adsorption/bioadsorption on activated carbon, J. Hazard. Mater. 170 (2009) 298–305. DOI: 10.1016/J.JHAZMAT.2009.04.096.

[100] S.G.J. Heijman, A.R.D. Verliefde, E.R. Cornelissen, G. Amy, J.C. Van Dijk, Influence of natural organic matter (NOM) fouling on the removal of pharmaceuticals by nanofiltration and activated carbon filtration, Water Sci. Technol. Water Supply. 7 (2007) 17–23. DOI: 10.2166/ws.2007.131.

[101] F. Saravia, F.H. Frimmel, Role of NOM in the performance of adsorption-membrane hybrid systems applied for the removal of pharmaceuticals, Desalination. 224 (2008) 168–171. DOI: 10.1016/j.desal.2007.02.089.

[102] J. Rivera-Utrilla, M. Sánchez-Polo, M.Á. Ferro-García, G. Prados-Joya, R. Ocampo-Pérez, Pharmaceuticals as emerging contaminants and their removal from water. A review, Chemosphere. 93 (2013) 1268–1287. DOI: 10.1016/j.chemosphere.2013.07.059.

[103] R. Andreozzi, V. Caprio, A. Insola, R. Marotta, Advanced oxidation processes (AOP) for water purification and recovery, Catal. Today. 53 (1999) 51–59. DOI: 10.1016/S0920-5861(99)00102-9.

[104] M.M. Huber, S. Canonica, G.Y. Park, U.V. Gunten, Oxidation of pharmaceuticals

during ozonation and advanced oxidation processes, Environ. Sci. Technol. 37 (2003) 1016–1024. DOI: 10.1021/ES025896H.

[105] W.H. Glaze, Drinking-water treatment with ozone, Environ. Sci. Technol. 21 (1987) 224–230. DOI: 10.1021/es00157a001.

[106] M. Cho, H. Chung, W. Choi, J. Yoon, Different inactivation behaviors of MS-2 phage and Escherichia coli in TiO_2 photocatalytic disinfection, Appl. Environ. Microbiol. 71 (2005) 270–275. DOI: 10.1128/AEM.71.1.270-275.2005.

[107] H. Ikai, K. Nakamura, M. Shirato, T. Kanno, A. Iwasawa, K. Sasaki, Y. Niwano, M. Kohno, Photolysis of hydrogen peroxide: An effective disinfection system via hydroxyl radical formation, Antimicrob. Agents Chemother. 54 (2010) 5086–5091. DOI: 10.1128/AAC.00751-10.

[108] C.P. Huang, C. Dong, Z. Tang, Advanced chemical oxidation: Its present role and potential future in hazardous waste treatment, Waste Manag. 13 (1993) 361–377. DOI: 10.1016/0956-053X(93)90070-D.

[109] C. Gottschalk, J.A. Libra, Ozonation of water and waste water: A practical guide to understanding ozone and its applications, 2nd Edition. John Wiley & Sons. (2009) Germany.

[110] Y. Du, J. Rabani, The Measure of TiO_2 Photocatalytic efficiency and the comparison of different photocatalytic titania, J. Phys. Chem. B. 107 (2003) 11970–11978. DOI: 10.1021/jp035491z.

[111] A. Tsitonaki, B. Petri, M. Crimi, H. Mosbk, R.L. Siegrist, P.L. Bjerg, In situ chemical oxidation of contaminated soil and groundwater using persulfate: A review, Crit. Rev. Environ. Sci. Technol. 40 (2010) 55–91. DOI: 10.1080/10643380802039303.

[112] G.R. Boyd, H. Reemtsma, D.A. Grimm, S. Mitra, Pharmaceuticals and personal care products (PPCPs) in surface and treated waters of Louisiana, USA and Ontario, Canada, Sci. Total Environ. 311 (2003) 135–149. DOI: 10.1016/S0048-9697(03)00138-4.

[113] D.W. Kolpin, E.T. Furlong, M.T. Meyer, E.M. Thurman, S.D. Zaugg, L.B. Barber, H.T. Buxton, Pharmaceuticals, hormones, and other Organic wastewater contaminants in U.S. streams, 1999−2000: A National Reconnaissance, Environ. Sci. Technol. 36 (2002) 1202–1211. DOI: 10.1021/ES011055J.

[114] T.A. Ternes, Occurrence of drugs in German sewage treatment plants and rivers, Water Res. 32 (1998) 3245–3260. DOI: 10.1016/S0043-1354(98)00099-2.

[115] R.R. Giri, H Ozaki, S Ota, R Takanami, S Taniguchi, Degradation of common pharmaceuticals and personal care products in mixed solutions by advanced oxidation techniques, Int. J. Environ. Sci. Tech. 7 (2010) 251–260.

[116] Z. Qiang, C. Adams, R. Surampalli, Determination of ozonation rate constants for lincomycin and spectinomycin, Ozone Sci. Eng. 26 (2010) 525–537. DOI: 10.1080/01919510490885334.

[117] M. Addamo, V. Augugliaro, A. Di Paola, Removal of drugs in aqueous systems by photoassisted degradation, Appl. Electrochem. 35 (2005) 765–774. DOI: 10.1007/s10800-005-1630-y.

[118] K. Ikehata, N. Jodeiri Naghashkar, M. Gamal El-Din, Degradation of aqueous pharmaceuticals by ozonation and advanced oxidation processes: A review, Ozone Sci. Eng. 28 (2006) 353–414. DOI: 10.1080/01919510600985937.

[119] R. Andreozzi, M. Canterino, R. Marotta, N. Paxeus, Antibiotic removal from wastewaters: The ozonation of amoxicillin, J. Hazard. Mater. 122 (2005) 243–250. DOI:

10.1016/J.JHAZMAT.2005.03.004.

[120] I.A. Balcioğlu, M. Ötker, Treatment of pharmaceutical wastewater containing antibiotics by O_3 and O_3/H_2O_2 processes, Chemosphere. 50 (2003) 85–95. DOI: 10.1016/S0045-6535(02)00534-9.

[121] D. Vogna, R. Marotta, A. Napolitano, R. Andreozzi, M. D'Ischia, Advanced oxidation of the pharmaceutical drug diclofenac with UV/H_2O_2 and ozone, Water Res. 38 (2004) 414–422. DOI: 10.1016/J.WATRES.2003.09.028.

[122] J. Teng, G. Liu, J. Liang, S. You, Electrochemical oxidation of sulfadiazine with titanium suboxide mesh anode, Electrochim. Acta. 331 (2020) 135441. DOI: 10.1016/J.ELECTACTA.2019.135441.

[123] H. Hai, X. Xing, S. Li, S. Xia, J. Xia, Electrochemical oxidation of sulfamethoxazole in BDD anode system: Degradation kinetics, mechanisms and toxicity evaluation, Sci. Total Environ. 738 (2020) 139909. DOI: 10.1016/J.SCITOTENV.2020.139909.

[124] R. Patidar, V.C. Srivastava, Mechanistic insight into ultrasound-induced enhancement of electrochemical oxidation of ofloxacin: Multi-response optimization and cost analysis, Chemosphere. 257 (2020) 127121. DOI: 10.1016/J.CHEMOSPHERE.2020.127121.

[125] D.M. Montoya-Rodríguez, Y. Ávila-Torres, E.A. Serna-Galvis, R.A. Torres-Palma, Data on treatment of nafcillin and ampicillin antibiotics in water by sonochemistry, Data Br. 29 (2020) 105361. DOI: 10.1016/J.DIB.2020.105361.

[126] M. Ötker, I.A. Balcıoğlu, Ozonation of enrofloxacin in solid and liquid phase, Adsorpt. J. Int. Adsorpt. Soc. (2006) International Conference Ozone and UV, April 3rd 2006 Istanbul.

[127] R. Andreozzi, R. Marotta, G. Pinto, A. Pollio, Carbamazepine in water: Persistence in the environment, ozonation treatment and preliminary assessment on algal toxicity, Water Res. 36 (2002) 2869–2877. DOI: 10.1016/S0043-1354(01)00500-0.

[128] T.A. Ternes, M.Meisenheimer, D.McDowell, F.Sacher, H.J. Brauch, B. Haist-Gulde, G.Preuss, U.Wilme, N. Zulei-Seibert, Removal of pharmaceuticals during drinking water treatment, Environ. Sci. Technol. 36 (2002) 3855–3863. DOI: 10.1021/ES015757K.

[129] T.E. Doll, F.H. Frimmel, Kinetic study of photocatalytic degradation of carbamazepine, clofibric acid, iomeprol and iopromide assisted by different TiO_2 materials—determination of intermediates and reaction pathways, Water Res. 38 (2004) 955–964. DOI: 10.1016/J.WATRES.2003.11.009.

[130] C. Zwiener, F.H. Frimmel, Oxidative treatment of pharmaceuticals in water, Water Res. 34 (2000) 1881–1885. DOI: 10.1016/S0043-1354(99)00338-3.

[131] T.A. Ternes, J. Stüber, N. Herrmann, D. McDowell, A. Ried, M. Kampmann, B. Teiser, Ozonation: a tool for removal of pharmaceuticals, contrast media and musk fragrances from wastewater?, Water Res. 37 (2003) 1976–1982. DOI: 10.1016/S0043-1354(02)00570-5.

[132] D. Vogna, R. Marotta, R. Andreozzi, A. Napolitano, M. D'Ischia, Kinetic and chemical assessment of the UV/H_2O_2 treatment of antiepileptic drug carbamazepine, Chemosphere. 54 (2004) 497–505. DOI: 10.1016/S0045-6535(03)00757-4.

[133] J.L. Packer, J.J. Werner, D.E. Latch, K. McNeill, W.A. Arnold, Photochemical fate of pharmaceuticals in the environment: Naproxen, diclofenac, clofibric acid, and ibuprofen, Aquat. Sci. 2003 654. 65 (2003) 342–351. DOI: 10.1007/S00027-003-0671-

8.

[134] M. Ravina, L. Campanella, J. Kiwi, Accelerated mineralization of the drug diclofenac via Fenton reactions in a concentric photo-reactor, Water Res. 36 (2002) 3553–3560. DOI: 10.1016/S0043-1354(02)00075-1.

[135] L.A. Pérez-Estrada, S. Malato, W. Gernjak, A. Agüera, E. M. Thurman, I. Ferrer, A.R. Fernández-Alba, Photo-Fenton degradation of diclofenac: Identification of main intermediates and degradation pathway, Environ. Sci. Technol. 39 (2005) 8300–8306. DOI: 10.1021/ES050794N.

[136] P. Bartels, W. von Tümpling, Solar radiation influence on the decomposition process of diclofenac in surface waters, Sci. Total Environ. 374 (2007) 143–155. DOI: 10.1016/j.scitotenv.2006.11.039.

[137] F. Sacher, F.T. Lange, H.J. Brauch, I. Blankenhorn, Pharmaceuticals in groundwaters: Analytical methods and results of a monitoring program in Baden-Württemberg, Germany, J. Chromatogr. A 938 (2001) 199–210. DOI: 10.1016/S0021-9673(01)01266-3.

[138] M. Rabiet, A. Togola, F. Brissaud, J.L. Seidel, H. Budzinski, F. Elbaz-Poulichet, Consequences of treated water recycling as regards pharmaceuticals and drugs in surface and ground waters of a medium-sized mediterranean catchment, Environ. Sci. Technol. 40 (2006) 5282–5288. DOI: 10.1021/es060528p.

[139] U. Jux, R.M. Baginski, H.G. Arnold, M. Krönke, P.N. Seng, Detection of pharmaceutical contaminations of river, pond, and tap water from Cologne (Germany) and surroundings, Int. J. Hyg. Environ. Health. 205 (2002) 393–398. DOI: 10.1078/1438-4639-00166.

[140] Q. Bu, B. Wang, J. Huang, S. Deng, G. Yu, Pharmaceuticals and personal care products in the aquatic environment in China: A review, J. Hazard. Mater. 262 (2013) 189–211. DOI: 10.1016/j.jhazmat.2013.08.040.

[141] L. Wang, G.G. Ying, J.L. Zhao, X.B. Yang, F. Chen, R. Tao, S. Liu, L.J. Zhou, Occurrence and risk assessment of acidic pharmaceuticals in the Yellow River, Hai River and Liao River of north China, Sci. Total Environ. 408 (2010) 3139–3147. DOI: 10.1016/j.scitotenv.2010.04.047.

[142] S. Bae, D. Kim, W. Lee, Degradation of diclofenac by pyrite catalyzed Fenton oxidation, Appl. Catal. B Environ. 134–135 (2013) 93–102. DOI: 10.1016/j.apcatb.2012.12.031.

[143] J. Schwaiger, H. Ferling, U. Mallow, H. Wintermayr, R.D. Negele, Toxic effects of the non-steroidal anti-inflammatory drug diclofenac. Part I: Histopathological alterations and bioaccumulation in rainbow trout, Aquat. Toxicol. 68 (2004) 141–150. DOI: 10.1016/j.aquatox.2004.03.014.

[144] Y. Zhang, S.U. Geißen, C. Gal, Carbamazepine and diclofenac: Removal in wastewater treatment plants and occurrence in water bodies, Chemosphere. 73 (2008) 1151–1161. DOI: 10.1016/j.chemosphere.2008.07.086.

[145] E.S. Rigobello, A.D.B. Dantas, L. Di Bernardo, E.M. Vieira, Removal of diclofenac by conventional drinking water treatment processes and granular activated carbon filtration, Chemosphere. 92 (2013) 184–191. DOI: 10.1016/j.chemosphere.2013.03.010.

[146] I.M. Jauris, C.F. Matos, C. Saucier, E.C. Lima, A.J.G. Zarbin, S.B. Fagan, F.M. Machado, I. Zanella, Adsorption of sodium diclofenac on graphene: A combined experimental and theoretical study, Phys. Chem. Chem. Phys. 18 (2016) 1526–1536. DOI: 10.1039/c5cp05940b.

[147] X. Lu, Y. Shao, N. Gao, J. Chen, Y. Zhang, Q. Wang, Y. Lu, Adsorption and removal of clofibric acid and diclofenac from water with MIEX resin, Chemosphere. 161 (2016) 400–411. DOI: 10.1016/j.chemosphere.2016.07.025.

[148] S. Mondal, S. Patel, S.K. Majumder, Naproxen removal capacity enhancement by transforming the activated carbon into a blended composite material, Water. Air. Soil Pollut. 231 (2020) 1–16. DOI: 10.1007/s11270-020-4411-7.

[149] S. Mondal, S. Patel, S.K. Majumder, Bio-extract assisted in-situ green synthesis of Ag-RGO nanocomposite film for enhanced naproxen removal, Korean J. Chem. Eng. 37 (2020) 274–289. DOI: 10.1007/s11814-019-0435-3.

[150] B.M.B. Ensano, L. Borea, V. Naddeo, V. Belgiorno, M.D.G. de Luna, F.C. Ballesteros, Removal of pharmaceuticals from wastewater by intermittent electrocoagulation, Water 9 (2017) 85. DOI: 10.3390/w9020085.

[151] K.A. Landry, P. Sun, C.H. Huang, T.H. Boyer, Ion-exchange selectivity of diclofenac, ibuprofen, ketoprofen, and naproxen in ureolyzed human urine, Water Res. 68 (2015) 510–521. DOI: 10.1016/j.watres.2014.09.056.

[152] V.S. Bessa, I.S. Moreira, M.E. Tiritan, P.M.L. Castro, Enrichment of bacterial strains for the biodegradation of diclofenac and carbamazepine from activated sludge, Int. Biodeterior. Biodegrad. 120 (2017) 135–142. DOI: 10.1016/j.ibiod.2017.02.008.

[153] P. Falås, P. Longrée, J. La Cour Jansen, H. Siegrist, J. Hollender, A. Joss, Micropollutant removal by attached and suspended growth in a hybrid biofilm-activated sludge process, Water Res. 47 (2013) 4498–4506. DOI: 10.1016/j.watres.2013.05.010.

[154] W. Zhang, L. Zhou, H. Deng, Ag modified g-C_3N_4 composites with enhanced visible-light photocatalytic activity for diclofenac degradation, J. Mol. Catal. A Chem. 423

(2016) 270–276. DOI: 10.1016/j.molcata.2016.07.021.

[155] P. Calza, V.A. Sakkas, C. Medana, C. Baiocchi, A. Dimou, E. Pelizzetti, T. Albanis, Photocatalytic degradation study of diclofenac over aqueous TiO_2 suspensions, Appl. Catal. B Environ. 67 (2006) 197–205. DOI: 10.1016/j.apcatb.2006.04.021.

[156] J.B. Ellis, Pharmaceutical and personal care products (PPCPs) in urban receiving waters, Environ. Pollut. 144 (2006) 184–189. DOI: 10.1016/j.envpol.2005.12.018.

[157] D.S. Gomes, L.M. Gando-Ferreira, R.M. Quinta-Ferreira, R.C. Martins, Removal of sulfamethoxazole and diclofenac from water: Strategies involving O_3 and H_2O_2, Environ. Technol. 39 (2018) 1658–1669. DOI: 10.1080/09593330.2017.1335351.

[158] K.H. Hama Aziz, H. Miessner, S. Mueller, D. Kalass, D. Moeller, I. Khorshid, M.A.M. Rashid, Degradation of pharmaceutical diclofenac and ibuprofen in aqueous solution, a direct comparison of ozonation, photocatalysis, and non-thermal plasma, Chem. Eng. J. 313 (2017) 1033–1041. DOI: 10.1016/J.CEJ.2016.10.137.

[159] S.K. Alharbi, W.E. Price, J. Kang, T. Fujioka, L.D. Nghiem, Ozonation of carbamazepine, diclofenac, sulfamethoxazole and trimethoprim and formation of major oxidation products, New Pub Balaban. 57 (2016) 29340–29351. DOI: 10.1080/19443994.2016.1172986.

[160] A. Aguinaco, F.J. Beltrán, J.F. García-Araya, A. Oropesa, Photocatalytic ozonation to remove the pharmaceutical diclofenac from water: Influence of variables, Chem. Eng. J. 189–190 (2012) 275–282. DOI: 10.1016/J.CEJ.2012.02.072.

[161] V. Naddeo, D. Ricco, D. Scannapieco, V. Belgiorno, Degradation of antibiotics in wastewater during sonolysis, ozonation, and their simultaneous application: Operating conditions effects and processes evaluation, Int. J. Photoenergy. 2012 (2012) 1–7. DOI:

10.1155/2012/624270.

[162] F.J. Beltrán, P. Pocostales, P. Alvarez, A. Oropesa, Diclofenac removal from water with ozone and activated carbon, J. Hazard. Mater. 163 (2009) 768–776. DOI: 10.1016/J.JHAZMAT.2008.07.033.

[163] M.M. Sein, M. Zedda, J. Tuerk, T.C. Schmidt, A. Golloch, C. Von Sonntag, Oxidation of diclofenac with ozone in aqueous solution, Environ. Sci. Technol. 42 (2008) 6656–6662. DOI: 10.1021/es8008612.

[164] J. Hofmann, U. Freier, M. Wecks, S. Hohmann, Degradation of diclofenac in water by heterogeneous catalytic oxidation with H_2O_2, Appl. Catal. B Environ. 70 (2007) 447–451. DOI: 10.1016/J.APCATB.2005.11.023.

[165] R. Rosal, A. Rodríguez, J.A. Perdigón-Melón, M. Mezcua, M.D. Hernando, P. Letón, E. García-Calvo, A. Agüera, A.R. Fernández-Alba, Removal of pharmaceuticals and kinetics of mineralization by O_3/H_2O_2 in a biotreated municipal wastewater, Water Res. 42 (2008) 3719–3728. DOI: 10.1016/J.WATRES.2008.06.008.

[166] L. Rizzo, S. Meric, D. Kassinos, M. Guida, F. Russo, V. Belgiorno, Degradation of diclofenac by TiO_2 photocatalysis: UV absorbance kinetics and process evaluation through a set of toxicity bioassays, Water Res. 43 (2009) 979–988. DOI: 10.1016/J.WATRES.2008.11.040.

[167] L. Yang, C. Hu, Y. Nie, J. Qu, Catalytic ozonation of selected pharmaceuticals over mesoporous alumina-supported manganese oxide, Environ. Sci. Technol. 43 (2009) 2525–2529. DOI: 10.1021/ES803253C.

[168] M. Stumpf, T.A. Ternes, R.D. Wilken, S.V. Rodrigues, W. Baumann, Polar drug residues in sewage and natural waters in the state of Rio de Janeiro, Brazil, Sci. Total

Environ. 225 (1999) 135–141. DOI: 10.1016/S0048-9697(98)00339-8.

[169] M.J. Benotti, R.A. Trenholm, B.J. Vanderford, J.C. Holady, B.D. Stanford, S.A. Snyder, Pharmaceuticals and endocrine disrupting compounds in U.S. drinking water, Environ. Sci. Technol. 43 (2008) 597–603. DOI: 10.1021/ES801845A.

[170] J. Park, N. Yamashita, C. Park, T. Shimono, D.M. Takeuchi, H. Tanaka, Removal characteristics of pharmaceuticals and personal care products: Comparison between membrane bioreactor and various biological treatment processes, Chemosphere. 179 (2017) 347–358. DOI: 10.1016/J.CHEMOSPHERE.2017.03.135.

[171] M. Hijosa-Valsero, V. Matamoros, J. Martín-Villacorta, E. Bécares, J.M. Bayona, Assessment of full-scale natural systems for the removal of PPCPs from wastewater in small communities, Water Res. 44 (2010) 1429–1439. DOI: 10.1016/J.WATRES.2009.10.032.

[172] X. Li, J. Xu, R.A. de Toledo, H. Shim, Enhanced removal of naproxen and carbamazepine from wastewater using a novel countercurrent seepage bioreactor immobilized with Phanerochaete chrysosporium under non-sterile conditions, Bioresour. Technol. 197 (2015) 465–474. DOI: 10.1016/J.BIORTECH.2015.08.118.

[173] F.A. Kibuye, H.E. Gall, K.R. Elkin, B. Ayers, T.L. Veith, M. Miller, S. Jacob, K.R. Hayden, J.E. Watson, H.A. Elliott, Fate of pharmaceuticals in a spray-irrigation system: From wastewater to groundwater, Sci. Total Environ. 654 (2019) 197–208. DOI: 10.1016/J.SCITOTENV.2018.10.442.

[174] G.R. Boyd, S. Zhang, D.A. Grimm, Naproxen removal from water by chlorination and biofilm processes, Water Res. 39 (2005) 668–676. DOI: 10.1016/J.WATRES.2004.11.013.

[175] Y. Liu, Y. Tang, Y. Wu, L. Feng, L. Zhang, Degradation of naproxen in chlorination and UV/chlorine processes: Kinetics and degradation products, Environ. Sci. Pollut. Res. 2019 2633. 26 (2019) 34301–34310. DOI: 10.1007/S11356-019-04472-Z.

[176] P. Thanekar, S. Garg, P.R. Gogate, Hybrid treatment strategies based on hydrodynamic cavitation, advanced oxidation processes, and aerobic oxidation for efficient removal of naproxen, Ind. Eng. Chem. Res. 59 (2019) 4058–4070. DOI: 10.1021/ACS.IECR.9B01395.

[177] R. Bai, Y. Xiao, W. Yan, S. Wang, R. Ding, F. Yang, J. Li, X. Lu, F. Zhao, Rapid and efficient removal of naproxen from water by $CuFe_2O_4$ with peroxymonosulfate, Environ. Sci. Pollut. Res. 27 (2020) 21542–21551. DOI: 10.1007/s11356-020-08613-7.

[178] Mingwei Pan, Zihao Wu, Changyuan Tang, Kaiheng Guo, Yingjie Cao, Jingyun Fang, Emerging investigators series: Comparative study of naproxen degradation by the UV/chlorine and the UV/H_2O_2 advanced oxidation processes, Environ. Sci. Water Res. Technol. 4 (2018) 1219–1230. DOI: 10.1039/C8EW00105G.

[179] E. Arany, R.K. Szabó, L. Apáti, T. Alapi, I. Ilisz, P. Mazellier, A. Dombi, K. Gajda-Schrantz, Degradation of naproxen by UV, VUV photolysis and their combination, J. Hazard. Mater. 262 (2013) 151–157. DOI: 10.1016/J.JHAZMAT.2013.08.003.

[180] A. Ghauch, A.M. Tuqan, N. Kibbi, Naproxen abatement by thermally activated persulfate in aqueous systems, Chem. Eng. J. 279 (2015) 861–873. DOI: 10.1016/J.CEJ.2015.05.067.

[181] F. Méndez-Arriaga, J. Gimenez, S. Esplugas, Photolysis and TiO_2 photocatalytic treatment of naproxen: Degradation, mineralization, intermediates and toxicity, J. Adv. Oxid. Technol. 11 (2008) 435–444. DOI: 10.1515/jaots-2008-0302.

[182] M.E. Dasenaki, N.S. Thomaidis, Multianalyte method for the determination of pharmaceuticals in wastewater samples using solid-phase extraction and liquid chromatography–tandem mass spectrometry, Anal. Bioanal. Chem. 2015 40715. 407 (2015) 4229–4245. DOI: 10.1007/S00216-015-8654-X.

[183] D. Dumanović, I. Juranić, D. Dželetović, V.M. Vasić, J. Jovanović, Protolytic constants of nizatidine, ranitidine and N,N′-dimethyl-2-nitro-1,1-ethenediamine; spectrophotometric and theoretical investigation, J. Pharm. Biomed. Anal. 15 (1997) 1667–1678. DOI: 10.1016/S0731-7085(96)01977-2.

[184] J. Rivas, O. Gimeno, A. Encinas, F. Beltrán, Ozonation of the pharmaceutical compound ranitidine: Reactivity and kinetic aspects, Chemosphere. 76 (2009) 651–656. DOI: 10.1016/J.CHEMOSPHERE.2009.04.028.

[185] D.A. Henry, I.A. Macdonald, G. Kitchingman, G.D. Bell, M.J. Langman, Cimetidine and ranitidine: Comparison of effects on hepatic drug metabolism., Br Med J. 281 (1980) 775–777. DOI: 10.1136/BMJ.281.6243.775.

[186] J.M. Conley, S.J. Symes, M.S. Schorr, S.M. Richards, Spatial and temporal analysis of pharmaceutical concentrations in the upper Tennessee River basin, Chemosphere. 73 (2008) 1178–1187. DOI: 10.1016/J.CHEMOSPHERE.2008.07.062.

[187] M.E. Dasenaki, N.S. Thomaidis, Multi-residue determination of 115 veterinary drugs and pharmaceutical residues in milk powder, butter, fish tissue and eggs using liquid chromatography–tandem mass spectrometry, Anal. Chim. Acta. 880 (2015) 103–121. DOI: 10.1016/J.ACA.2015.04.013.

[188] Y. Valcárcel, S. González Alonso, J.L. Rodríguez-Gil, A. Gil, M. Catalá, Detection of pharmaceutically active compounds in the rivers and tap water of the Madrid Region

(Spain) and potential ecotoxicological risk, Chemosphere. 84 (2011) 1336–1348. DOI: 10.1016/J.CHEMOSPHERE.2011.05.014.

[189] P.F. Carey, L.E. Martin, P.E. Owen, Determination of ranitidine and its metabolites in human urine by reversed-phase ion-pair high-performance liquid chromatography, J. Chromatogr. B Biomed. Sci. Appl. 225 (1981) 161–168. DOI: 10.1016/S0378-4347(00)80255-8.

[190] L.E. Martin, J. Oxford, R.J.N. Tanner, The use of on-line high-performance liquid chromatography-mass spectrometry for the identification of ranitidine and its metabolites in urine, Xenobiotica 11 (2009) 831–840. DOI: 10.3109/00498258109045320.

[191] C. Carlesi Jara, D. Fino, V. Specchia, G. Saracco, P. Spinelli, Electrochemical removal of antibiotics from wastewaters, Appl. Catal. B Environ. 70 (2007) 479–487. DOI: 10.1016/J.APCATB.2005.11.035.

[192] D.E. Latch, B.L. Stender, J.L. Packer, W.A. Arnold, K. McNeill, Photochemical fate of pharmaceuticals in the environment: Cimetidine and ranitidine, Environ. Sci. Technol. 37 (2003) 3342–3350. DOI: 10.1021/ES0340782.

[193] M. Jamrógiewicz, B. Wielgomas, Detection of some volatile degradation products released during photoexposition of ranitidine in a solid state, J. Pharm. Biomed. Anal. 76 (2013) 177–182. DOI: 10.1016/J.JPBA.2012.12.019.

[194] C. Christophoridis, M.C. Nika, R. Aalizadeh, N.S. Thomaidis, Ozonation of ranitidine: Effect of experimental parameters and identification of transformation products, Sci. Total Environ. 557–558 (2016) 170–182. DOI: 10.1016/J.SCITOTENV.2016.03.026.

[195] J. Radjenović, C. Sirtori, M. Petrović, D. Barceló, S. Malato, Characterization of

intermediate products of solar photocatalytic degradation of ranitidine at pilot-scale, Chemosphere. 79 (2010) 368–376. DOI: 10.1016/J.CHEMOSPHERE.2010.02.014.

[196] X. Zou, J. Zhang, X. Zhao, Z. Zhang, MoS_2/RGO composites for photocatalytic degradation of ranitidine and elimination of NDMA formation potential under visible light, Chem. Eng. J. 383 (2020) 123084. DOI: 10.1016/J.CEJ.2019.123084.

[197] Y. Lester, H. Mamane, I. Zucker, D. Avisar, Treating wastewater from a pharmaceutical formulation facility by biological process and ozone, Water Res. 47 (2013) 4349–4356. DOI: 10.1016/J.WATRES.2013.04.059.

[198] R.B.P. Marcelino, M.M.D. Leão, R.M. Lago, C.C. Amorim, Multistage ozone and biological treatment system for real wastewater containing antibiotics, J. Environ. Manage. 195 (2017) 110–116. DOI: 10.1016/J.JENVMAN.2016.04.041.

[199] Z.P. Xing, D.Z. Sun, X.J. Yu, J.L. Zou, W. Zhou, Treatment of antibiotic fermentation-based pharmaceutical wastewater using anaerobic and aerobic moving bed biofilm reactors combined with ozone/hydrogen peroxide process, Environ. Prog. Sustain. Energy. 33 (2014) 170–177. DOI: 10.1002/EP.11775.

[200] M.I. Badawy, R.A. Wahaab, A.S. El-Kalliny, Fenton-biological treatment processes for the removal of some pharmaceuticals from industrial wastewater, J. Hazard. Mater. 167 (2009) 567–574. DOI: 10.1016/j.jhazmat.2009.01.023.

[201] S.N. Malik, S.M. Khan, P.C. Ghosh, A.N. Vaidya, G. Kanade, S.N. Mudliar, Treatment of pharmaceutical industrial wastewater by nano-catalyzed ozonation in a semi-batch reactor for improved biodegradability, Sci. Total Environ. 678 (2019) 114–122. DOI: 10.1016/J.SCITOTENV.2019.04.097.

[202] N.Q. Thang, A. Sabbah, L.C. Chen, K.H. Chen, C.M. Thi, P. Van Viet, High-efficient

photocatalytic degradation of commercial drugs for pharmaceutical wastewater treatment prospects: A case study of Ag/g-C_3N_4/ZnO nanocomposite materials, Chemosphere. 282 (2021) 130971. DOI: 10.1016/j.chemosphere.2021.130971.

[203] S. Sircar, W.C. Kratz, Oxygen Production by Pressure Swing Adsorption, Sep. Sci. Technol. 24 (1989) 429–440.DOI: 10.1080/01496398908049779.

[204] C.A. Grande, Advances in pressure swing adsorption for gas separation, ISRN Chem. Eng. 2012 (2012) 1–13. DOI: 10.5402/2012/982934.

[205] R. Peyrous, R.M. Millot, Ozone generation in oxygen by corona discharges in a point-to-plane gap subjected to a chopped DC positive voltage, J. Phys. D. Appl. Phys. 14 (1981) 2237–2242. DOI: 10.1088/0022-3727/14/12/012.

[206] J.L. Means, S.J. Anderson, Comparison of five different methods for measuring biodegradability in aqueous environments, Water. Air. Soil Pollut. 16 (1981) 301–315. DOI: 10.1007/BF01046911.

[207] J. Szabo, J. Hall, On-line water quality monitoring for drinking water contamination, Compr. Water Qual. Purif. (2014) 266–282. DOI: 10.1016/B978-0-12-382182-9.00038-4.

[208] W.G. Walter, Standard methods for the examination of water and wastewater (11th ed.), Am. J. Public Heal. Nations Heal. 51 (1961) 940–940. DOI: 10.2105/ajph.51.6.940-a.

[209] F.R. Kalt, I.E. Cock, Gas chromatography-mass spectroscopy analysis of bioactive petalostigma extracts: Toxicity, antibacterial and antiviral activities, Pharmacogn. Mag. 10 (2014) S37–S49. DOI: 10.4103/0973-1296.127338.

[210] A. Bertella, K. Benlahcen, S. Abouamama, D.C.G.A. Pinto, K. Maamar, M. Kihal, A.M.S. Silva, Artemisia herba-alba Asso. essential oil antibacterial activity and acute

toxicity, Ind. Crops Prod. 116 (2018) 137–143. DOI: 10.1016/j.indcrop.2018.02.064.

[211] S. Patel, S.K. Majumder, P. Das, P. Ghosh, Ozone microbubble-aided intensification of degradation of naproxen in a plant prototype, J. Environ. Chem. Eng. 7 (2019) 103102. DOI: 10.1016/j.jece.2019.103102.

[212] J.Y. Hu, T. Aizawa, S. Ookubo, Products of aqueous chlorination of bisphenol A and their estrogenic activity, Environ. Sci. Technol. 36 (2002) 1980–1987. https://doi.org/10.1021/es011177b.

[213] B. Legube, N. Karpel Vel Leitner, Catalytic ozonation: A promising advanced oxidation technology for water treatment, Catal. Today. 53 (1999) 61–72. DOI: 10.1016/S0920-5861(99)00103-0.

[214] J.A. Roth, D.E. Sullivan, Solubility of ozone in water, Ind. Eng. Chem. Fundam. 20 (1981) 137–140. DOI: 10.1021/i100002a004.

[215] Y. Gendel, O. Lahav, A novel approach for ammonia removal from fresh-water recirculated aquaculture systems, comprising ion exchange and electrochemical regeneration, Aquac. Eng. 52 (2013) 27–38. DOI: 10.1016/j.aquaeng.2012.07.005.

[216] F.J. Beltrán, J. Encinar, J.F. González, Industrial wastewater advanced oxidation. Part 2. Ozone combined with hydrogen peroxide or UV radiation, Water Res. 31 (1997) 2415–2428.

[217] J.L. Sotelo, F.J. Beltran, F.J. Benitez, J. Beltran-Heredia, Ozone decomposition in water: Kinetic study, Ind. Eng. Chem. Res. 26 (1987) 39–43.

[218] F.J. Beltran, Ozone reaction kinetics for water and wastewater systems. Lewis Publishers, (2004) Boca Ratón Florida.

[219] J. Wang, Axial-dispersion models of fluid-fluid reactors based on the two-film theory, Chem. Eng. Process. Process Intensif. 34 (1995) 447–453. DOI: 10.1016/0255-2701(95)00580-3.

[220] M. Skoumal, P.L. Cabot, F. Centellas, C. Arias, R.M. Rodríguez, J.A. Garrido, E. Brillas, Mineralization of paracetamol by ozonation catalyzed with Fe^{2+}, Cu^{2+} and UVA light, Appl. Catal. B Environ. 66 (2006) 228–240. DOI: 10.1016/j.apcatb.2006.03.016.

[221] H. Tomiyasu, H. Fukutomi, G. Gordon, Kinetics and mechanism of ozone decomposition in basic aqueous solution, Inorg. Chem. 24 (1985) 2962–2966. DOI: 10.1021/ic00213a018.

[222] K. Sehested, J. Holcman, E. Bjergbakke, E.J. Hart, A pulse radiolytic study of the reaction hydroxyl+ ozone in aqueous medium, J. Phys. Chem. A. 88 (1984) 4144–4147.

[223] J. Staehelin, J. Holgné, Decomposition of ozone in water: Rate of initiation by hydroxide ions and hydrogen peroxide, Environ. Sci. Technol. 16 (1982) 676–681. DOI: 10.1021/es00104a009.

[224] Y.L. Lin, B.K. Li, Removal of pharmaceuticals and personal care products by Eichhornia crassipe and Pistia stratiotes, J. Taiwan Inst. Chem. Eng. 58 (2016) 318–323. DOI: 10.1016/j.jtice.2015.06.007.

[225] N. Jallouli, K. Elghniji, O. Hentati, A.R. Ribeiro, A.M.T. Silva, M. Ksibi, UV and solar photo-degradation of naproxen: TiO_2 catalyst effect, reaction kinetics, products identification and toxicity assessment, J. Hazard. Mater. 304 (2016) 329–336. DOI: 10.1016/j.jhazmat.2015.10.045.

[226] B. Zheng, Z. Zheng, J. Zhang, Q. Liu, J. Wang, X. Luo, L. Wang, Degradation kinetics and by-products of naproxen in aqueous solutions by gamma irradiation, Environ. Eng.

Sci. 29 (2012) 386–391. DOI: 10.1089/ees.2010.0215.

[227] R. Andreozzi, M. Canterino, R. Marotta, N. Paxeus, Antibiotic removal from wastewaters: The ozonation of amoxicillin, J. Hazard. Mater. 122 (2005) 243–250. DOI: 10.1016/j.jhazmat.2005.03.004.

[228] K. Ikehata, N. Jodeiri Naghashkar, M. Gamal El-Din, Degradation of aqueous pharmaceuticals by ozonation and advanced oxidation processes: A review, Ozone Sci. Eng. 28 (2006) 353–414. DOI: 10.1080/01919510600985937.

[229] M.M. Huber, A. GÖbel, A. Joss, N. Hermann, D. LÖffler, C.S. McArdell, A. Ried, H. Siegrist, T.A. Ternes, U. von Gunten, Oxidation of pharmaceuticals during ozonation of municipal wastewater effluents: A pilot study, Environ. Sci. Technol. 39 (2005) 4290–4299. DOI: 10.1021/es048396s.

[230] R. Rosal, A. Rodríguez., M.S. Gonzalo, E. García-Calvo, Catalytic ozonation of naproxen and carbamazepine on titanium dioxide, Appl. Catal. B Environ. 84 (2008) 48–57. DOI: 10.1016/j.apcatb.2008.03.003.

[231] F. Javier Benitez, J.L. Acero, F.J. Real, G. Roldán, Ozonation of pharmaceutical compounds: Rate constants and elimination in various water matrices, Chemosphere. 77 (2009) 53–59. DOI: 10.1016/j.chemosphere.2009.05.035.

[232] A.D. Coelho, C. Sans, A. Agüera, M.J. Gómez, S. Esplugas, M. Dezotti, Effects of ozone pre-treatment on diclofenac: Intermediates, biodegradability and toxicity assessment, Sci. Total Environ. 407 (2009) 3572–3578. DOI: 10.1016/j.scitotenv.2009.01.013.

[233] Z. Qiu, J. Sun, D. Han, F. Wei, Q. Mei, B. Wei, X. Wang, Z. An, X. Bo, M. Li, J. Xie, M. He, Ozonation of diclofenac in the aqueous solution: Mechanism, kinetics and ecotoxicity assessment, Environ. Res. 188 (2020) 109713. DOI:

10.1016/j.envres.2020.109713.

[234] D. Vogna, R. Marotta, A. Napolitano, R. Andreozzi, M. D'Ischia, Advanced oxidation of the pharmaceutical drug diclofenac with UV/H_2O_2 and ozone, Water Res. 38 (2004) 414–422. DOI: 10.1016/j.watres.2003.09.028.

[235] C.V. Sonntag, U.V. Gunten, Chemistry of ozone in water and wastewater treatment IWA Publishing, London, United Kingdom.

[236] K.M.S. Hansen, A. Spiliotopoulou, R.K. Chhetri, M. Escolà Casas, K. Bester, H.R. Andersen, Ozonation for source treatment of pharmaceuticals in hospital wastewater - Ozone lifetime and required ozone dose, Chem. Eng. J. 290 (2016) 507–514. DOI: 10.1016/j.cej.2016.01.027.

[237] K. Shang, X. Wang, J. Li, H. Wang, N. Lu, N. Jiang, Y. Wu, Synergetic degradation of acid orange 7 (AO7) dye by DBD plasma and persulfate, Chem. Eng. J. 311 (2017) 378–384. DOI: 10.1016/j.cej.2016.11.103.

[238] M.F. Sevimli, H.Z. Sarikaya, Ozone treatment of textile effluents and dyes: Effect of applied ozone dose, pH and dye concentration, J. Chem. Technol. Biotechnol. 77 (2002) 842–850. DOI: 10.1002/jctb.644.

[239] G. Márquez, E.M. Rodríguez, F.J. Beltrán, P.M. Álvarez, Solar photocatalytic ozonation of a mixture of pharmaceutical compounds in water, Chemosphere. 113 (2014) 71–78. DOI: 10.1016/J.CHEMOSPHERE.2014.03.093.

[240] J.F. Gomes, I. Leal, K. Bednarczyk, M. Gmurek, M. Stelmachowski, M. Diak, M. Emília Quinta-Ferreira, R. Costa, R.M. Quinta-Ferreira, R.C. Martins, Photocatalytic ozonation using doped TiO_2 catalysts for the removal of parabens in water, Sci. Total Environ. 609 (2017) 329–340. DOI: 10.1016/J.SCITOTENV.2017.07.180.

[241] J. Hartmann, P. Bartels, U. Mau, M. Witter, W.V. Tümpling, J. Hofmann, E. Nietzschmann, Degradation of the drug diclofenac in water by sonolysis in presence of catalysts, Chemosphere. 70 (2008) 453–461. DOI: 10.1016/j.chemosphere.2007.06.063.

[242] X. Li, M. Zhou, Y. Pan, Degradation of diclofenac by H_2O_2 activated with pre-magnetization Fe0: Influencing factors and degradation pathways, Chemosphere. 212 (2018) 853–862. DOI: 10.1016/j.chemosphere.2018.08.144.

[243] J. Nackiewicz, Ł. Kołodziej, A. Poliwoda, M.A. Broda, Oxidation of diclofenac in the presence of iron(II) octacarboxyphthalocyanine, Chemosphere. 265 (2020) 129145. DOI: 10.1016/j.chemosphere.2020.129145.

[244] Q. Dai, J. Wang, L. Chen, J. Chen, Degradation of p-acetamidophenol in aqueous solution by ozonation: Performance optimization and kinetics study, Ind. Eng. Chem. Res. 53 (2014) 11593–11600. DOI: 10.1021/ie501616r.

[245] D. Stülten, S. Zühlke, M. Lamshöft, M. Spiteller, Occurrence of diclofenac and selected metabolites in sewage effluents, Sci. Total Environ. 405 (2008) 310–316. DOI: 10.1016/j.scitotenv.2008.05.036.

[246] B. Bonnefille, E. Gomez, F. Courant, A. Escande, H. Fenet, Diclofenac in the marine environment: A review of its occurrence and effects, Mar. Pollut. Bull. 131 (2018) 496–506. DOI: 10.1016/j.marpolbul.2018.04.053.

[247] H.R. Buser, T. Poiger, M.D. Müller, Occurrence and fate of the pharmaceutical drug diclofenac in surface waters: Rapid photodegradation in a lake, Environ. Sci. Technol. 32 (1998) 3449–3456. DOI: 10.1021/es980301x.

[248] M.G. Antoniou, G. Hey, S. Rodríguez Vega, A. Spiliotopoulou, J. Fick, M. Tysklind, J. la Cour Jansen, H.R. Andersen, Required ozone doses for removing pharmaceuticals

from wastewater effluents, Sci. Total Environ. 456–457 (2013) 42–49. DOI: 10.1016/J.SCITOTENV.2013.03.072.

[249] J. Fick, R.H. Lindberg, M. Tysklind, D.G.J. Larsson, Predicted critical environmental concentrations for 500 pharmaceuticals, Regul. Toxicol. Pharmacol. 58 (2010) 516–523. DOI: 10.1016/j.yrtph.2010.08.025.

[250] R. Loos, B.M. Gawlik, G. Locoro, E. Rimaviciute, S. Contini, G. Bidoglio, EU-wide survey of polar organic persistent pollutants in European river waters, Environ. Pollut. 157 (2009) 561–568. DOI: 10.1016/j.envpol.2008.09.020.

[251] J.F. Ericson, R. Laenge, D.E. Sullivan, Pharmaceuticals, hormones, and other organic wastewater contaminants in U.S. streams, 1999-2000: A national reconnaissance., Environ. Sci. Technol. 36 (2002) 1202–1211. DOI: 10.1021/es011055j.

[252] D. Gerrity, S. Snyder, Review of ozone for water reuse applications: Toxicity, regulations, and trace organic contaminant oxidation, Ozone Sci. Eng. 33 (2011) 253–266. DOI: 10.1080/01919512.2011.578038.

[253] J. Radjenović, M. Petrović, D. Barceló, Fate and distribution of pharmaceuticals in wastewater and sewage sludge of the conventional activated sludge (CAS) and advanced membrane bioreactor (MBR) treatment, Water Res. 43 (2009) 831–841. DOI: 10.1016/j.watres.2008.11.043.

[254] Y. Lee, U.V. Gunten, Oxidative transformation of micropollutants during municipal wastewater treatment: Comparison of kinetic aspects of selective (chlorine, chlorine dioxide, ferrateVI, and ozone) and non-selective oxidants (hydroxyl radical), Water Res. 44 (2010) 555–566. DOI: 10.1016/j.watres.2009.11.045.

[255] P. Falås, A. Baillon-Dhumez, H.R. Andersen, A. Ledin, J. La Cour Jansen, Suspended

biofilm carrier and activated sludge removal of acidic pharmaceuticals, Water Res. 46 (2012) 1167–1175. DOI: 10.1016/j.watres.2011.12.003.

[256] R. Triebskorn, H. Casper, A. Heyd, R. Eikemper, H.R. Köhler, J. Schwaiger, Toxic effects of the non-steroidal anti-inflammatory drug diclofenac: Part II. Cytological effects in liver, kidney, gills and intestine of rainbow trout (Oncorhynchus mykiss), Aquat. Toxicol. 68 (2004) 151–166. DOI: 10.1016/j.aquatox.2004.03.015.

[257] D.B. Huggett, B.W. Brooks, B. Peterson, C.M. Foran, D. Schlenk, Toxicity of select beta adrenergic receptor-blocking pharmaceuticals (β-blockers) on aquatic organisms, Arch. Environ. Contam. Toxicol. 43 (2002) 229–235. DOI: 10.1007/s00244-002-1182-7.

[258] M. Palmiotto, S. Castiglioni, E. Zuccato, A. Manenti, F. Riva, E. Davoli, Personal care products in surface, ground and wastewater of a complex aquifer system, a potential planning tool for contemporary urban settings, J. Environ. Manage. 214 (2018) 76–85. DOI: 10.1016/j.jenvman.2017.10.069.

[259] J.M. Brausch, G.M. Rand, A review of personal care products in the aquatic environment: Environmental concentrations and toxicity, Chemosphere. 82 (2011) 1518–1532. DOI: 10.1016/j.chemosphere.2010.11.018.

[260] A. Nikolaou, S. Meric, D. Fatta, Occurrence patterns of pharmaceuticals in water and wastewater environments, Anal. Bioanal. Chem. 387 (2007) 1225–1234. DOI: 10.1007/s00216-006-1035-8.

[261] J. Derco, A.Ž. Gotvajn, O. Čižmárová, J. Dudáš, L. Sumegová, K. Šimovičová, Removal of micropollutants by ozone-based processes, Processes. 9 (2021) 1–48. DOI: 10.3390/pr9061013.

[262] S.D. Richardson, Environmental mass spectrometry: Emerging contaminants and current issues, Anal. Chem. 84 (2012) 747–778. DOI: 10.1021/ac202903d.

[263] D.G.J. Larsson, C. de Pedro, N. Paxeus, Effluent from drug manufactures contains extremely high levels of pharmaceuticals, J. Hazard. Mater. 148 (2007) 751–755. DOI: 10.1016/j.jhazmat.2007.07.008.

[264] X.S. Miao, F. Bishay, M. Chen, C.D. Metcalfe, Occurrence of antimicrobials in the final effluents of wastewater treatment plants in Canada, Environ. Sci. Technol. 38 (2004) 3533–3541. DOI: 10.1021/es030653q.

[265] S. Ben Abdelmelek, J. Greaves, K.P. Ishida, W.J. Cooper, W. Song, Removal of pharmaceutical and personal care products from reverse osmosis retentate using advanced oxidation processes, Environ. Sci. Technol. 45 (2011) 3665–3671. DOI: 10.1021/es104287n.

[266] P. Drillia, S.N. Dokianakis, M.S. Fountoulakis, M. Kornaros, K. Stamatelatou, G. Lyberatos, On the occasional biodegradation of pharmaceuticals in the activated sludge process: the example of the antibiotic sulfamethoxazole, J. Hazard. Mater. 122 (2005) 259–265. DOI: 10.1016/j.jhazmat.2005.03.009.

[267] T.G. Vasconcelos, K. Kümmerer, D.M. Henriques, A.F. Martins, Ciprofloxacin in hospital effluent: Degradation by ozone and photoprocesses, J. Hazard. Mater. 169 (2009) 1154–1158. DOI: 10.1016/j.jhazmat.2009.03.143.

[268] M. Klavarioti, D. Mantzavinos, D. Kassinos, Removal of residual pharmaceuticals from aqueous systems by advanced oxidation processes, Environ. Int. 35 (2009) 402–417. DOI: 10.1016/j.envint.2008.07.009.

[269] M.A.S. Pastor, A.B. Botelho Junior, D.C.R. Espinosa, J.A.S. Tenório, M.D.P.G.

Baltazar, Application of advanced oxidation process using ozonation assisted with hydrogen peroxide for organic compounds removal from bayer liquor, Ozone Sci. Eng. 00 (2021) 1–11. DOI: 10.1080/01919512.2021.1924118.

[270] S.N. Malik, P.C. Ghosh, A.N. Vaidya, S.N. Mudliar, Hybrid ozonation process for industrial wastewater treatment: Principles and applications: A review, J. Water Process Eng. 35 (2020) 101193. DOI: 10.1016/j.jwpe.2020.101193.

[271] S. Khuntia, S.K. Majumder, P. Ghosh, Oxidation of As (III) to As (V) using ozone microbubbles, Chemosphere. 97 (2014) 120–124. DOI: 10.1016/j.chemosphere.2013.10.046.

[272] J. Villadsen, W.E. Stewart, N. Wakao, J.M. Smith, J.B. Wang, A. Varma, Ozone decomposition in water: Kinetic study, Ind. Eng. Chem. Res. 26 (1987) 39–43. DOI: 10.1021/ie00061a008.

[273] R. Rosal, A. Rodríguez, M. Zerhouni, Enhancement of gas-liquid mass transfer during the unsteady-state catalytic decomposition of ozone in water, Appl. Catal. A Gen. 305 (2006) 169–175. DOI: 10.1016/j.apcata.2006.02.059.

[274] J. Staehelin, J. Holgné, Decomposition of ozone in water: Rate of initiation by hydroxide Ions and hydrogen peroxide, Environ. Sci. Technol. 16 (1982) 676–681. DOI: 10.1021/es00104a009.

[275] W. Chu, C.W. Ma, Quantitative prediction of direct and indirect dye ozonation kinetics, Water Res. 34 (2000) 3153–3160. DOI: 10.1016/S0043-1354(00)00043-9.

[276] L. Zhang, Y.R. Yang, H.Y. Yang, Z.X. Chang, D.L. Li, Degradation of *p*-toluene sulfonic acid wastewater by combined photocatalysis and ozonization, Asian J. Chem. 25 (2013) 1609–1612. DOI: 10.14233/ajchem.2013.13437.

[277] F.J. Beltrán, F.J. Rivas, L.A. Fernández, P.M. Álvarez, R. Montero-de-Espinosa, Kinetics of catalytic ozonation of oxalic acid in water with activated carbon, Ind. Eng. Chem. Res. 41 (2002) 6510–6517. DOI: 10.1021/ie020311d.

[278] H. Dong, Z. Qiang, J. Lian, J. Qu, Degradation of nitro-based pharmaceuticals by UV photolysis: Kinetics and simultaneous reduction on halonitromethanes formation potential, Water Res. 119 (2017) 83–90. DOI: 10.1016/j.watres.2017.04.049.

[279] M.G. Seid, C. Lee, K. Cho, S.W. Hong, Degradation of ranitidine and changes in N-nitrosodimethylamine formation potential by advanced oxidation processes: Role of oxidant speciation and water matrix, Water Res. 203 (2021) 117495. DOI: 10.1016/j.watres.2021.117495.

[280] X. Wang, H. Yang, B. Zhou, X. Wang, Y. Xie, Effect of oxidation on amine-based pharmaceutical degradation and N-Nitrosodimethylamine formation, Water Res. 87 (2015) 403–411. DOI: 10.1016/j.watres.2015.07.045.

[281] R. Zou, X. Liao, L. Zhao, B. Yuan, Reduction of N-nitrosodimethylamine formation from ranitidine by ozonation preceding chloramination: influencing factors and mechanisms, Environ. Sci. Pollut. Res. 25 (2018) 13489–13498. DOI: 10.1007/S11356-018-1470-Z/FIGURES/6.

[282] IBEF, Indian pharmaceuticals industry analysis: A sectoral presentation, India Brand Equity Found. (2019). https://www.ibef.org/archives/industry/indian-pharmaceuticals-industry-analysis-reports/indian-pharmaceuticals-industry-analysis-october-2019.

[280] V. Chander, B. Sharma, V. Negi, R.S. Aswal, P. Singh, R. Singh, R. Dobhal, Pharmaceutical compounds in drinking water, J. Xenobiotics. 6 (2016) 1–7. DOI: 10.4081/xeno.2016.5774.

[283] C. Sirtori, A. Zapata, I. Oller, W. Gernjak, A. Agüera, S. Malato, Decontamination industrial pharmaceutical wastewater by combining solar photo-Fenton and biological treatment, Water Res. 43 (2009) 661–668. DOI: 10.1016/j.watres.2008.11.013.

[284] A.M. Deegan, B. Shaik, K. Nolan, K. Urell, M. Oelgemöller, J. Tobin, A. Morrissey, Treatment options for wastewater effluents from pharmaceutical companies, Int. J. Environ. Sci. Technol. 8 (2011) 649–666. DOI: 10.1007/BF03326250.

[285] J. Zhan, Z. Li, G. Yu, X. Pan, J. Wang, W. Zhu, X. Han, Y. Wang, Enhanced treatment of pharmaceutical wastewater by combining three-dimensional electrochemical process with ozonation to in situ regenerate granular activated carbon particle electrodes, Sep. Purif. Technol. 208 (2019) 12–18. DOI: 10.1016/j.seppur.2018.06.030.

[286] J.P. Scott, D.F. Ollis, Integration of chemical and biological oxidation processes for water treatment: II. Recent illustrations and experiences, J. Adv. Oxid. Technol. 2 (1997) 374–381. DOI: 10.1515/jaots-1997-0304.

[287] H.W. Chen, Y.L. Kuo, C.S. Chiou, S.W. You, C.M. Ma, C.T. Chang, Mineralization of reactive black 5 in aqueous solution by ozone/H_2O_2 in the presence of a magnetic catalyst, J. Hazard. Mater. 174(1–3) (2010) 795–800. DOI: 10.1016/j.jhazmat.2009.09.122.

[288] H. Jürg, Comparison of ozone and hydroxyl radical-induced oxidation of chlorinated hydrocarbons in water, Ozone Sci. Eng. 14 (1992) 197–214. DOI: 10.1080/01919519208552475.

[289] S. Khuntia, S.K. Majumder, P. Ghosh, Quantitative prediction of generation of hydroxyl radicals from ozone microbubbles, Chem. Eng. Res. Des. 98 (2015) 231–239. DOI: 10.1016/j.cherd.2015.04.003.

[290] D. Rajkumar, K. Palanivelu, Electrochemical treatment of industrial wastewater, J. Hazard. Mater. 113 (2004) 123–129. DOI: 10.1016/j.jhazmat.2004.05.039.

[291] V. Preethi, K.S. Parama Kalyani, K. Iyappan, C. Srinivasakannan, N. Balasubramaniam, N. Vedaraman, Ozonation of tannery effluent for removal of cod and color, J. Hazard. Mater. 166 (2009) 150–154. DOI: 10.1016/j.jhazmat.2008.11.035.

[292] F.J. Beltrán, G. Ovejero, J. Rivas, Oxidation of polynuclear aromatic hydrocarbons in water. 4. Ozone combined with hydrogen peroxide, Ind. Eng. Chem. Res. 35 (1996) 891–898. DOI: 10.1021/ie9503757.

[293] C. Tizaoui, L. Bouselmi, L. Mansouri, A. Ghrabi, Landfill leachate treatment with ozone and ozone/hydrogen peroxide systems, J. Hazard. Mater. 140 (2007) 316–324. DOI: 10.1016/j.jhazmat.2006.09.023.

[294] M.D. Gurol, R. Vatistas, Oxidation of phenolic compounds by ozone and ozone + u.v. radiation: A comparative study, Water Res. 21 (1987) 895–900. DOI: 10.1016/S0043-1354(87)80006-4.

[295] P.C. Singer, W.B. Zilli, Ozonation of ammonia in wastewater, Water Res. 9 (1975) 127–134. DOI: 10.1016/0043-1354(75)90001-9.

[296] J. Hoigne, H. Bader, Ozonation of water: Kinetics of oxidation of ammonia by ozone and hydroxyl radicals, Environ. Sci. Technol. 12 (1978) 79–84. DOI: 10.1021/es60137a005.

[297] C.H. Kuo, F. Yuan, D.O. Hill, Kinetics of oxidation of ammonia in solutions containing ozone with or without hydrogen peroxide, Ind. Eng. Chem. Res. 36 (1997) 4108–4113. DOI: 10.1021/ie9702082.

[298] J. Hoigné, H. Bader, The role of hydroxyl radical reactions in ozonation processes in

aqueous solutions, Water Res. 10 (1976) 377–386. DOI: 10.1016/0043-1354(76)90055-5.

[299] C.H. Liao, S.F. Kang, F.A. Wu, Hydroxyl radical scavenging role of chloride and bicarbonate ions in the H_2O_2/UV process, Chemosphere. 44 (2001) 1193–1200. DOI: 10.1016/S0045-6535(00)00278-2.

[300] M. Anbar, J.K. Thomas, Pulse radiolysis studies of aqueous sodium chloride solutions, J. Phys. Chem. 68 (1964) 3829–3835. DOI: 10.1021/j100794a050.

[301] G.G. Jayson, B.J. Parsons, A.J. Swallow, Some simple, highly reactive, inorganic chlorine derivatives in aqueous solution. Their formation using pulses of radiation and their role in the mechanism of the Fricke dosimeter, J. Chem. Soc. Faraday Trans. 1 Phys. Chem. Condens. Phases. 69 (1973) 1597–1607. DOI: 10.1039/F19736901597.

[302] U.K. Klaning, T. Wolff, Laser flash photolysis of HClO, ClO^-, HbrO and BrO^- in aqueous solutions, Ber. Bunsen-Ges. Phys. Chem. 89 (1985) 243–245. DOI: 10.1002/bbpc.19850890309.

[303] W.H. Glaze, J.W. Kang, D.H. Chapin, The chemistry of water treatment processes involving ozone, hydrogen peroxide and ultraviolet radiation, Ozone Sci. Eng. 9 (1987) 335–352. DOI: 10.1080/01919518708552148.

[304] A. Shokri, K. Mahanpoor, D. Soodbar, Degradation of *o*-toluidine in petrochemical wastewater by ozonation, UV/O_3, O_3/H_2O_2 and UV/O_3/H_2O_2 processes, Desalin. Water Treat. 57 (2016) 16473–16482. DOI: 10.1080/19443994.2015.1085454.

[305] C.D. Adams, P.A. Scanlan, N.D. Secrlst, Oxidation and biodegradability enhancement of 1,4-Dioxane using hydrogen peroxide and ozone, Environ. Sci. Technol. 28 (1994) 1812−1818. DOI: 10.1021/es00060a010.

[306] F.J. Beltrán, J.F. García-Araya, J. Frades, P. Álvarez, O. Gimeno, Effects of single and combined ozonation with hydrogen peroxide or UV radiation on the chemical degradation and biodegradability of debittering table olive industrial wastewaters, Water Res. 33 (1999) 723–732. DOI: 10.1016/S0043-1354(98)00239-5.

[307] R. Tosik, S. Wiktorowski, Color removal and improvement of biodegradability of wastewater from dyes production using ozone and hydrogen peroxide, Ozone Sci. Eng. 23 (2001) 295–302. DOI: 10.1080/01919510108962012.

[308] J.H. Suh, M. Mohseni, A study on the relationship between biodegradability enhancement and oxidation of 1,4-dioxane using ozone and hydrogen peroxide, Water Res. 38 (2004) 2596–2604. DOI: 10.1016/j.watres.2004.03.002.

[309] I.A. Balcioğlu, F. Çeçen, Treatability of kraft pulp bleaching wastewater by biochemical and photocatalytic oxidation, Water Sci. Technol. 40 (1999) 281–288. DOI: 10.1016/S0273-1223(99)00396-0.

[310] F.J. Beltrán, J.F. García-Araya, P.M. Álvarez, Integration of continuous biological and chemical (ozone) treatment of domestic wastewater: 1. Biodegradation and post-ozonation, J. Chem. Technol. Biotechnol. 74 (1999) 877–883. DOI: 10.1002/(SICI)1097-4660(199909)74:9<877::AID-JCTB117>3.0.CO;2-2.

[311] R. Baccar, M. Sarrà, J. Bouzid, M. Feki, P. Blánquez, Removal of pharmaceutical compounds by activated carbon prepared from agricultural by-product, Chem. Eng. J. 211–212 (2012) 310–317. DOI: 10.1016/j.cej.2012.09.099.

[312] A.W.M. Ip, J.P. Barford, G. McKay, A comparative study on the kinetics and mechanisms of removal of reactive black 5 by adsorption onto activated carbons and bone char, Chem. Eng. J. 157 (2010) 434–442. DOI: 10.1016/j.cej.2009.12.003.

[313] Y. Zhu, P. Kolar, Adsorptive removal of *p*-cresol using coconut shell-activated char, J. Environ. Chem. Eng. 2 (2014) 2050–2058. DOI: 10.1016/j.jece.2014.08.022.

[314] D. Mohan, H. Kumar, A. Sarswat, M. Alexandre-Franco, C.U. Pittman, Cadmium and lead remediation using magnetic oak wood and oak bark fast pyrolysis bio-chars, Chem. Eng. J. 236 (2014) 513–528. DOI: 10.1016/j.cej.2013.09.057.

[315] C. Jung, J. Park, K.H. Lim, S. Park, J. Heo, N. Her, J. Oh, S. Yun, Y. Yoon, Adsorption of selected endocrine disrupting compounds and pharmaceuticals on activated biochars, J. Hazard. Mater. 263 (2013) 702–710. DOI: 10.1016/j.jhazmat.2013.10.033.

[316] S. Mondal, S. Patel, S.K. Majumder, Naproxen removal capacity enhancement by transforming the activated carbon into a blended composite material, Water. Air. Soil Pollut. 231 (2020) 1–16. DOI: 10.1007/s11270-020-4411-7.

[317] O. Cardoso, J.M. Porcher, W. Sanchez, Factory-discharged pharmaceuticals could be a relevant source of aquatic environment contamination: Review of evidence and need for knowledge, Chemosphere. 115 (2014) 20–30. DOI: 10.1016/J.CHEMOSPHERE.2014.02.004.

[318] J. Lalwani, A. Gupta, S. Thatikonda, C. Subrahmanyam, An industrial insight on treatment strategies of the pharmaceutical industry effluent with varying qualitative characteristics, J. Environ. Chem. Eng. 8 (2020) 104190. DOI: 10.1016/j.jece.2020.104190.

[319] R. Gothwal, T. Shashidhar, Antibiotic pollution in the environment: A Review, Clean - Soil, Air, Water. 43 (2015) 479–489. DOI: 10.1002/clen.201300989.

[320] M. Dular, T. Griessler-Bulc, I. Gutierrez-Aguirre, E. Heath, T. Kosjek, A. Krivograd Klemenčič, M. Oder, M. Petkovšek, N. Rački, M. Ravnikar, A. Šarc, B. Širok, M.

Zupanc, M. Žitnik, B. Kompare, Use of hydrodynamic cavitation in (waste)water treatment, Ultrason. Sonochem. 29 (2016) 577–588. DOI: 10.1016/j.ultsonch.2015.10.010.

[321] J. Lalwani, S. CJ, S. Thatikonda, S. Challapalli, Sequential treatment of crude drug effluent for the elimination of API by combined electro-assisted coagulation-photocatalytic oxidation, J. Water Process Eng. 28 (2019) 195–202. DOI: 10.1016/j.jwpe.2019.01.006.

[322] I. Sirés, E. Brillas, Remediation of water pollution caused by pharmaceutical residues based on electrochemical separation and degradation technologies: A review, Environ. Int. 40 (2012) 212–229. DOI: 10.1016/J.ENVINT.2011.07.012.

[323] I. Oller, S. Malato, J.A. Sánchez-Pérez, Combination of advanced oxidation processes and biological treatments for wastewater decontamination: A review, Sci. Total Environ. 409 (2011) 4141–4166. DOI: 10.1016/J.SCITOTENV.2010.08.061.

[324] C. Comninellis, A. Kapalka, S. Malato, S.A. Parsons, I. Poulios, D. Mantzavinos, Advanced oxidation processes for water treatment: Advances and trends for R&D, J. Chem. Technol. Biotechnol. 83 (2008) 769–776. DOI: 10.1002/jctb.1873.

[325] E. Brillas, I. Sirés, M.A. Oturan, Electro-fenton process and related electrochemical technologies based on fenton's reaction chemistry, Chem. Rev. 109 (2009) 6570–6631. DOI: 10.1021/cr900136g.

[326] N. San Sebastián Martínez, J.F. Fernández, X.F. Segura, A.S. Ferrer, Pre-oxidation of an extremely polluted industrial wastewater by the Fenton's reagent, J. Hazard. Mater. 101 (2003) 315–322. DOI: 10.1016/S0304-3894(03)00207-3.

[327] M. Panizza, G. Cerisola, Direct and mediated anodic oxidation of organic pollutants,

Chem. Rev. 109 (2009) 6541–6569. DOI: 10.1021/cr9001319.

[328] A. Monteoliva-García, J. Martín-Pascual, M.M. Muñío, J.M. Poyatos, Effects of carrier addition on water quality and pharmaceutical removal capacity of a membrane bioreactor – Advanced oxidation process combined treatment, Sci. Total Environ. 708 (2020) 135104. DOI: 10.1016/J.SCITOTENV.2019.135104.

[329] C. Köhler, S. Venditti, E. Igos, K. Klepiszewski, E. Benetto, A. Cornelissen, Elimination of pharmaceutical residues in biologically pre-treated hospital wastewater using advanced UV irradiation technology: A comparative assessment, J. Hazard. Mater. 239–240 (2012) 70–77. DOI: 10.1016/J.JHAZMAT.2012.06.006.

[330] D. Mousel, D. Bastian, J. Firk, L. Palmowski, J. Pinnekamp, Removal of pharmaceuticals from wastewater of health care facilities, Sci. Total Environ. 751 (2021) 141310. DOI: 10.1016/J.SCITOTENV.2020.141310.

[331] G. Laera, M.N. Chong, B. Jin, A. Lopez, An integrated MBR-TiO_2 photocatalysis process for the removal of carbamazepine from simulated pharmaceutical industrial effluent, Bioresour. Technol. 102 (2011) 7012–7015. DOI: 10.1016/j.biortech.2011.04.056.

[332] S.H. Lee, K.H. Kim, M. Lee, B.D. Lee, Detection status and removal characteristics of pharmaceuticals in wastewater treatment effluent, J. Water Process Eng. 31 (2019) 100828. DOI: 10.1016/J.JWPE.2019.100828.

[333] M.F. Sevimli, H.Z. Sarikaya, Ozone treatment of textile effluents and dyes: Effect of applied ozone dose, pH and dye concentration, J. Chem. Technol. Biotechnol. 77 (2002) 842–850. DOI: 10.1002/jctb.644.

[334] S. Patel, S.K. Majumder, S. Mondal, P. Das, P. Ghosh, Treatment of a pharmaceutical

industrial effluent by a hybrid process of advanced oxidation and adsorption, ACS Omega. 5 (2020) 32305–32317. DOI: 10.1021/acsomega.0c04139.

[335] S. Khuntia, S.K. Majumder, P. Ghosh, Removal of ammonia from water by ozone microbubbles, Ind. Eng. Chem. Res. 52 (2012) 318–326. DOI: 10.1021/ie302212p.

[336] U. von Gunten, J. Hoigné, Bromate formation during ozonization of bromide-containing waters: Interaction of ozone and hydroxyl radical reactions, Environ. Sci. Technol. 28 (1994) 1234–1242. DOI: 10.1021/es00056a009.

[337] A.Y.C. Lin, C.F. Lin, J.M. Chiou, P.K.A. Hong, O3 and O3/H2O2 treatment of sulfonamide and macrolide antibiotics in wastewater, J. Hazard. Mater. 171 (2009) 452–458. DOI: 10.1016/j.jhazmat.2009.06.031.

[338] J. Staehelin, J. Hoigne, Decomposition of ozone in water: rate of initiation by hydroxide ions and hydrogen peroxide, Environ. Sci. Technol. 16 (1982) 676–681.

[339] O. Levenspiel, Chemical Reaction Engineering, 3rd Edition, Wiley (1998).

[340] C.L. Hsueh, Y.H. Huang, C.C. Wang, C.Y. Chen, Degradation of azo dyes using low iron concentration of Fenton and Fenton-like system, Chemosphere. 58 (2005) 1409–1414. DOI: 10.1016/J.CHEMOSPHERE.2004.09.091.

[341] M.A. Tony, Y.Q. Zhao, A.M. Tayeb, Exploitation of Fenton and Fenton-like reagents as alternative conditioners for alum sludge conditioning, J. Environ. Sci. 21 (2009) 101–105. DOI: 10.1016/S1001-0742(09)60018-8.

[342] K. Ntampegliotis, A. Riga, V. Karayannis, V. Bontozoglou, G. Papapolymerou, Decolorization kinetics of Procion H-exl dyes from textile dyeing using Fenton-like reactions, J. Hazard. Mater. 136 (2006) 75–84. DOI: 10.1016/j.jhazmat.2005.11.016.

[343] H.J. Fan, S.T. Huang, W.H. Chung, J.L. Jan, W.Y. Lin, C.C. Chen, Degradation pathways of crystal violet by Fenton and Fenton-like systems: Condition optimization and intermediate separation and identification, J. Hazard. Mater. 171 (2009) 1032–1044. DOI: 10.1016/j.jhazmat.2009.06.117.

[344] M.W. Chang, C.C. Chung, J.M. Chern, T.S. Chen, Dye decomposition kinetics by UV/H_2O_2: Initial rate analysis by effective kinetic modelling methodology, Chem. Eng. Sci. 65 (2010) 135–140. DOI: 10.1016/J.CES.2009.01.056.

[345] G. V. Buxton, C.L. Greenstock, W.P. Helman, A.B. Ross, Critical review of rate constants for reactions of hydrated electrons, hydrogen atoms and hydroxyl radicals (·OH/·O− in Aqueous Solution, J. Phys. Chem. Ref. Data. 17 (1988) 513–886. DOI: 10.1063/1.555805.

APPENDIX

Table A1. Table for uncertainty analysis of concentration measured for NPX

Time (min)	[NPX]/ [NPX]$_0$	[NPX]/ [NPX]$_0$	[NPX]/ [NPX]$_0$	Mean	STDEV	U	U_r (%)
1	0.934	0.905	0.889	0.909	0.022	0.013	1.431
2	0.890	0.846	0.832	0.856	0.039	0.018	2.087
3	0.800	0.782	0.759	0.779	0.029	0.012	1.693
4	0.698	0.672	0.659	0.676	0.023	0.017	1.731
5	0.654	0.613	0.599	0.622	0.028	0.013	2.621
6	0.587	0.545	0.531	0.554	0.028	0.016	2.993
7	0.467	0.446	0.436	0.450	0.015	0.090	2.004
8	0.443	0.407	0.373	0.407	0.035	0.025	5.025
9	0.378	0.338	0.309	0.342	0.036	0.019	5.835
10	0.307	0.272	0.243	0.275	0.032	0.019	6.552

Table A2. Mean, standard deviation, and standard and relative uncertainty for the DCF concentration

Appendix

Time (min)	$[DCF]/[DCF]_0$	$[DCF]/[DCF]_0$	$[DCF]/[DCF]_0$	Mean	STDEV	U	U_r (%)
1	0.803	0.826	0.856	0.827	0.025	0.015	1.78
2	0.543	0.583	0.609	0.578	0.033	0.019	3.35
3	0.428	0.474	0.441	0.447	0.023	0.014	3.08
4	0.262	0.285	0.251	0.266	0.016	0.009	3.65
5	0.156	0.162	0.187	0.168	0.016	0.009	5.67
6	0.077	0.085	0.096	0.087	0.008	0.005	5.83
7	0.064	0.051	0.054	0.056	0.007	0.004	7.13
8	0.030	0.025	0.026	0.027	0.002	0.001	4.03
9	0.017	0.016	0.017	0.016	0.001	0.001	2.64
10	0.012	0.014	0.015	0.013	0.002	0.001	6.83

Table A3. Mean, standard deviation, and standard and relative uncertainty for the RNT concentration

Time (min)	[RNT]/ [RNT]$_0$	[RNT]/ [RNT]$_0$	[RNT]/ [RNT]$_0$	Mean	STDEV	U	U_r (%)
1	0.887	0.870	0.853	0.870	0.016	0.009	1.111
2	0.752	0.720	0.709	0.727	0.022	0.012	1.758
3	0.659	0.617	0.641	0.639	0.021	0.012	1.904
4	0.525	0.470	0.495	0.497	0.027	0.015	3.217
5	0.431	0.363	0.387	0.393	0.034	0.019	5.042
6	0.328	0.284	0.296	0.303	0.022	0.013	4.299
7	0.239	0.218	0.254	0.237	0.018	0.010	4.384
8	0.149	0.134	0.126	0.136	0.011	0.006	4.844
9	0.121	0.102	0.117	0.113	0.009	0.005	5.043
10	0.096	0.071	0.068	0.078	0.015	0.009	11.613

LIST OF PUBLICATIONS

Publications

[1] **S. Patel**, S. K. Majumder, P. Ghosh, P. Das, Ozone microbubble-aided intensification of degradation of naproxen in a plant prototype, J. Environ. Chem. Eng. 7:3 (2019) 103102. DOI: 10.1016/j.jece.2019.103102.

[2] **S. Patel**, R. Agarwal, S. K. Majumder, P. Ghosh, P. Das, Kinetics of ozonation and mass transfer of pharmaceuticals degraded by ozone fine bubbles in a plant prototype, Heat and Mass Trans. 56:2 (2019) 385–397. DOI: 10.1007/s00231-019-02718-7.

[3] **S. Patel**, S Mondal, S. K. Majumder, P. Ghosh, P. Das, Treatment of a pharmaceutical industrial effluent by a hybrid process of advanced oxidation and adsorption. ACS Omega. 5:50 (2020) 32305–32317. DOI: 10.1021/acsomega.0c04139.

[4] **S. Patel**, S. K. Majumder, P. Ghosh, Ozonation of diclofenac in a laboratory scale bubble column: Intermediates, mechanism, and mass transfer study. J. Water Process. Eng. (2021), 44, 102325. DOI: 10.1016/j.jwpe.2021.102325.

[5] **S. Patel**, S. K. Majumder, P. Ghosh, Degradation of ranitidine by $O_3 + H_2O_2$: Kinetics, modeling, and mechanism (under preparation).

[6] **S. Patel**, S. K. Majumder, P. Ghosh, Treatment of a mixture of real pharmaceutical industrial effluents by coagulation and perozonation (under preparation).

Conferences

[1] **S. Patel**, R. Agarwal, S. K. Majumder, P. Das, P. Ghosh, Kinetic study of degradation of pharmaceutical drugs by ozone microbubbles. AIChE Annual Meeting, 26 – 28 October 2018, Pittsburgh, USA.

[2] **S. Patel**, S. K. Majumder, P. Ghosh, Degradation and kinetics of naproxen by using peroxone. Reflux, 28 – 29 Sep 2019, IIT Guwahati, India.

[3] **S. Patel**, S. K. Majumder, P. Ghosh, Degradation and kinetics of naproxen by peroxone in a fine-bubbles system. ICAMEES, 14 – 15 Dec 2019, UPES Dehradun, India.

[4] **S. Patel**, S. K. Majumder, P. Ghosh, Ozonation of synthetic and real industrial pharmaceutical wastewater. Recycle, 13 – 14 Feb 2020, IIT Guwahati, India.

Award

[1] Runner-up, Reflux, 28 – 29 Sep 2019, organized by Indian Institute of Technology Guwahati, India.